Tampere University

SURESH PALANIVEL

Evaluation of Cytotoxic Effects and Underlying Mechanism of Phenolic Compounds on Breast Cancer Cell Lines

Tampere University Dissertations 619

Tampere University Dissertations 619

SURESH PALANIVEL

Evaluation of Cytotoxic Effects and Underlying Mechanism of Phenolic Compounds on Breast Cancer Cell Lines

ACADEMIC DISSERTATION
To be presented, with the permission of
the Faculty of Medicine and Health Technology
of Tampere University,
for public discussion at Tampere University,
on 31st May 2022, at 15 o'clock.

ACADEMIC DISSERTATION
Tampere University, Faculty of Medicine and Health Technology
Finland

Responsible supervisor	Adjunct Professor Meenakshisundaram Kandhavelu Tampere University Finland	
Supervisor	Professor Olli Yli-Harja Tampere University Finland	
Pre-examiners	Professor Jeyakanthan Jeyaram Alagappa University India	PhD Clement B. Penny University of Witwatersrand South Africa
Opponent	Associate Professor Raghu Sinha Penn State College of Medicine USA	
Custos	Professor Olli Yli-Harja Tampere University Finland	

Cover design: Roihu Inc.

ISBN 978-952-03-2446-9 (print)
ISBN 978-952-03-2447-6 (pdf)
ISSN 2489-9860 (print)
ISSN 2490-0028 (pdf)
http://urn.fi/URN:ISBN:978-952-03-2447-6

PunaMusta Oy – Yliopistopaino
Joensuu 2022

ACKNOWLEDGEMENTS

My heartfelt gratitude is to my supervisor, Docent, Dr. Meenakshisundaram Kandhavelu, and Prof. Olli Yli-Harja, who instructed my doctoral research. Dr. Meenakshisundaram Kandhavelu supported me with the most profound knowledge and encouragement to do my research work. I sincerely thank him for allowing me to engage in his laboratory and complete my research work successfully. Likewise, I extend my sincere gratitude and respect to Prof. Olli Yli-Harja, who gave me expert guidance, inspiration, and support to succeed in my research work.

I thank my colleagues and lab members Anisha Vishwanathan, Phuong Doan, Angelika Karjalainen, and Adrien Sala, who helped me a lot with the scientific concerns during my research. I also thank Akshaya Murugesan, who supported me in manuscript preparation.

It's my immense pleasure to mention some true-hearted people in my life Ilamathi Thirusenthilarasan and Gnanavel Mutharasu, who gave their precious time to support my research work. This is my sincere thanks to them for their effort to make me succeed in my research career.

I would love to mention the most significant support given by my family, who were behind me throughout my journey. My father Palanivel and my mother Muthumari trusted me and my talent more than anyone in my life. Likewise, I would like to be grateful to my better half Anjugam and my little fella Vel Atheeran, who sacrificed many of their precious moments to support my research career. Last but not least, I would like to thank my Godfather Pekka Lepisto, my Finnish guardian, and my best friend Lauri Koskela, who supported me without any expectations and encouraged me a lot to grow in my career.

Finally, I would like to thank the Faculty of Medicine and Health Technology, Tampere University, for providing the financial support and infrastructure to complete my research work. I also thank the Centre for International Mobility (CIMO) for providing financial support through the fellowship, TM-15-9720.

ABSTRACT

Breast cancer (BC) is the second most common cancer that causes higher mortality rates worldwide. It is a complex and heterogeneous disease with a median survival range of around three years. Breast cancer patients' overall survival has increased due to using chemotherapeutic medicines, namely anthracyclines and taxanes. However, drug resistance and subsequent progression of this disease were still observed in metastatic patients. Furthermore, the efficacy failure of even today's sophisticated chemotherapeutics negatively impacts breast cancer patients with side effects, highlighting the urgent need for the development of nontoxic medications, that have low side effects, and are patient-friendly. Tumor cell death has been associated with the activation of apoptotic signal transduction pathways in cancer cells, such as the intrinsic and/or extrinsic pathways. Thus, understanding the molecular mechanism of apoptosis opens the future perspective for drug development for breast cancer treatment. The present study focuses on the possibility of using newly synthesized indoline analogs as targeted therapy for breast cancer, which could selectively induce apoptosis in cancer cells. Advances in anticancer drug discovery using broad-spectrum drugs, such as substituted alkylamino phenolic rings or indoline rings, have emerged as promising molecules. Thus, investigating the effects of these compounds in inducing apoptosis would provide opportunities that directly evade the significant challenges in current breast cancer therapies.

The present research work focuses on the in-vitro analysis of the anti-breast cancer activity of three novel indoline derivatives, 2-((1, 2, 3, 4-Tetrahydroquinolin-1-yl) (4 methoxyphenyl) methyl) phenol (THMPP), 2-((3,4-Dihydroquinolin-1(2H)-yl) (ptolyl)methyl)phenol)(THTMP) and N-(2-hydroxy-5-nitrophenyl (4'-methyl

phenyl)methyl) indoline (HNPMI). The present study's findings have been published in four publications, each of which highlights the mechanism of action of each compound's cytotoxic potential, its apoptotic induction potential, the regulation of the genes involved in the Epithelial Growth Factor Receptor (EGFR) signaling pathway, and the in-silico analysis to identify the compound's interaction with the target receptor, EGFR. Absorption, distribution, metabolism, excretion, and toxicity (ADME/ T) analysis also confirms the drug likeliness of the compound to be used as a potent anticancer drug. The compounds' cytotoxicity was tested in breast cancer cells like MCF7 (ER+PR+/HER-), SkBr3 (ER-PR-/HER+), MDA MB-231, and non-tumorous cells like HEK293 and H9C2.

The first compound we analyzed was 2-((1, 2, 3, 4-Tetrahydroquinolin-1-yl) (4 methoxyphenyl) methyl) phenol (THMPP). In human breast cancer cell lines MCF-7 and SkBr3 and non-cancerous mouse myoblast cells, H9C2, it was evaluated for its potential cytotoxicity and method of action. THMPP induced cell death in MCF-7 and SkBr3 cells at their IC50 concentration of 83.23 μM and 113.94 μM, respectively. The toxicity was 36.4% in MCF-7 cells and 18.86% in SkBr3 cells at 10μM concentrations. Interestingly, THMPP showed the lowest percentage of cytotoxicity to H9C2 cells (0.91%) than the other breast cancer cell line. The compound induced apoptosis through increased caspase three and caspase 9 with the fold level of 0.17-fold and 0.47-fold in MCF-7 cells and 0.07 and 0.25 in SkBr3 cells, respectively. THMPP also enhanced apoptosis of the breast cancer cells, causing inter-nucleosomal DNA fragmentation, thus leading to DNA strand breakage and cell death. FACS analysis has proved that THMPP improves breast cancer cells to enter various stages of apoptosis, especially in the late apoptotic stage. With a score of 5.79 kJ/mol, molecular docking validates THMPP's substantial interaction with EGFR, predicted to activate the downstream signaling pathway. The downregulation of PI3K and S6K1 genes involved in the Phosphatidylinositol 3-Kinase (PI3K)/AKT signaling pathway, which were considerably overexpressed in

cancer cells, was validated by gene expression analysis. Quantitative Structure-Activity Relationship (QSAR) analysis confirmed the toxicity of THMPP against breast cancer cells. ADME/T analysis predicts the drug-likeliness of THMPP.

The second important compound that was analyzed for its anti-breast cancer activity was 2-((3,4-Dihydroquinolin-1(2H)-yl) (p-tolyl) methyl) phenol) (THTMP), the derivative of THMPP. A methyl group replaced the 4-OMe substituent of the aryl ring in THMPP to synthesize THMPP. The compound exhibits a cytotoxic effect against MCF7 and SK-BR3 cells, with IC50 values of 87.92 μM and 172.51 μM, respectively. THTMP caused cell death in breast cancer cells by regulating critical apoptosis enzymes, caspase-3 and-9, with 33 percent of cells in the late apoptotic stage after 24 hours of treatment. The significant interaction of THTMP with EGFR inhibits PI3K/S6K1 gene expression, thus enhancing the apoptotic response of the breast cancer cells. Structural validation of QSAR also confirms the anticancer property of THTMP. ADME/T screening suggested the compound's oral availability and better intestinal absorption with acceptable metabolism and toxicity parameters.

Furthermore, seven N-substituted indoline derivatives have been assessed for their ability to interact with the EGFR protein. Among the seven compounds analyzed by molecular docking, it was confirmed that the N-(2-hydroxy-5-nitrophenyl (4'-methyl phenyl) methyl) indoline (HNPMI) possesses a stronger affinity with EGFR active sites. As a result, the EGFR signaling pathway was activated, which reduced the expression of PI3K and S6K1 to about 0.4-fold and 0.3-fold, respectively, thereby inducing cell death via inter-nucleosomal DNA fragmentation. The IC50 value of HNPMI was found to be 64.10 μM in MCF-7 cells and 119.99 μM in SkBr3 cells. Furthermore, HNPMI stimulated DNA fragmentation, which was validated by FACS analysis, resulting in caspase-mediated apoptosis. Structural elucidation also revealed the bi-molecular interaction of HNPMI-EGFR, relating its activity to the anti-proliferative and apoptotic activity.

Finally, a combined computational analysis was performed to predict the compounds' interaction with the tyrosine kinase receptor of EGFR. The study revealed that the HNPMI, THMPP, and THTMP interact with the active site region of the EGFR structure (PDB ID: 1M17). The interactions include hydrogen bonds, hydrophobic interactions, pi stacking, and salt bridges. HNPMI was found to have the lowest Glide docking score among the three compounds, reflecting that it can be a better inhibitor than the other two compounds. The investigation of the MMGB/ SA and QM/MM analysis also showed a coherent pattern. It was also found that the protein-ligand complex was stable when it was simulated for 100ns. The Molecular dynamics results also revealed that the ligand interacted with the protein for more than 30% of the simulation time. The compounds also possessed good pharmacokinetic properties, which were predicted by ADME/T analysis.

Overall, the study demonstrates the effect of cytotoxicity and apoptotic induction of indoline derivatives THMPP, THTMP, and HNPMI. Furthermore, our results revealed the anti-breast cancer property of all three phenolic compounds with HNPMI as the lead molecule. HNPMI was also observed to be a potent EGFR pathway inhibitor, inhibiting the PI3K/ S6K1 signaling pathway and causing cell death in breast cancer cells. Thus, HNPMI can be subjected to further clinical testing and developed as a promising therapeutic medication for the treatment of breast cancer.

CONTENTS

List of Figures

List of Tables

ABBREVIATIONS

BC	Breast cancer
ER	Estrogen Receptor
PR	Progesterone Receptor
HER2	Human Epidermal Growth Factor Receptor 2
ELISA	Enzyme-Linked Immunosorbent Assay
cDNA	Complementary Deoxyribonucleic Acid
mRNA	Messenger Ribonucleic Acid
PCR	Polymerase Chain Reaction
PI3K	Phosphatidylinositol 3-Kinase
S6K1	S6 Kinase beta 1
EGFR	Epidermal Growth Factor Receptor
AKT	Protein Kinase B
mTOR	Mammalian Target of Rapamycin
PDB	Protein Data Bank

MM-GB/SA	Molecular mechanics with generalized born and surface area solvation
QM/MM	Quantum Mechanics/Molecular Mechanics

ORIGINAL PUBLICATIONS

This thesis comprises four publications: Publication I, Publication II, Publication III, and Publication IV. With permission from the respective publishers, the publications are reproduced.

Publication I Palanivel S, Murugesan A, Yli-Harja O, and Kandhavelu M, Anticancer activity of THMPP: Downregulation of PI3K/ S6K1 in breast cancer cell line, *Saudi Pharmaceutical Journal*; Volume 28(4), 19 March 2020, Pages 495-503.

doi.org: 10.1016/j.jsps.2020.02.015

Publication II Palanivel S, Yli-Harja O and Kandhavelu M, Alkylamino phenol derivative induces apoptosis by inhibiting EGFR signaling pathway in breast cancer cells, *Anticancer Agents in Medicinal Chemistry;* Volume 20(7):03 July 2020, Pages 809-819.

doi.org: 10.2174/1871520620666200213101407

Publication III Palanivel S, Murugesan A, Subramanian K, Yli-Harja O, and Kandhavelu M, Antiproliferative and apoptotic effects of indole derivative, N-(2-hydroxy-5-nitrophenyl (4'-methylphenyl) methyl) indoline in breast cancer cells, *European Journal of Pharmacology*; Volume 881:15 August 2020, Pages 173-195.

doi.org: 10.1016/j.ejphar.2020.173195

Publication IV Palanivel S, Yli-Harja O, and Kandhavelu M, Molecular interaction study of novel indoline derivatives with EGFR-kinase domain using

multiple computational analysis, *Journal of BiomolecularStructure and. Dynamics*; 1-10.

doi: 10.1080/07391102.2021.1900917

AUTHOR'S CONTRIBUTIONS

Publication I Palanivel S performed *in-vitro* techniques, such as confocal microscopy and RT-PCR analysis, and *in-silico* methods, such as molecular docking and QSAR analysis. Palanivel S contributed to analyze the results with Kandhavelu M. Palanivel S, Murugesan A., Yli-Harja O., and Kandhavelu M. contributed to write the manuscript.

Publication II Palanivel S performed a high-throughput *in-vitro* experiment and validated the *in-vitro* experiment results with the *in-silico* experiment results. Furthermore, Palanivel S and Kandhavelu M. contributed to analyze the results. In addition, Palanivel S participated in writing the manuscript along with Yli-Harja O. and Kandhavelu M.

Publication III Palanivel S conceived the study with Kandhavelu M. Palanivel S designed and conducted all the *in-vitro* experiments. Subramanian K. and Palanivel S conducted a few *in-silico* experiments to validate the *in-vitro* results. Palanivel S, Kandhavelu M., and Subramanian K. contributed to analyze the results. Palanivel S, Murugesan A., Subramanian K., Yli-Harja O., and Kandhavelu M. supported the writing of the manuscript.

Publication IV Palanivel S utilized many *in-silico* techniques, such as molecular docking, molecular dynamics simulation, and DFT analysis. Palanivel S is the corresponding author of the article. In addition,

Palanivel S, Yli-Harja O., and Kandhavelu M. contributed to write the manuscript.

Kandhavelu M. and Yli-Harja O. supervised the experimental & computational studies and manuscript preparation.

1 INTRODUCTION

1.1 Background and motivation

Cancer is the second most widespread disorder worldwide[1]. Among the various types of cancer, breast cancer in women is the most formidable cancer type globally. The statistics of GLOBOCAN 2020 assert that breast cancer diagnosis has surpassed lung cancer, colorectal cancer, prostate cancer, and stomach cancer[2]. Breast cancer sometimes results in mortality, predominantly due to metastasis rather than cancer during the early stages of diagnosis. Despite the unprecedented advancements in treatment options, nearly 40% of patients suffer from recurrence of breast cancer; however, in another 35% to 40% of patients, cancer eventually progresses to the metastatic stage.[3]

The treatment approach for each patient is different since it is dependent on the nature of the breast cancer cells and the stage of the tumor. The major cancer treatment modalities aim to eliminate the tumor through surgical procedures, radiotherapy, and chemotherapy. Chemotherapy is administered via drugs during the initial phase of the disease to inhibit the growth of the tumor and its further replication. It is mainly used in cases that do not require surgical treatment. The drugs are given at regular intervals in cycles based on the patient's health condition and cancer stage.[4]

The cell's many metabolic pathways mediate the pathogenesis of breast cancer and the development of cancerous cells.[5] Many biomarkers are used in breast cancer

diagnosis. Any of these markers can be targeted by a compound and can be established as a treatment approach. In addition, the targeted therapies may provide new insights into cancer therapeutics by explicitly altering the signaling pathway involved in cell proliferation, metastasis, apoptosis, and cell cycle regulation.[6] Most chemotherapeutic drugs exert anticancer activity by altering the cell cycle progression.

Chemotherapeutic drugs, hormone-mediated therapies, and immunotherapies are the essential spotlights of the current cancer cure.[7] The poor response by many cancer patients to conventional chemotherapy in a clinical context triggers the development of resistance. Many current chemotherapeutics' poor efficacy and considerable toxicity urge an immediate need for novel, effective, and nontoxic cent-per-cent results that are oriented as patient-friendly drugs for cancer treatment. The administration of such drugs should be combined with predictive biomarkers, which would enable a personalized therapeutic approach for each patient. Furthermore, such drugs must ensure the total absence of side effects. Hence, the design and development of new drugs for cancer therapeutics has emerged as an essential and challenging task for medicinal chemists worldwide.

The substituted alkylamino phenolic rings or indoline rings represent an interesting class of hetero compounds. They have a broad spectrum of pharmacological activities, including antifungal, antioxidant, analgesic, anti-inflammatory modulations, and so on.[8–11]

Various past studies clearly describe the efficacy and effectiveness of phenolic compounds in controlling cancer progression. Their antioxidant properties make them attractive for the sake of exploring further anti-oncogenic activities.[12,13] Their potential to modulate cell activity depends on the number and length of the presented side chains, especially the hydroxyl groups. Phenolic compounds occur naturally in many plant species and mainly consist of single or multiple aromatic rings

with hydroxylic residues. Many theoretical experts and practitioners in the field have highlighted the existence and ability of phenol moieties that act as free radical scavengers; they have shown that natural compounds such as quinones, flavonoids, lignans, coumarins, stilbenes, and tannins have multiple biological properties.[11,14,15] Phenols are abundant in nature, but only a few chemically synthesized derivatives such as eugenol dimmers have exhibited strong anticancer activity.[8] Resveratrol is a non-flavonoid polyphenol that exhibits both chemopreventive and chemotherapeutic potential against breast carcinogenesis; it is present in several nutritional sources such as grapes and berries, soybeans, pomegranates, and peanuts.[16] It modulates EGF and leads to the activation of EGFR, which, in turn, triggers the downstream PI3K signaling pathway and increases cellular migration.[17] The EGFR-induced T47D breast cancer cells enhance cell proliferation, which requires both PI3K and MAPK pathways.[18]

The present research was conducted amid this background to evaluate the anticancer activity of synthetic phenolic compounds. The ability of the compounds was examined in different breast cancer cell lines by performing many *in-vitro* and *in-silico* experiments.

1.2 Aim of the study

This thesis aims to evaluate the anticancer potential of three synthesized phenolic compounds in breast cancer cell lines and investigate their action inside the cells. The following five objectives are fulfilled through this research:

The first objective involved examining the cytotoxicity capability of the compounds in breast cancer cells. The cytotoxicity was evaluated in three cell lines, namely HNPMI, THTMP, and THMPP, using the MTT assay. This study depicts the

inhibitory concentration (IC_{50}) of the compounds against breast cancer cells. The lower their IC_{50} value, the higher the probability of their utility as a chemo drug. The compound's activity in normal, noncancerous H9C2 cells was also examined to prove its specificity to cancer cells.

The second objective involved verifying whether the cytotoxic activity was due to the induction of apoptosis in cancer cells. Throughout this thesis, apoptosis was examined and considered a major hallmark. Therefore, assays such as caspases 3 and 9 enzyme assays and DNA fragmentation assays were performed to determine the occurrence of apoptosis and to check whether the cell death was due to necrosis or apoptosis.

The third objective involved experimentally proving and quantifying the apoptotic induction in the cancer cells after treatment of the compounds. Fluorescence microscopic analysis was conducted using Annexin V staining on cell differentiation and cell death due to apoptosis. Flow cytometry-based cell sorting aided in the analysis of the number of cells present in different cell stages. These two methods made it simple and possible to enumerate the percentage of cells that shifted to apoptosis after the appropriate compound exposure to the cell lines.

The fourth objective involved examining the expression of the gene involved in the PI3K/S6K1 signaling pathway. Reverse Transcriptase Polymerase Chain Reaction (RT-PCR) is a highly sensitive molecular technique used to detect the presence of cancer cells at the smallest size possible. This technique aided in detecting the alteration in the gene expression in the cancer signaling pathway after treatment.

The fifth objective involved utilizing multiple computational approaches to understand the interaction of EGFR protein and the compounds (ligands). Molecular docking is used to predict ligand-protein interaction, binding energies required for the compounds to bind to the active site and analyze the type of weak

interaction involved. Apart from this, the correlation of the structure of a molecule to biological activity as a function of molecular descriptors can be recognized by using a statistical tool called Quantitative Structure-Activity Relationship (QSAR). ADME/T analysis is used to predict Adsorption, Distribution, Metabolism, Excretion, Toxicity (ADME/T), etc., which is an important step in the early stage of drug discovery. Finally, Molecular Dynamic Simulation (MD-Simulation) investigates biological molecules' structure, dynamics, thermodynamics, and complexes. Overall, the fifth objective aided in substantiating the experimental evidence on the anticancer property of the compounds.

1.3 General scheme of the study and limitations

This thesis is a foot-proof document of the *in-vitro* anticancer activity of the three phenolic derivatives synthesized under laboratory conditions. Furthermore, the study proposes to accomplish the detailed anticancer activity of these compounds in breast cancer cells *in-vitro*.

The cell cytotoxicity of the compounds in three different cancer cell lines was initially studied. The determination of IC_{50} values enabled the determination of the best compound among the three compounds. The lower IC_{50} value prompted a further and deeper investigation into the understanding of the activity of compounds in apoptosis induction. The IC_{50} values were substantially low, so the activity of compounds in apoptosis induction was studied. Different methods were employed to study the apoptosis induction posttreatment, such as caspase's enzyme activity determination, DNA fragmentation analysis, cell sorting to find the cell cycle stage, and the microscopic technique to comprehend the morphological changes of the cell.

The gene expression of key molecules PI3K and S6K1 was evaluated using the RT-PCR technique, based on the total mRNA of cells after treatment. Apart from

the gene expression analysis *in-vitro*, the combined computational analysis of the compounds' interaction with EGFR protein was conducted. This includes molecular docking and molecular dynamics simulation. QM/MM analysis and MM-GB/SA analysis support docking data, which give a precise idea of the molecular mechanism of action behind the biological activity. The study also identified the best cancer compound among the three compounds selected. However, this provides only preliminary *in-vitro* and *in-silico* data. The efficacy observed in animal models and pharmacological and pharmacokinetic studies are not included in this thesis. Being a clinical study, the efficacy of the co-drugs must be assessed before they are used as drugs.

1.4 Thesis outline

This thesis is organized into six chapters. Chapter 1 describes and articulates the research issue or question; it presents the background and motivation behind the study, the aims and objectives, limitations, a general overview, and an outline of the thesis. Chapter 2 presents an overview of breast cancer research; it details the breast cancer mechanisms, the background of targeted chemotherapy, apoptosis, and the role of receptors in signaling pathways and various phenolic compounds in breast cancer therapeutics. Chapter 3 describes the methods implemented in the study. This chapter provides adequate details of the methodology used to characterize and identify the most potent anticancer agents. Chapter 4 illustrates the results collectively obtained from the experiments in the publication, which are presented in tabular and/or pictorial form. Chapter 5 discusses the outcomes obtained from the experiments and compares them with previous reports from similar research. Finally, chapter 6 includes the conclusion, summary, significance, and future perspectives of the research work.

2 REVIEW OF LITERATURE

2.1 BREAST CANCER

2.1.1 Statistics of breast cancer

Breast carcinoma is a tumor formed in the tissues of the breast. The three types of breast cancer are classified based on their origin of cell type. (1) Ductal carcinoma is the most commonly occurring type of breast cancer and is found in the epithelial cells of ducts in the breast. (2) Lobular carcinoma originates in the lobules. (3) Invasive carcinoma originates in the ducts or lobules and spreads to other surrounding breast tissues. Breast cancer occurs in both men and women but is rare among men.

Hormonal, environmental, and lifestyle factors can cause breast cancer. Mutations in breast cancer gene 1 (BRCA1) and breast cancer gene 2 (BRCA2) also aggravate the risk of developing breast cancer. Other minor causes of breast cancer among women include aging, radiation exposure, obesity, late or no pregnancies, alcohol consumption, and changes in hormones. The International Agency for Research on Cancer (IARC), Global Cancer Observatory GLOBOCAN, reported in 2018 on the periodic cancer statistics related to the incidence and mortality rates caused by different cancers worldwide. The report elucidates the cancer rates among men and women separately. It has been observed that breast cancer is the most commonly occurring cancer among women and the second most common cancer overall. Nearly two million incidences of breast cancer occurred globally in 2018. Among the

various cancers in women, 24.2% of new cases were breast cancer, resulting in 15% of deaths globally[19] (Figure 1).

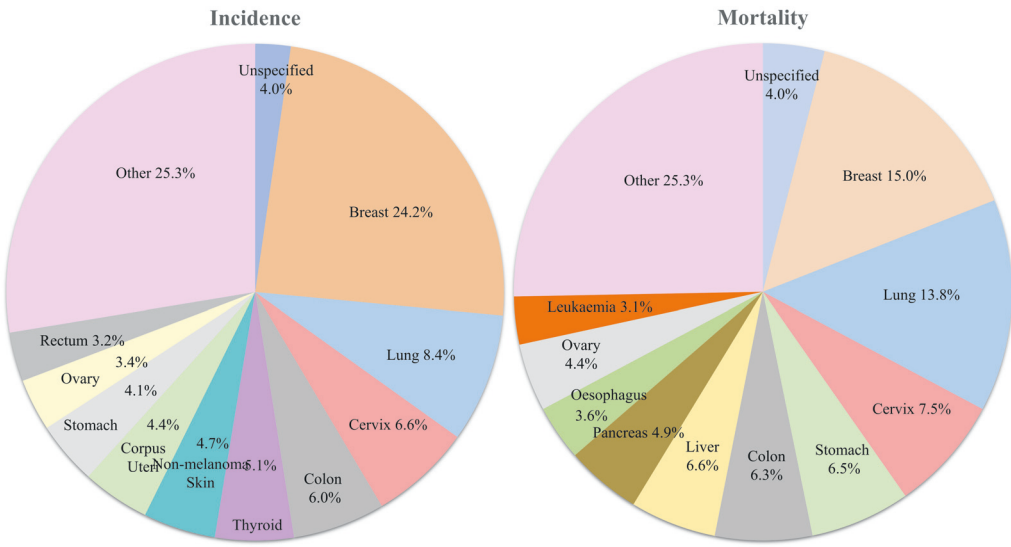

Figure 1: Incidence and mortality of cancers in women: The figure represents the incidence and mortality of the ten most common cancers in women surveyed in 2018 globally. The fraction of the total number of cases and deaths is represented in the pie chart. Figure reproduced from GLOBOCAN, 2018, reported by the International Agency for Research in Cancer.

It was estimated that by 2020, the new cases of breast cancer in the United States would exceed 276,480, which would account for 15.3% of all cancers. Furthermore, the estimated death cases would be 42,170, or 7% of all cancers. In the European Union, comprising 27 countries, it was anticipated that by 2020 a fall in breast cancer incidence would be observed in almost 355,000 women (13.3% of all cancer diagnoses). The second most commonly occurring cancer is colorectal cancer, followed by prostate and lung cancer. The death rate due to female breast cancer is low compared with lung and colorectal carcinoma. Among the deaths caused by cancer, 7.3% are observed to be due to breast cancer. Based on the 2015–2017 data, nearly 13% of women were diagnosed with female breast cancer at some point

during their lifetime. The convincing fact is that the five-year relative survival rate of the patients with breast cancer was an average of 90.06% from 2010 to 2016, which is reasonably higher than other cancers. Among the EU-27 countries, the highest rate of female breast cancer occurrence is observed in Belgium, followed by Luxembourg; Finland ranks 13th among the European countries.

2.1.2 Breast cancer subtypes

Carcinoma is a heterogeneous disease with a myriad of variations in its pathological features and molecular characteristics.[20].

Medical practitioners classify breast cancer into major subtypes based on certain tumor markers in the breast cells. The key markers are the expression of estrogen receptor (ER), progesterone receptor (PR), and human epidermal growth factor receptor 2 (HER2). The subtypes are ER+/PR+, ER+/PR-, ER-/PR+, and ER-/PR- with HER2 positive or negative in each case. Advancements in molecular technologies have generated gene profiling models for a complete categorization of the disease. Compared with molecular or genetic profiling, ER, PR, and HER2 markers are commonly used, cheaper, and more reliable for deciding the treatment regimen. St. Gallen risk categories have reported eight combinations of ER, PR, and HER2 for all breast cancer stages: They describe the demographics, tumor characteristics, and survival based on these subtypes.[21–23] Among the eight combinations, triple-negative, ER-/PR-/HER2- breast cancer is graded higher than the others, and it is also more aggressive and difficult for prognosis.

2.1.3 Treatment modalities of breast cancer

Each patient's treatment plan differs based on the biology of the breast cancer cells. The major factors include the type of breast cells affected, the expression of the hormone receptors, the tumor stage, the genetic markers expressed, the patient's

general health and age, her menstrual status, and the presence or absence of BRCA mutations. Therefore, the regimen differs for every patient. Still, common steps are followed for most patients.[24] (1) Surgery: A lumpectomy is performed during which the tumor and a smaller portion surrounding the tumor are removed. Another option would be a mastectomy, during which a surgical procedure removes the entire breast with the tumor. This also includes cancerous lymph node removal. (2) Chemotherapy: Drugs are administered to prevent the growth of cancer cells. These can be administered before or after the surgery to reduce the tumor size and ultimately eliminate the tumor. The drugs are given at regular intervals in cycles depending on the patient's condition. A few commonly administered chemotherapeutic drugs for breast cancer include Docetaxel, Paclitaxel, Epirubicin, Doxorubicin, Carboplatin, Cisplatin, Cyclophosphamide, Fluorouracil, Methotrexate, etc. (3) Radiotherapy: High-energy X-rays or other forms of radiation are used to destroy cancer cells. Radiation can be given as an external beam or in the tumor site using a probe or brachytherapy. (4) Hormonal therapy: For the hormone receptor-positive cases, the "anti-hormone" inactivates the hormone (ER, PR, or HER2). This can prevent the recurrence of cancer, for instance, Tamoxifen and Aromatase inhibitors. (5) Immunotherapy: This is often an adjuvant therapy to enhance the body's immunity to fight against cancer. Atezolizumab and Pembrolizumab are the commonly used immunotherapy drugs.

2.2 Chemotherapy and breast cancer

The exceptional and phenomenal advancements in the understanding, screening, diagnosis, and treatment of breast cancer have resulted in a sharp decline in mortality rates, despite a rise in the incidence of breast cancer globally. In addition, molecular-level research has provided potential new therapies to manage breast cancer effectively. For example, the new compounds found and recommended in the recent past precisely target breast cancer cells, decreasing mortality rates.

Most research at preclinical and clinical levels is conducted to examine the role of chemotherapy. Debates and trials are also conducted to find the efficacy of polytherapy or combined chemotherapy versus single chemotherapy.[24] The widespread chemotherapeutic agents are anthracyclines, taxanes, and Trastuzumab. The use of anthracyclines as an adjuvant after surgery has been reported since early 1958, and these showed significant improvement in the overall survival of patients with breast cancer. Notwithstanding the database issues on using these compounds, it has already been established that they decrease the death rate among women with breast cancer. Reports in 1980 proved that anthracyclines enhanced the survival rate by up to 3% for five years and by 4% for ten years. Since then, they have been combined with Fluorouracil and Cyclophosphamide to manage breast cancer at an initial stage. The commonly used anthracyclines include Epirubicin and Adriamycin.[25] These are a lifeline for patients with both breast cancer and heart diseases who require chemotherapy.[26] Similarly, Taxanes (commonly Paclitaxel and docetaxel) are widely used to treat metastatic breast cancer. Clinical data have proven that Paclitaxel usage before the FEC (Fluorouracil, Epirubicin, and Cyclophosphamide) significantly increases the overall survival rate; however, docetaxel is more active and ensures an extended half-life time, increased cellular uptake, and intracellular retention time compared with Paclitaxel.[27] However, Trastuzumab is a drug designed to target the HER2 protein in breast cancer. It is a monoclonal IgG1 class humanized murine antibody, binding the extracellular domain of the HER2 transmembrane receptor.[28] These antibodies are always administered as co-drugs with other chemo drugs, especially to patients exhibiting a HER2-positive breast cancer type. Since 20% of patients with breast cancer are HER2+, the role of Trastuzumab is crucial; it is also reported to decrease the recurrence rate by up to 53%.[29]

2.3 Apoptosis and cancer

All the cell activities are well organized in higher multicellular organisms. The cells in this system of higher organisms are tightly controlled—both by regulating cell division rates and by controlling cell death rates. Cells activate an intracellular death program and commit suicide when they are no longer required. This mechanism is generally referred to as programmed cell death or apoptosis. Kerr, Wyllie, and Currie coined the term "apoptosis" (a-po-toe-sis) in 1972 to define a morphologically distinct mode of cell death; however, some components related to the definition of apoptosis had been specifically defined much earlier.

Cell death and cell division are perfectly balanced in adult tissues, preventing uncontrollable growth and tissue shrinkage. Cell death caused by a severe injury inevitably results in their swelling and bursting. These cells inject their intracellular contents into the neighboring cells, triggering a potentially harmful inflammatory reaction. This kind of cell death is known as "cell necrosis." On the contrary, a cell that undergoes apoptosis dies without harming its neighbors. A perfect example of apoptosis is found in people's behavior during embryonic development when they have web hands, feet, and tails; the cells that constitute those parts later undergo apoptosis. Apoptosis also occurs upon the nonreceipt of any trophic factors, such as a survival signal, or upon detecting extensive DNA damage or repair in their nucleus. Apoptosis involves five major steps after receiving its "ON" signal: Initially, the cells shrink and condense; then the cytoskeleton disintegrates; the nuclear envelope disintegrates, and the nuclear DNA fragments. After that, the cells release apoptotic bodies, the morphologic phenomena observed as blebs having small membrane-enclosed nuclear fragments. This change in the cell surface enables the dying cell to be phagocytosed quickly, either by a neighboring cell or a macrophage, until its contents leak out. This not only prevents cell necrosis but also enables the organic components of the dead cell to be recycled by the cell that consumes it (Figure 2).

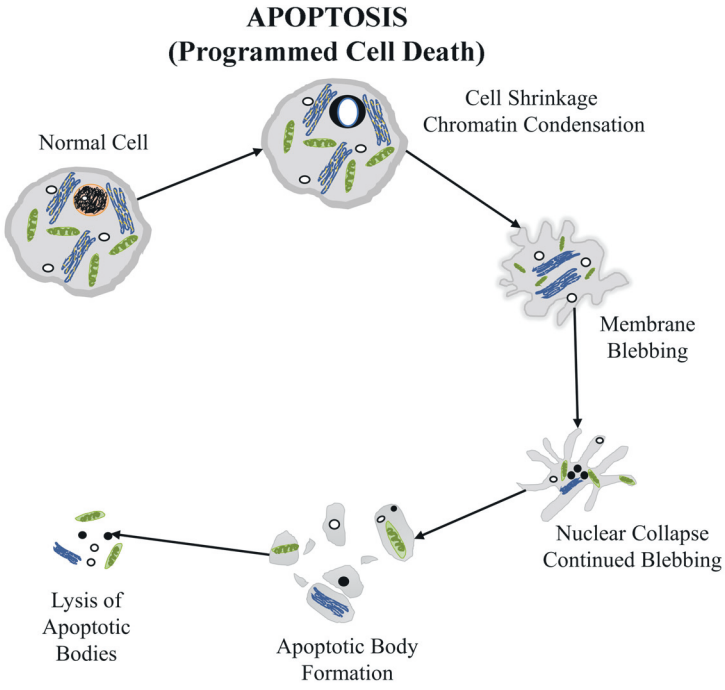

Figure 2: Morphological cell changes during apoptosis. The schematic diagram represents the various kinds of transformation of a normal cell into an apoptotic cell during apoptosis.

Apoptosis occurs either intrinsically or extrinsically. The difference is observed in the signals received by cells. The intrinsic pathway is chosen if the cell death is due to an error or aging of cells; the extrinsic pathway is selected if the cell death is due to external factors. Figure 2 illustrates the differences in signals and their molecular cascade. The death ligands bind to the transmembrane death receptors present on the cell destined to die in the extrinsic pathway. The ligand binding to the receptors on the target cell triggers receptor clustering on the cell surface. This aggregation recruits the adaptor proteins on the cytoplasmic site of the receptors, forming a death-inducing signaling complex (DISC). The formation of a DISC

brings procaspase molecules close to one another, facilitating their autocatalytic activation and releasing them into the cytoplasm, where they activate the caspase cascade. Active caspase-8 also mediates the cleavage of pro-apoptotic protein BID, which subsequently releases mitochondrial proapoptotic factors linking the two pathways. The stress signal causes the binding of cytoplasmic proteins BAX and BID to the outer membrane of the mitochondria in the case of the intrinsic pathway. Another mitochondrial protein, BAK, interacts with BAX and BID, causing the release of cytochrome c into the cytosol. This binds to Apaf-1, which later forms an apoptosome that triggers the activation of procaspase-9. Activated caspase-9 further initiates the caspase cascade, leading to apoptosis. Tumor suppressor p53 protein is a sensor of cellular stress, which plays a vital role in initiating apoptosis by transcriptionally activating proapoptotic proteins BID and BAX.

Apoptotic evasion is a major hallmark in almost all cancers. The cells have their way of preventing cancer; they achieve this by inducing their death when there is a mistake in their function. In many ways, apoptosis is inhibited by prolonging the life of the cancer cells despite an error in their DNA. This will subsequently lead to other hallmarks of cancer, such as angiogenesis progression and metastasis. The cancer cells exhibit a disruption in the intrinsic pathway of apoptosis. This includes the loss of caspase function and the deregulation of antiapoptotic and proapoptotic controls. It is found that caspases are inhibited in many cancers; the overexpression of proapoptotic breast cancer is also commonly observed.[30–32]

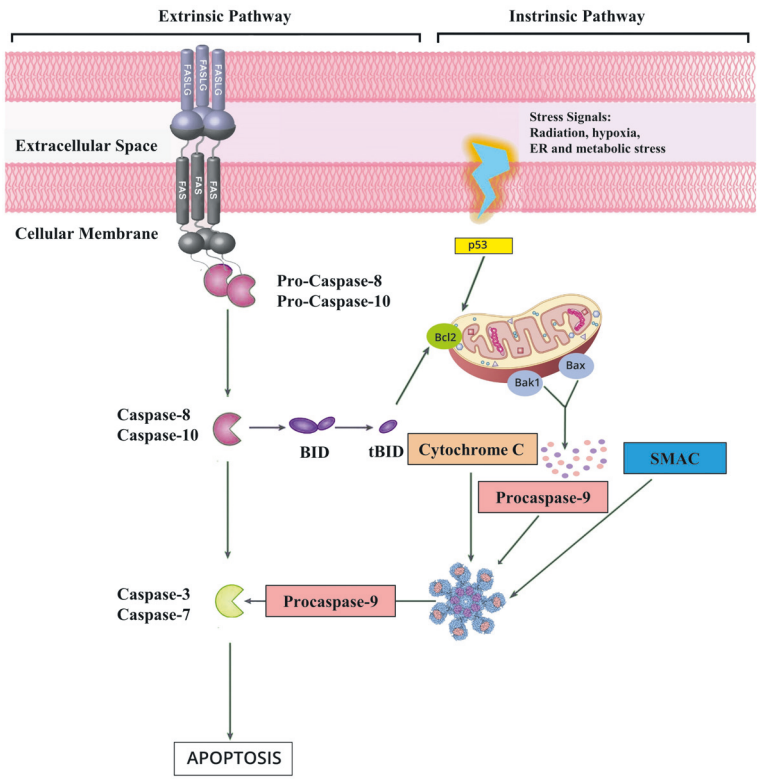

Figure 3: Extrinsic and intrinsic pathways of apoptosis, activation of initiator and executioner caspases.

A better approach for treating cancer involves inducing the cells to shift toward apoptosis rather than proliferation. This includes directly targeting molecules that target pro-apoptotic proteins or indirectly targeting other molecules that increase pro-apoptotic signals (Figure 3). Nowadays, more apoptosis-inducing anticancer drugs are being designed.

Most targeted chemotherapeutic drugs are small molecules or monoclonal antibodies that inhibit the tyrosine/serine kinases.[7,33] However, research on cancer molecular biology sheds light on many different targets such as other receptors, enzymes, cofactors, and critical molecules involved in the cell and tissue biology networks.

2.4 Drug discovery in breast cancer

Drug development is a challenging, expensive, and time-consuming process often characterized by unsuccessful attempts. Developing a marketable drug can take 12–15 years and cost more than $1 billion.

The preclinical phase of drug discovery involves the identification, validation, and optimization of the candidates. The next step involves investigating the drug molecules' efficacy and toxicity in animal models. The entire preclinical stage alone lasts six years. Clinical trials begin after receiving FDA approval under the Investigational New Drug (IND) category. According to reports, almost one-third of drugs fail to reach the first stage of clinical trials. The majority of compounds found to be nontoxic in animals have manifested toxicity in humans. Besides this, a small number of candidates fail in clinical trials because of the drug's ineffectiveness in humans; thus, the testing of substances for safety and efficacy during the early stages of drug development should be prioritized. It is beneficial to do so in a high-throughput manner because of the vast combinatorial space associated with drug candidates, testable effects, and organ systems within the human body.

Conventional drug discovery methods, which involve proteins and nucleotides, rely heavily on target recognition. The validation of such targets is needed to demonstrate a sufficient degree of confidence and to determine the pharmacological relevance to the disease under study. This can be done at all levels, from cellular to molecular to animal levels. Efficient substances such as antagonists, stimulators, or inhibitors of these targets should be listed upon completion of the target validation. The design and development of an appropriate assay to estimate the effect on the target are referred to as "lead identification." This critical step, which requires testing many chemical compounds on the target, is known as high-throughput screening (HTS). Lead compounds exhibit dose-dependent target modulation in terms of a certain degree of reliability (Figure 4). Studies are then carried out in animal models,

with the positive outcomes being refined in terms of potency and selectivity. Finally, candidates' physicochemical properties and pharmacokinetic and safety characteristics are evaluated before being selected for drug production.[34] Even though most of the processes depend on experimental tasks, *in-silico* methods are vital at any point in the drug development process.

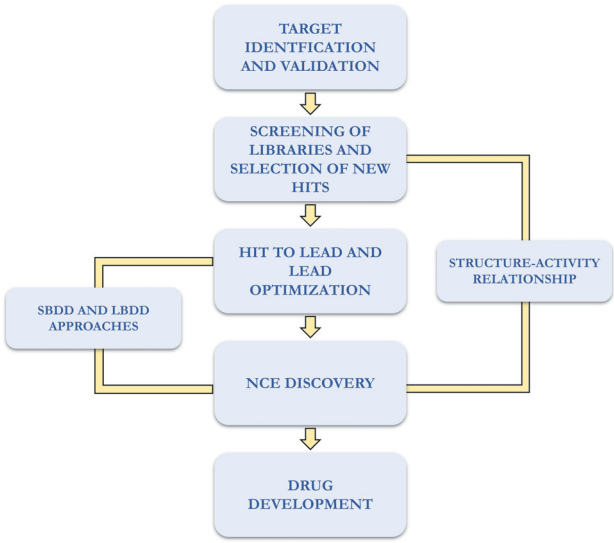

Figure 4: High-throughput screening: Flowchart elucidating the steps involved in the high-throughput screening of drugs during the Investigational New Drug Discovery process.

High-throughput screening entails identifying a lead molecule by synthesizing and analyzing lead derivatives to establish Structure-Activity Relationships (SARs), calculating physicochemical properties, and using them for lead refinement utilizing techniques such as Quantitative Structure-Activity Relationships (QSARs) (Figure 5). Modern techniques such as combinatorial chemistry combined with HTS provide many New Chemical Entities (NCEs). Still, the use of modernized equipment and the exorbitant reagent cost make these techniques highly effective. As a result, there

is a strong demand for computer-assisted techniques, which are fast, reliable, and cost-effective. [35]

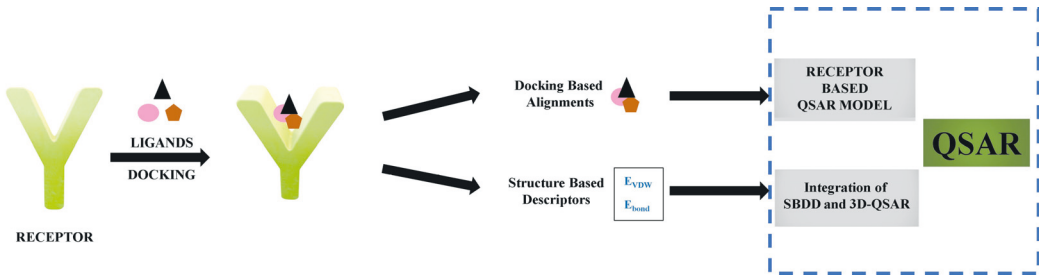

Figure 5: Representation of drug development techniques: The figure demonstrates the molecular docking-based QSAR analysis during the process of Structure-Based Drug Design (SBDD).

It is anticipated that *in-silico* techniques will play a crucial role in target and lead discovery and contribute significantly to early drug discovery. They are proposed to become a part of every drug discovery researcher's toolkit.[36]

Cell-based assays are powerful laboratory tools used during the process of drug discovery and preclinical validation. However, to date, a wide range of assays that target different cellular mechanisms has been used for anticancer drug evaluation in cells. Measuring the cytotoxicity of a drug to the cancer cells is a major step during the preclinical phase. Cytotoxicity can be measured in two ways: the toxic effect itself (cytotoxicity assays) or the effect on cell viability (viability assay). The latter is, in reality, a calculation of the number of viable cells and is inversely proportional to the cytotoxicity assay measurement (which measures cell death or destruction). Toxicity is measured in the inhibitory concentration (IC_{50}), the test substance concentration that decreases cell viability by 50% compared with untreated control cells, the median cellular cytotoxicity concentration. It is also known as cellular cytotoxicity 50% (CC_{50}) or cellular cytotoxicity inhibitory concentration 50% ($CCIC_{50}$). While using a cytotoxicity assay, the IC_{50} refers to the test substance concentration that causes 50% toxicity compared with the positive control (a cell exposed to a toxin

such as Triton X-100, which is assumed to cause 100% toxicity or cell lysis).[37] However, there is always an uncertainty in determining the effectiveness of a drug against cancer cells. This is due to the wide difference in the outcome of the experimental study performed at different time points. Thus, the cell-based assays face difficulties in reproducibility.[38]

2.4.1 Small-molecule inhibitors as cancer therapeutics

Targeted therapy denotes the design of a therapeutic drug that can kill the tumor cells specifically at the molecular level by binding to a well-defined carcinogenic target. The use of low-molecular-weight compounds (small molecules) for targeted therapy exhibits advantages over other drugs. Among the 59 new drugs approved by the U.S. FDA in 2018, 64% of those drugs were small molecules. Statistically, antitumor drugs account for 50% of small-molecule targeted drugs that are in common use. Compared with conventional cytotoxic drugs, these targeted drugs are specific to cancer cells and less toxic to normal cells. They are designed to bind to key proteins/factors involved in cell regulation, the cell signaling pathway, angiogenesis, or any carcinogenic process. These result in higher selectivity toward cancer cells, causing lower resistance and lower dosage requirements.

Many strands of research on the targeted drugs that enter clinical trials are emerging in breast cancer therapy. Among them, the following, plus another 40 kinase inhibitors, are currently used in clinical trials: epidermal growth factor receptor (EGFR) inhibitors, extracellular signal-regulated kinase/extracellular signal-regulated kinase (MEK/ERK) inhibitors, PI3K/AKT/mTOR inhibitors, poly(ADP-ribose) polymerase (PARP) inhibitors, Janus kinase (JAK)/signal transducer and activator of transcription 3 (STAT3) inhibitors, SRC inhibitors, Unc-51-like autophagy activating kinase (ULK1) inhibitors, eukaryotic elongation factor 2 kinase (eEF2K) inhibitors, bromodomain 4 (BRD4) inhibitors.

2.4.2 New molecules in targeted therapy

Phosphatidylinositol 3-Kinase (PI3K) / Protein Kinase B (Akt) /Mammalian Target of Rapamycin (mTOR) Pathway Inhibitors:

The PI3K–Akt–mTOR pathway is activated in 70% of breast cancer and contributes mainly to hormonal resistance. p110α of PI3K is the common gene mutated in breast cancer, causing its constitutive activation. The compound that inhibits the pathway successfully overcomes resistance and reduces proliferation.[39,40] A few of the latest drugs that target HER2- breast cancer include Buparlisb (in phase III trials), Pictilisib, Pilaralisib (in phase II trials), and mTOR inhibitor Voxtalisib (in phase II clinical studies).[41] Everolimus, another new drug in phase III trials against HER2+ breast cancer, is administered with Trastuzumab.

Several PI3K or Akt inhibitors are currently used in clinical or preclinical trials; however, the FDA has not approved any drug. Wortmannin is a fungal metabolite that targets the p110 subunit and is a powerful pan-specific, irreversible PI3K inhibitor. In addition, Wortmannin was observed to limit cell proliferation in various cancer cell lines. LY294002 is the first designed PI3K inhibitor that works similarly to wortmannin and has been shown to improve cytotoxicity in various cancers in preclinical tests.

PX-866 (a synthetic derivative of wortmannin) is a potent inhibitor of PI3K that interacts irreversibly with the ATP binding site. The combination of PX-866 with docetaxel in solid tumors has shown similar toxicity and promising results on entering the phase I trials in patients with breast cancer. A few other PI3K inhibitor drugs that are involved in the clinical trials in breast carcinoma include BYL719 (alpelisib), GDC-0032 (Taselisib), BAY 80-6946 (Copanlisib), and NK-1117.

BGT226 is an oral drug exhibiting dual PI3K/mTOR inhibitory activity; in a phase I trial, it is reported to be effective in patients with advanced solid tumors. BKM120, also known as Buparlisib, is a pan-class I PI3K inhibitor that inhibits class IA PI3Ks but does not affect class III PI3Ks or mTOR. BKM120 is now being explored in combination with chemotherapy or endocrine therapy in several breast cancer clinical trials.

2.4.3 Cyclin-Dependent Kinases 4 and 6 (CDK4/6) Inhibitors

CDK4 and CDK6 interact with cyclin D1 and favor cell cycle progression. The inhibitors are designed to target these kinases and arrest the cycle at the G1-S stage. Nearly 29% of patients have cyclin D1 overexpression in breast cancer and 14% exhibit amplification of CDKs. CDK4/6 inhibitors are administered along with hormonal therapy to arrest cells at the G1-S stage.[42,43] The kinase inhibitors usually inhibit the site of phosphorylation from deactivating the function of the specific protein. Recent efficient FDA-approved (in 2017) CDK4/6 inhibitors against advanced breast cancer are Palbociclib, Ribociclib, and Abemaciclib, which are used against ER+/PR+/HER2- breast cancer[44].

2.4.4 Poly (ADP-Ribose) Polymerase (PARP) Inhibitors

The PARP enzyme repairs DNA single-strand breaks, whereas the BRCA1/BRCA2 genes encode tumor-suppressor proteins that repair DNA double-strand breaks through homologous recombination. The PARP inhibitors are effective in patients with germline BRCA1/BRCA2 mutation (gBRCA+), probably by synthetic lethality from DNA damage and replication detain because of physical obstruction of DNA replication forks.[45] The PARP inhibitors or the DNA-targeting platinum drug (carboplatin) are used in combination with traditional chemo drugs in triple-negative

breast cancer. One such novel drug, Olaparib, crossed phase III trials for triple-negative, gBRCA-mutated breast cancer. The other compounds, Talazoparib and Veliparib, have not yet entered clinical studies.[46]

2.4.5 Histone Deacetylase (HDAC) Inhibitors

The deacetylation of Histone proteins mediates the loss of estrogen receptor expression in breast cancer cells. This results in hormonal resistance in the case of patients with ER+ breast cancer. The inhibitors of this HDAC enzyme upregulate the ER and aromatase expression and reduce the resistance in cancer cells.[47] Entinostat and Vorinostat are novel HDAC inhibitors that are studied as combination chemotherapies with exemestane and tamoxifen, respectively.[48]

2.4.6 Inhibitors targeting HER-family receptors

Growth factor ligands of HER-family receptors [HER1 (EGFR), HER3, or HER4] exhibit resistance to the trastuzumab. Moreover, the overexpression of HER2/HER3 heterodimers has been reported to cause trastuzumab resistance. They are more active than other heterodimers or homodimers formed by the HER family. A broader inhibition of HER-family receptors may, therefore, elicit a greater anti-cancer effect than trastuzumab alone.[49] Neratinib is an irreversible binder of HER1, HER2, and HER4 involved in the clinical development of early breast cancer cases pre-treated with other drugs and has developed resistance.[50] Apart from these, there are evolving compounds that are anti-angiogenic agents, or SRC inhibitors, and Farnesyl transferase inhibitors.[4]

The milestones of every decade are next recapitulated to summarize the development of treatments that reduce the risk of mortality that breast cancer has caused among women. A switch occurred in the 1960s from radical to simple mastectomy.

Tamoxifen was approved for metastatic breast cancer in the 1970s. Breast-conserving lumpectomy with radiation was introduced in the 1980s, making chemotherapy the standard treatment for breast cancer during the beginning stage. HER2 was also identified as an important gene in carcinogenesis during that decade. BRCA1/2 gene mutations were linked to hereditary breast cancer, and the Aromatase inhibitors were found to target hormone receptor-positive breast cancer in the 1990s. The HER2 protein therapy was incorporated during the early stage of breast cancer, and radiotherapy became more targeted toward the site in 2000. New treatments such as PARP inhibitor/immunotherapy were introduced in 2010. A major setback in handling advanced breast cancer is the resistance of breast cancer to chemo drugs. Chemo agents should be selected based on the molecular characteristics of the cancer tissue to enhance their benefits. New drugs are also essential to successfully treat many variant cases that do not respond to existing drugs.

2.5 S6K1 as a potential target for ER+ BC

S6K1 is among the most well-studied mTORC1 downstream targets that affect cell size homeostasis, protein translation, and cell proliferation. S6K1 is tightly regulated by multiple phosphorylation events that mTORC1 and PI3K mediate. This was proved by the rapamycin therapy that causes S6K1 to be rapidly dephosphorylated and inactivated.

S6K1 gets autophosphorylated frequently after phosphorylation of their four proline-directed sites in the C terminus regions. The kinases phosphorylating these sites are unknown, but ERK- and p38-MAPK are mediated in their regulation. Apart from these kinases, S6K1 is activated by PI3K-dependent Akt, PKCζ, and λ, and the small G proteins Rac1 and Cdc42.

S6K1 also controls cell proliferation by regulating G1/S cell cycle progression. Thus, the overexpression of S6K1 is also studied as a marker for proliferation in neoplastic transformation. This overexpression and activation of S6K1 are due to the frequent mutations of its upstream signal proteins of the mTORC1 pathway, including PIK3CA, PTEN, AKT, PDK1, and TSC1/2.

Many studies reported that the mTORC1/S6K1 pathway and ERα signaling have a close relationship. The stimulation of ERα signaling even in the absence of a ligand is known to cause endocrine resistance. This was caused by the hyperstimulation of the mTORC1 signaling pathway, which can be reversed *in-vitro* by the mTORC1 inhibitor everolimus. S6K1 is the key activator of ERα inducing proliferation in ER+ breast cancer. Some reports point to S6K1 activation as the cause of poor prognosis in ER+ tumors and are not related to ER- patients. This makes them a potential therapeutic target in ER-positive breast cancer.

The data support the following three reasons to target S6K1: (1) 17q23 amplification is one of the most common abnormalities in ER+ invasive ductal carcinoma and closely corresponds with ER-positive status. S6K1 hyperactivation is also caused by several other common breast cancer mutations that cause abnormal expression and activation of IGF-1R, ErbB2, FGFR, PIK3CA, PTEN, and Akt1/2. (2) RPS6KB1 has been identified as a gene associated with the ability of tumors to spread in ER+ breast cancer. Furthermore, the activation of S6K1 in ER+ tumors (not in ER-) was associated with a worse prognosis and the development of endocrine resistance. (3) The genomic and non-genomic co-stimulatory correlation between ER and S6K1 could explain RPS6KB1 amplification and S6K1 overexpression in ER-driven breast tumors.

Maintaining significant co-overexpression of S6K1 and ER in breast cancer cells may thus give them a selection advantage and contribute to uncontrolled cell proliferation during carcinogenesis and breast cancer progression. Finally, in a genome-wide

screening for crucial kinases for MCF7/LTED cell development (ER+ cells chosen after long-term estrogen deprivation), S6K1 was found as a significant contributor.

2.6 Future treatment and its scope

Despite the remarkable achievements in therapies in the recent past, chemotherapy has undesirable effects. These include the drugs that kill normal cells and cancer cells, cancerous cells exhibit multidrug resistance, and the drug causes toxicity at the dosage level.

There is an urgent need to find new and effective targeted treatments based on the tumor cells' molecular biology changes. Many novel drugs make their appearance on the healthcare horizon; these drugs can obstruct transduction pathways and induce the death of cancer cells through apoptosis and stimulation of the immune system or potentially deliver chemotherapeutic agents to cancer cells.

New drug development is encouraged by the expedition process for approval by the Accelerated Approval Program, cohort expansion trial design, and tumor-agnostic mutational drug indications.[51] This would favor progress in precision medicine to treat advanced breast cancer. Despite rapid advances in medicinal science and improved regulatory processes, which allow patients to get from bench to bedside in three to five years, chemotherapy remains a significant component of solid tumor and hematologic malignancy treatment today. It is assumed to remain constant for many years.

The current arsenal of chemotherapeutic treatments, while successful, poses its own set of patient-centric issues because the agents influence the quality of life, limited efficacy, and potentially lethal side effects.[52] Traditional systemic cytotoxic drug research should not be abandoned owing to those challenges and the explosion in

targeted and immunologic therapy approvals accompanied by the assumption of the extension of a number of limitations of the ongoing research. The end of chemotherapy is not foreseeable, as it will continue to play a critical life-saving role in treating breast cancer and several other common cancers in the near future, if not decades. More study is needed to evaluate the comparative effectiveness based on previously approved chemotherapeutic drugs and investigate new agents with a significant emphasis on the patient.

2.6.1 Synthetic compounds in breast cancer

The FDA-approved synthetic compounds against breast cancer include fulvestrant, lapatinib, eribulinmesylate, pertuzumab, everolimus, etc.[53] Many new synthetic compounds are emerging as anticancer agents. However, they are still in different clinical phases of drug development. The major synthetic drugs would certainly contain one common functional group and are known to have biological activity. A few of them are highlighted next based on their functional groups.

First, quinoline and quinazoline derivatives are a class of aromatic compounds that are widely studied in anticancer screening.[8] Many compounds with these functional groups are reported in recent research and show promising cytotoxic potential against breast cancer cells. The 4-(imidazolylmethyl) quinoline derivative was reported to have an IC_{50} value of less than 5μM and was found to inhibit COX-2 in MCF-7cells.[54] Similarly, N-piperazinyl quinolone derivatives were found to have IC_{50} values of 2 to 10μM in different breast cancer cell lines.[55]. Chlorophenyl-quinazoline derivatives synthesized by a research group have also exhibited a very low IC_{50} value compared with doxorubicin.[56] Two oxazolo-quinazoline compounds were analyzed in the Skbr3 cell line; they exerted significant cytotoxic potential by inhibiting EGFR and HER2 receptors.[57]

Pyridine and pyrimidine rings with various functional group modifications have also been proved to exhibit various biological properties. A study published on hexahydropyridone derivatives and their anticancer activity was comparable to 5-fluorouracil *in-vitro*. A novel series of pyrimidine compounds was documented in which chemically synthesized compounds exhibited good cytotoxicity in MDA-MB-231 by inhibiting Src kinase activity and blocking the MAPK signaling pathway.[58]

Nevertheless, Imidazole and its derivatives are a group of compounds exhibiting potent anti-breast cancer activity. A few exhibited agonist activities against the Estrogen receptor, which is significant in the metastatic and advanced stages of breast cancer. These compounds are also various other groups of synthesized compounds effective against breast cancer and produce encouraging results against cell lines *in-vitro*.[59]

2.6.2 Phenolic derivatives in breast cancer

The phenolic derivatives are a group of compounds with multiple known biological activities. Phenolics are primarily extracted from natural sources, especially plants.[60] Secondary metabolites such as tannins, flavonoids, and coumarins are all phenolic compounds.[61] These compounds are extensively examined and demonstrated to possess good antioxidant and anti-inflammatory properties.[62] This allures the researchers toward choosing them for an in-depth study against various cancers. It was documented by multiple research groups that the phenolic compounds can arrest the cell cycle and cell growth, reduce oxidative stress, upregulate the expression of tumor suppressors, and inhibit many signaling pathways that play a vital role in cell proliferation, apoptosis, and angiogenesis.[13] For instance, hydroxybenzoic acids,[63] protocatechuic acids, gallic acids,[64] ferulic acid,[65], and cinnamic acid[66] isolated from multiple plants show cytotoxic activity against breast cancer cell lines.[64]

Based on natural sources, hundreds of synthetic phenol compounds were designed and derived to enhance the pharmacological properties and overcome the demerits of natural phenol derivatives. The Indole ring-containing compounds are also reported in recent literature to have many pharmaceutical activities, such as anti-virus, anti-inflammatory, and even anticancer activity. A novel group of indole-9, 10-dione derivatives were synthesized and reported to have Human Casein Kinase II (CK2) inhibiting properties.[67] A few series of indole alkaloid meleagrin derivatives were documented to have a low IC_{50} value in five breast cancer cell lines and are c-Met inhibitors, resulting in cytotoxic effects in breast cancer cells.[68]

Aminophenol analogs are another group of phenolic compounds reported to have anticancer potential against various cancers. The p-alkylaminophenols and p-acylaminophenols synthesized by researchers inhibited cell growth in human leukemia cell lines.[69] They have shown that the inhibitory potential was imposed by preventing lipid peroxidation. A similar group of amino phenols, 3,5-dimethylaminophenol, was designed, synthesized and found to have an anti-tumorigenic property in non-small cell lung cancer by inducing apoptosis and promoting cell cycle arrest.[70] Another strand of research has derived aminophenol substituted compounds showing anticancer potential in the liver cancer cell line. The cytotoxicity was comparable to doxorubicin and a docking study against EGFR, for instance, a repeat of the lipoprotein receptor. Fenretinide (N-(4-hydroxyphenyl) retinamide-based analogs were synthesized and reported to have anticancer potential against many cancer cells, including the MCF-7 breast cancer cell line.[71]

3 MATERIALS AND METHODS

3.1 Synthetic phenolic compounds used in the study

Phenolic compounds have been reported to possess potent antioxidant activity. They have anticancer or anticarcinogenic/antimutagenic, anti-atherosclerotic, antibacterial, antiviral, and anti-inflammatory properties to a greater or lesser degree extent.[62,72–75] Phenolic compounds have preventive effects on tumor initiation through numerous mechanisms, such as the avoidance of genotoxic molecule formation, the blockade of mutagenic transforming enzyme activity, the regulation of phase I and II enzymes, such as cytochrome P450s (CYP), and S-transferase (GST), and the prevention of DNA damage.[76]

Phenolic compounds play a key role in breast cancer cells. These compounds inhibit cancer progression by regulating the genes responsible for the growth and development of the tumors. Three different compounds are synthesized and treated against breast cancer cell lines. The indoline compounds named as N-(2-hydroxy-5-nitrophenyl (4'-methyl phenyl) methyl) indoline (HNPMI), Alkyl amino phenolic compound 2-((3,4-Dihydroquinolin-1(2H)-yl)(p-tolyl)methyl)phenol) (THTMP) and 2-((1, 2, 3, 4-Tetrahydroquinolin-1-yl) (4 methoxyphenyl)methyl) phenol (THMPP) are examined (Figure 6).

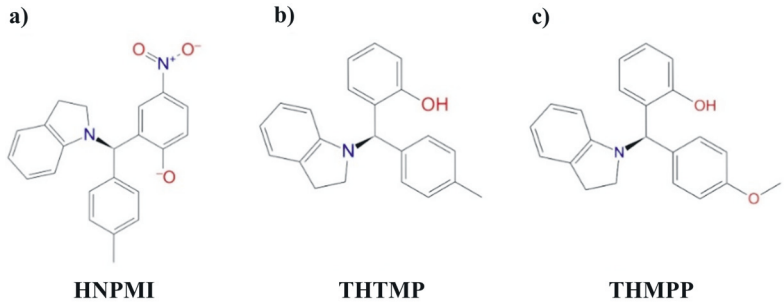

Figure 6: Chemical structure of HNPMI, THMPP, and THTMP.

3.2 *In-vitro* analysis of the selected compounds in breast cancer cells

3.2.1 Cell lines used

Three cell lines were used for the *in-vitro* study to investigate the anticancer properties of the synthetic compounds, where MCF-7 and SkBr3 are breast cancer cell lines and H9C2 is a normal cardiomyocyte cell line (Publications I, II, and III).

MCF-7 cells are the most common cancer cell line used to study breast cancer; these were established in 1973 at the Michigan Cancer Foundation.[77] MCF7 cells are an ideal model to study the hormone response since they express the estrogen receptor on their surface (ER+).[78] The most important signaling pathway that promotes cell survival and cell proliferation, the PI3K/AKT/S6K1/mTOR signaling pathway, is continuously overexpressed in the MCF-7 cell line.[79] The two growth factor receptors that play a vital role in breast cancer cells are Epidermal Growth Factor Receptor (EGFR) and Human Epidermal Growth Factor Receptor-2 (HER-2); these are present in MCF-7 cells.[80] Chemotherapy treatment has increased the rate of autophagy level in MCF7 compared with MDA-MB231.[81]

SkBr3 are breast epithelial cells derived from metastatic sites isolated by G. Trempe and L. J. Old in 1970 from a patient's pleural effusion cells.[82] The Her2 (Neu/ErnB-2) gene product is always overexpressed in the human breast cancer cell line SkBr3.[83] The signaling pathway ErbB2/ER-PI3K-Akt-mTOR-S6K1 exhibits an abnormal effect after being treated with Sulforaphane (SFN) in SkBr3 cell lines.[84] A shift in drug susceptibility has been caused by the overexpression of EGFR in the SkBr3/EGFR clone.[85] ATRA induces autophagic flux through RARα in retinoid-sensitive SkBr3 breast cancer cells.[86]

H9C2 is a normal myoblast, non-cancerous cell that this study used as normal control.[87] Small-molecule inhibitors showed that H9C2 cells have a high EGFR expression level and inhibit EGFR activation.[88] Trastuzumab-emtansine (TDM1), a novel antibody-drug conjugate, showed a stronger effect than Pertuzumab in H9C2 cardiomyoblast cells.

MDA-MB231 are epithelial cells of the human breast cancer cell line. These cell lines are derived from the pleural effusion of the metastatic mammary adenocarcinoma patients. The cell line lacks estrogen receptor (ER) expression, progesterone receptor (PR) expression, and HER2 amplification[89]. Tetrandrine has been reported as a promising anti-triple negative breast cancer drug that inhibits the PI3K/AKT/mTOR pathway by inducing autophagy on the MDA-MB231 cell lines[90].

3.2.2 Cell culture and maintenance

All cell lines (MCF-7 cells, SkBr3 cells, H9C2, and MDA-MB231) were cultured in Dulbecco's Modified Eagle Medium, high glucose (DMEM, Catalogue # L0102, Biowest). The complete media consisted of DMEM supplemented with 10% Fetal Bovine Serum (FBS, Product # F1051, Sigma-Aldrich, St Louis, MO), 1% Antibiotic

(Penicillin–Streptomycin) (Product # P4333, Sigma-Aldrich, St. Louis, MO), and antimycotic reagent Amphotericin B (Sigma-Aldrich, St. Louis, MO). The cells were grown on tissue culture-coated plasticware. The cells were incubated at 37°C with a 5% CO2-supplied incubator. They achieved a split ratio of 1:3 when they reached 70–80% confluence.

3.2.3 Cytotoxicity assay

The toxicity of compounds can be determined by using different methods. The MTT assay, rather than the trypan blue staining method, is the better assay to predict toxicity in cancer cells; this is mainly because the MTT method is preferred when the cells are rapidly dividing. The 3-(4,5-dimethylthiazol-2-yl)-2,5-diphenyltetrazolium bromide (MTT) is a yellow-colored tetrazolium dye reduced to an insoluble formazan crystal, which is purple. The principle of the MTT assay is that the live cells contain NAD(P)H-dependent oxidoreductase enzymes that reduce the MTT dye and form a purple color. Thus, the intensity of the purple color indicates the number of viable cells. The toxicity is calculated from the cell viability percentage.[91,92] The cytotoxicity of the three compounds THMPP, THTMP, and HNMP1 against MCF-7 cells and SkBr3 cells was measured in five different concentrations after a 24-h treatment.

The procedure followed was as stated by Mosmann et al. The cells were plated in 96-well flat-bottom tissue culture plates at a cell density of 1.2 × 104 cells/well and were allowed to adhere overnight at 37°C. Different concentrations of the drugs (10, 25, 50, 75, and 100μM) were added to the cells and incubated for 24 h. After the incubation, 100μl of fresh medium was added with 10μl of MTT (5mg/ml) and left undisturbed for four h. The spent medium was discarded, and the formazan crystals formed were solubilized using DMSO (100 μl). The purple color thus formed was

measured at 570nm.[93] Cyclophosphamide was used as a positive control, and the cells with the medium (untreated) served as a negative control.

Cell survival was calculated by the following formula:

Percentage of viable cells = $(OD_{Test} / OD_{Control}) X 100$

Cytotoxicity % = 100 – Viability percentage

The MTT assay was performed in MCF-7, SkBr3, and H9C2 cells to understand the cytotoxic effect of the three drugs in breast cancer cells. This also helps to determine the IC_{50} value of the drugs against breast cancer cells.

3.2.4 Determination of apoptosis induction

The evasion of apoptosis is one of the major hallmarks of cancer. A drug that can induce programmed cell death in cancerous cells can effectively prevent the further spread of the tumor.[94] Thus, four different assays have been performed to determine a drug's potential to induce apoptosis.

3.2.5 CASPASE Quantification Assay

Caspases are a group of enzymes involved in apoptosis, and they belong to the cysteine proteases family. They are formed as procaspases, which are activated after cleavage to caspases.[95] The cleaved caspases, in turn, lyse many downstream proteins and other caspases, ultimately leading to cell death.[96] Of the 12 existing caspases, a few are not involved in the apoptosis mechanism. Two important caspases that play

a major role in the initialization and execution of apoptosis are caspase three and caspase 9, respectively.[97]

The activities of caspase-3 and caspase-9 were measured by the colorimetric assay kit, following the manufacturer's protocol (Calbiochem, Merck). In this method, a labeled substrate (DEVD-pNA for caspase three and LEHD-pNA for caspase 9) is used, which produces a chromogenic p-nitroaniline (pNA) that can be measured spectrophotometrically. The basic principle of this method is that the caspases cleave the substrate to produce a pNA-forming color.[98] Thus, the intensity of the color formed is found to be proportional to the caspases present.

MCF7 and SkBr3 cells were cultured in 96-well plates and treated with the drugs at their respective IC_{50} concentrations. The protein content was initially measured by using the Bradford method of protein estimation.[99] Approximately 200 μg of protein was incubated in 96-well plates with 5 μL of the substrates for 2 h at 37°C. The activities of caspase-3 and caspase-9 were analyzed by measuring the cleaved substrate to free pNA at 405 nm in a microplate reader. The relative level of caspase-3 and caspase-9 was quantified using the absorbance ratio of treated to untreated cells.

3.2.6 DNA Fragmentation Assay

Caspase's action activates DNases or endonucleases, resulting in DNA cleavage inside the nucleus to form nucleosomal fragments of 180bp length.[100] Thus, DNA fragmentation is an important marker for apoptosis in the cell; the DNA laddering or fragmentation assay is used to determine apoptosis. The capacity of the drug in apoptotic induction is examined indirectly by observing DNA fragmentation using electrophoresis. The MCF7 cells were treated with the drugs and subjected to agarose gel electrophoresis.

MCF-7 cells were briefly lysed using a cell lysis buffer, and the debris was removed by centrifugation. The supernatant was mixed with an equal proportion of phenol, chloroform, and isoamyl alcohol to elute DNA from the cell. The DNA was then precipitated using 3.5 M ammonium acetate and ice-cold isopropanol during the aqueous phase, and it was incubated at a cold temperature. The pellet with DNA was washed with ethanol and stored in TE buffer for further use. The DNA samples were electrophoresed in a 2% agarose gel (w/v) at 50 V The DNA was detected under UV light using EtBr staining and a 1 kb DNA ladder as a control.[101]

3.2.7 Annexin V/Propidium Iodide Staining

Annexin V is a phospholipid-binding protein that has a high affinity to phospholipid phosphatidylserine (PS). PS is located on the inner cytoplasmic surface of the plasma membrane under normal cellular conditions; however, the PS is translocated to the outer/extracellular side of the plasma membrane in apoptotic cells. The principle behind this experiment is as follows: Annexin V stains PS and enables the detection of the location of PS, and this is conjugated to give green fluorescence.[102] Propidium Iodide (PI) is a red nuclear stain that detects dead cells and is impermeable to live cells. Thus, cells showing green fluorescence are apoptotic; those showing red fluorescence are dead cells. Live cells show no fluorescence. The emitted fluorescence is detected and analyzed by using FACS.

The breast cancer cells MCF-7 were treated with the selected three drugs (THMPP, THTMP, and HNPMI) at their IC_{50} concentration. After 24 h of treatment, 5 µl of FITC Annexin V and 5 µl PI were added to the cells and incubated for 15 min at 25° C in the dark. These were then subjected to flow cytometry analysis.[103] All of the measurements were checked in one hour using the same equipment settings.

3.2.8 Acridine Orange/Ethidium Bromide (Ao/EtBr) Staining

AO/EtBr staining is a microscopic technique performed to substantiate Annexin V/PI staining procedures. The apoptotic cell changes observed in the plasma membrane result from the staining by dyes differentiating the early apoptotic cells, late apoptotic cells, live cells, and necrotic cells observed under a fluorescence microscope. Early apoptotic cells are marked with yellow-green color and are stained by AO; late apoptotic cells are found with orange nuclei and are stained by EtBr; necrotic cells exhibit an uneven orange-red fluorescence at the periphery.[104]

MCF-7 cells were cultured and treated with different drug concentrations for 24 h. In a staining solution, they were collected in PBS and stained with a 1:1 mixture of 100mg/ml AO and 100mg/ml EB. A fluorescence microscope was used to observe the cell suspension (10ml) using a blue (420–495 nm) and green (510–560 nm) filter, and at least 300 cells/well were used for quantification in different fields.[105]

3.2.9 Gene expression analysis

The genes associated with carcinogenicity are studied to identify the potential of the drugs in treating breast cancer. The hypothesis that the drugs have an apoptotic induction property led to the investigation of the capability of the drugs to alter the expression of the genes involved in the EGFR-regulated pathway. The major targets studied were PI3K, S6K1, and EGFR genes. The gene expression analysis further leads to examining the change in the functional genes expressed in the cancer cells before and after drug treatment. The RNA is isolated from the cells and converted to cDNA using a reverse transcriptase enzyme to study the expression levels. The

cDNA thus formed is subjected to PCR analysis with specific gene primers. Thus, the PCR product formed will be the only gene of interest, which can then be used to compare samples using agarose gel electrophoresis. In this research, a one-step RNA reagent and synthesized cDNA were used with EasyScript Plus™ Reverse Transcriptase primed using oligo-dT.[106] For PCR amplification, primers specific for EGFR, PI3K, and S6K1 were designed (Table1) and used. The PCR reaction was set up with appropriate Ta for each gene, and it was performed under the conditions mentioned in the table. The gene products thus formed were visualized after running electrophoresis in 1.5% agarose gel. The band intensity was calculated by using ImageJ and then compared between the treated and untreated cells.

Table 1: PCR primer sequences, thermocycling conditions, and T_a of the respective genes

Gene	Primer Sequence (5'-3')	Thermocycling Conditions	T_a
EGFR	TCCCCGTAATTATGTGGTGACAGATC ACCCCTAAATGCCACCGGC	94° C for 2 min (94° C for 30 s, T_a for 1 min, 72° C for 1 min 20 s) x 32cycles, 72° C for 7 min	56° C
PI3K	AACACAGAAGACCAATACTC TTCGCCATCTACCACTAC	94° C for 2 min (94° C for 30 s, T_a for 1 min, 72° C for 1 min 20 s) x 32cycles, 72° C for 7 min	54° C
S6K1	CACATAACCTGTGGTCTGTTGCTG AGATGCAAAGCGAACTTGGGATA	94° C for 2 min (94° C for 30 s, T_a for 1 min, 72° C for 1 min 20 s) x 32cycles, 72° C for 7 min	56° C
β-ACTIN	CACCCGCGAGTACAACCTT CCCATACCCACCATCACACC	94° C for 2 min (94° C for 30 s, T_a for 1 min, 72° C for 1 min 20 s) x 32cycles, 72° C for 7 min	54° C

3.3 *In-silico* analysis of the selected compounds in breast cancer cells

3.3.1 QSAR Modeling

A Quantitative Structure-biological Activity-property Relationship (QSAR) approach was performed to quantitatively depict and provide mechanistic insights into interactions between the chemical structure of drugs by considering the compounds with similar structures.[107] QSAR is a method for determining the interaction between a compound's molecular descriptors and its biological activity.[108] In this study, 32 molecules with significant structural similarities to the drugs were examined. In addition, the literature also explored biological activity in terms of IC_{50} (Table 1). The descriptors of the compounds are calculated using the Dragon software, which has 1497 descriptors sorted into 18 groups. A total of 18 descriptors were discovered for each molecule in the training set. A set of descriptors that were the most appropriate to the IC_{50} of the compounds was selected for further analysis, the MLR models were built, and QSAR equations eliminating the variables were established with the use of BUILDQSAR software.[109]

3.3.2 *In-silico* analysis of the interaction of drugs with EGFR

The earlier experimental data clearly shows that the drugs exhibited good antiproliferative activity and induced apoptosis in breast cancer cell lines. Therefore, a combined computational analysis was performed with EGFR as the target protein following the gene expression studies.

For more than three decades, computational drug discovery or drug designing methods have been the key tools in developing therapeutically important small molecules. Many such drugs are on the market, and many more are in clinical trials designed and synthesized after computational screening methods. Among the various computational analysis methods, structure-based drug design is the most important because the structural information of the target and the ligands is well known. This method can be used either to screen the best compound among a group of compounds or to understand the interaction of the known drug with a particular molecular target. Here, the protein of interest is the target molecule, and the compounds (drug candidates) are called ligands. Structure-based approaches include molecular docking, pharmacophore, and ligand design methods.[110,111]

EGFR has been chosen as the protein target in this study, and the synthesized compounds HNPMI, THTMP, and THMPP have been chosen as the ligands. The structure of Gefitinib, a well-known drug for breast cancer and a potent inhibitor of EGFR, is used as the positive control (standard) for all the computational analyses.[112] A combined approach has been employed, including QSAR, ADME/Tox prediction, Molecular Docking, MM-GB/SA, QM/MM analysis, and molecular dynamics simulation to understand the protein-ligand interactions. To study the Protein-ligand interaction computationally, the following tools are used: Maestro, Qikprop, Prime, Glide, LigPrep, and Phase software of Schrödinger Inc (Schrödinger Release 2020-4), New York, USA.

3.3.3 Protein and ligand structures

The receptor tyrosine kinases family includes EGFR, which is a transmembrane protein. It mediates cell proliferation, apoptosis, angiogenesis, and metastasis in many cancers by mediating various signaling pathways, including PI3K-AKT-mTOR, JAK-STAT, and ERK–MAPK pathways. EGFR is one of the most

common molecules altered in cancers and is mostly overexpressed. The two domains of the EGFR protein are the tyrosine kinase domain and the ligand (EGF) binding domain.[113–115]

The three-dimensional crystal structure of the Epidermal Growth Factor Receptor (EGFR) protein was retrieved from the RCBS PDB database. The PDB ID chosen was 1M17, the three-dimensional structure of the tyrosine kinase domain of human EGFR. The uniport database shows that the total EGFR protein (ID: P00533) constitutes 1210 amino acid residues, of which 1M17 covers 333 residues, from 695 to 1022, representing the tyrosine kinase domain. The structure is determined by the X-ray diffraction method at an atomic resolution of 2.60 Å; it is deposited as a complex with a ligand. The 3D structure was downloaded as a PDB file, and the bound ligand was removed. It was then energy minimized by using Protein Preparation Wizard.[116] This is a promising step in molecular modeling, which would optimize the protein structure and ensure the best final structure. This was used as the target structure for all the forthcoming analyses.

Similar to the target structure, the structures of synthesized ligands were drawn by using Chemdraw. Then, the Ligprep tool was used to convert them to their three-dimensional structures, generate tautomers for each ligand, and optimize and neutralize the charge on the ligands.

3.3.4 ADME/TOX Analysis

The ADME/Tox (absorption, distribution, metabolism, and excretion/ Toxicity) analysis was carried out using the QikProp program. Qikprop accurately predicts physically significant descriptors and indicates the pharmaceutically relevant properties of organic molecules. This tool examines around 50 biological descriptors with relevance to drug likeliness.

3.3.5 Molecular docking

The interaction of the ligands with the EGFR kinase domain (1M17) was established through molecular docking. Docking is used here to predict the binding affinity between the compounds and EGFR. It also provides a target-ligand complex structure that will be valuable for lead optimization. In addition, the docking results will provide insights into the interaction of the ligand to the target protein at their specific active site. The interactions between the target and the ligand mainly include hydrogen bond interactions, hydrophobic interactions, van der Waals force, pi stacking, etc.

The Glide software contains three different modes of docking: rigid, flexible, and extra precision (XP). Among them, the ligand is kept flexible and provides the elimination of false positives in Glide XP mode. The key active site residues (Lys 721, Ala 719, Ile 720, Glu 738, Met 742, Leu 753, Ile 765, Thr 766, Gln 767, Leu 768, Leu 820, Gly 772, Leu 694, Asn 818, Asp 831, Phe 699, Val 702, and Met 769)[117] were confined, and a protein grid box of size 10 Å × 10 Å × 10 Å was defined. The Glide score function used here is a more sophisticated version of ChemScore with force field-based components and additional terms accounting for solvation and repulsive interactions. The best binding pose is made by using a model energy score (Emodel) that combines the energy grid score, Glide score, and the internal strain of the ligand.[118]

3.3.6 Molecular Mechanics / Generalized Born Surface Area (MM/GBSA) Analysis

MM-GB/SA (Molecular mechanics-generalized-Born/surface area) was calculated to estimate the binding free energy of ligand-protein complexes. The

output file of XP docking was provided as an input for the MM-GB/SA tool of the Prime module.[119] The docked poses were energy minimized using the OPLS-AA (2005) force field, and the energies of the protein-ligand complexes were calculated using generalized-Born/surface area (GB/SA). The free energy binding affinity (ΔG bind) was calculated as follows:

$$\Delta G_{bind} = \Delta E + \Delta G_{solv} + \Delta GSA$$

where E, Gsolv, and GSA represent the minimized energy of the protein-ligand complex, solvation free energies, and surface area energies; the delta represents the difference in energy between the protein-ligand complex, protein, and that of the ligand.

3.3.7 e-Pharmacophore Mapping

E-pharmacophores were implemented to screen the molecules further obtained from the initial docking of the selected compounds. Based on the protein-ligand structural information, a hypothesis will be computed by imposing Glide XP energy properties over pharmacophore sites. An e-pharmacophore map was generated from the ligands by using Phase software. The pharmacophore sites were developed automatically based on the default settings applied for refinement and scoring. The map includes chemical features such as hydrogen bond acceptor (A), HB donor (D), hydrophobic (H) region, positive ionizable (P), negative ionizable (N) atoms, and aromatic ring (R). Each of the pharmacophore feature sites is assigned with an energy value equal to the sum of XP contributions of the atoms comprising the sites, which allows sites to be ranked based on the energy values obtained.[120]

3.3.8 Quantum Mechanics / Molecular Mechanics QM/MM Methodology

The QSITE program can study the geometries and energies of structures by combining Quantum Mechanics (QM) and Molecular Mechanics (MM). It was used for QM/MM calculations. QSITE constructs the interface between QM and MM regions by utilizing the frozen localized molecular orbitals along with covalent bonds. The Density Functional Theory (DFT) method determines the molecular electronic properties, such as electron density, highest occupied molecular orbital (HOMO), and lowest unoccupied molecular orbital density (LOMO), to predict the biological activity and molecular features of compounds plays a significant role in representing the QM region, SPC is calculated at each configuration, and the outputs are analyzed. The optimization of the QM wave function is carried out by integrating the MM point charges, which are accountable for the polarization of the ligand charge distribution.[121]

3.3.9 Molecular Dynamics: Simulation

The macromolecules in the cells including proteins are in highly dynamic state in a solution state when a drug or any other molecule interacts with it. However, the docking algorithms mostly assume the target structure is a single static structure. Thus, the drug can naturally be bound to a particular region and stabilize only a subset of many conformations sampled by its dynamic receptor, causing the population of all possible conformations to shift toward those that can best accommodate binding. In addition, the ligand may further impact conformational changes that are not typically sampled when the ligand is absent on binding. Nevertheless, receptor emotions play an essential role in the binding of most small-

molecule drugs. Molecular dynamics simulations can provide information about these motions.

In Schrödinger software, the Desmond module was used to perform the molecular dynamics simulation for the protein-ligand complexes such as EGFR-HNPMI, EGFR-THTMP, and EGFR-THMPP (1M17-EGFR). The protein and ligand are prepared for simulation by applying the OPLS 2005 force field in the protein preparation wizard. Docked complexes were embedded in the TIP3P (Transferable Intermolecular Potential 3P) water model. The system specified periodic boundary conditions, the Particle Mesh Ewald (PME) method for electrostatics, a 10 A° cutoff for Lennard–Jones interactions, and the SHAKE algorithm for limiting the movement of all covalent bonds involving hydrogen atoms. With the addition of Na+ and Cl-ions, the system was neutralized. At first, a relaxation simulation was run with an NPT ensemble at 300K temperature and 1 bar pressure to relax the system. Then, for every 8.4 ps, trajectories were recorded. Berendsen thermostats and barostats were used to control the temperatures and pressures during the initial simulations.

Furthermore, a 100 ns unrestrained production run with an interval of every 1.0 picoseconds was carried out. The temperature was set to 300K during the production run. It was constantly maintained by invoking the Nose–Hoover thermostat with the pressure set to 1 atom, maintained through the Martyna–Tobias Klein pressure bath. Each trajectory's RMSD of complex and protein-ligand interactions was plotted against time. The Root Mean Square Deviation (RMSD) was used to analyze the stability of EGFR drug complexes, while the Root Mean Square Fluctuations were used to assess the system's adaptability (RMSF)[122].

4 SUMMARY OF RESULTS

This chapter summarizes the study's results that are published as four research articles. The potential of the three synthesized compounds - THMPP, THTMP, and HNPMI - against the growth of the cancer cells was studied in two different breast cancer cell lines: MCF-7 and SkBr3. The induction of apoptosis in cancer cells caused by these compounds was examined and reported in multiple ways. The mechanism of these compounds as anticancer drugs was evaluated at the molecular level, specifically in the EGFR-mediated pathway. The interaction of the compounds with the key oncogenic protein EGFR and their subsequent alterations in the expression of PI3K and S6K1 genes were observed. The results of each compound are cited in the different publications.

Publication 1 reports the effect of THMPP in breast cancer cells. Experiments showed that the THMPP has significant cytotoxic potential in MCF-7 and SkBr3 cells. The metabolic activities of the cells measured by using the MTT assay indicated that there is dose-dependent cytotoxicity in cancer cells when treated with THMPP. From the treatment of cells with 10–100 μM THMPP, the IC_{50} concentration was 83.23 μM in MCF-7 and 113.94μM in SkBr3 cells (Figure 7a). Apart from this, THMPP was less toxic with a higher IC_{50} value after 24 h of treatment in non-cancerous H9C2 cells. The induction of apoptosis by THMPP was examined and described next.

The apoptotic mechanism is induced in cells when there is a defect in DNA or a mistake in the DNA strand that the cell's DNA repair mechanism cannot repair. The endonucleases break down the DNA strands to small nucleotides (size ranging in

multiples of ~180bp length) and are packed in apoptotic blebs upon identifying such defective DNA. However, apoptosis is inhibited in cancer cells, and the cells continue to proliferate with defective DNA. Hence, DNA fragmentation is not observed in cancerous conditions of the cell. The apoptotic enzymes, namely caspases, are downregulated in cancer cells for many reasons, such as a mutation in epigenetic regulatory modulators such as p53. Among the 12 caspases reported, initiator caspase (caspase 9) and executioner caspase (caspase 3) play a major role in apoptosis's extrinsic and intrinsic pathways. Therefore, these two enzymes are often dysregulated in cancerous conditions, leading to inhibition of apoptosis.

The cancer cells MCF-7 and SkBr3 exhibited meager activity of the apoptotic enzymes caspase-3 and caspase-9, agreeing with these discussions. The treatment of the cells with THMPP led to a 0.17-fold increase in the level of caspase-3 in MCF-7 cells and a 0.47-fold increase in SkBr3 cells. Similarly, the treatment of the cells with THMPP led to a 0.07-fold increase in the level of caspase-9 in MCF-7 cells and a 0.25-fold increase in SkBr3 cells (Figure 8a). Substantiating these results of increased caspase activity, DNA fragmentation was also observed in MCF-7 cells after treatment with THMPP. However, untreated cells had intact genomic DNA when visualized in an agarose gel.

The apoptotic induction in cells was validated further by using a cell sorter facilitated by the FITC-labeled annexin V/PI staining. The percentage of MCF-7 cells undergoing apoptosis during THMPP treatment and untreated conditions provides a quantitative expression of the apoptotic induction caused by THMPP. Around 39% of cells were in the apoptotic stage when treated with THMPP, whereas only 2% of untreated cells were in the apoptotic stage (Figure 7b).

The changes in apoptotic cells are revealed in morphological analysis using AO/EB staining of MCF-7 cells with THMPP, with a clear separation between normal cells,

apoptotic cells, and necrotic cells. Upon treating MCF-7 cells with THMPP at IC_{50} concentration, 42% of the cells exhibited apoptotic features, including blebs (Figure 7c). These results prove that THMPP increases the sensitivity of cancer cells toward apoptosis.

This led to a further study of the gene expression of cells posttreatment by THMPP at its IC_{50} concentration. The PI3K/Akt pathway genes, namely EGFR, PI3k, and S6K1, were specifically considered. The total mRNA of treated and untreated cells was isolated, and complementary DNA was synthesized and amplified. THMPP downregulated the overexpressing PI3K and S6K1 genes to 0.5-fold in breast cancer cells (Figure 8b). Our results showed that there was no alteration in the expression of the EGFR gene after THMPP treatment.

The EGFR gene expression was not altered in cells by the THMPP, so the interaction of the compound with the protein was studied by using computational molecular docking analysis. The compound showed a hydrogen–bond interaction with active site residues and a docking score of 33.02 (GOLD-CCDC). The structure-activity relationship of THMPP was studied by creating a QSAR model equation. The model was generated with a correlation coefficient of 0.953 for the training set and 0.982 for the test set, proving its efficiency[79]. THMPP fits in the equation well, where it is predicted as a potent anticancer agent. Finally, the pharmacokinetic properties (ADME) predicted based on the structure of THMPP revealed that it is a good candidate as a drug for oral administration.

The second compound of interest, THTMP, which had a similar backbone to THMPP, was studied for its activity against breast cancer. Publication 2 reports the results of the experiments with THTMP treatment in breast cancer cell lines and computational analysis made with EGFR protein, QSAR model generation, and the ADME properties of THTMP.

THTMP has shown good antiproliferative activity, has induced apoptosis in cancer cells by enhancing caspases activity, and has effectively regulated the expression of the genes involved in the PI3K/AKT pathway after treatment at its IC_{50} concentration. The complete data are available in Publication 2[123]. The significant results are presented here. Similar to THMPP, THTMP has an IC_{50} concentration value of 87.92μM in MCF-7 cells and 172.51μM in SkBr3 cells (Figure 7a); THTMP reduced cell viability in a dose-dependent manner and was nontoxic to the normal non-cancerous cell H9C2.

THTMP mediated the stimulation of apoptosis in breast cancer cells, which was confirmed by using caspases quantification and DNA fragmentation. THTMP increased the levels of caspase-3 and caspase-9 by 0.331-fold and 0.388-fold, respectively, in SkBr3 cells and 0.295-fold in MCF-7 cells (Figure 8a). The genomic DNA of THTMP-treated cells also showed fragmented nucleotides when visualized on an Agarose gel, whereas intact genomic DNA was maintained in untreated cells. The observations were corroborated when cells were stained with Annexin V/PI and sorted through FACS. In MCF-7 cells posttreatment with THTMP for 24 h, 32% of the cell population was shifted to apoptotic stages (early and late stages) (Figure 7c).

Using fluorescent dye AO/EB, morphological changes in the nucleus were examined through fluorescence microscopy. The untreated cells appeared green with the usual nuclear morphology, indicating the avoidance of apoptosis in cancer cells. Alternatively, after THTMP treatment, apoptotic events were envisaged as the bright yellow-green color and orange staining representing the cells during the early and late apoptotic stages, respectively, along with distorted cell shapes' appearance blebbing. The early apoptotic stage was observed in 11.63% of cells, while the late apoptotic stage was 22.96% (Figure 7b).

The evasion of apoptosis is mainly due to the overexpression of genes related to growth proliferation. In untreated MCF-7 cells, gene expression studies revealed that the PI3k and S6K1 genes were expressed constitutively. However, THTMP treatment significantly altered the expression of these genes and downregulated them by 0.5-fold compared with untreated cells (Figure 8b).

Furthermore, similar to THMPP, a QSAR model study was performed with THTMP, and an equation was constructed based on its IC_{50} values. The model equation validated that THTMP is a potent anti-cancer compound. The docking score of THTMP with the EGFR protein was 37.25 in a molecular docking analysis, and it interacts with the active site residues by forming hydrogen bonds. The computational prediction of ADME properties revealed that THTMP has a drug-likeliness structure.

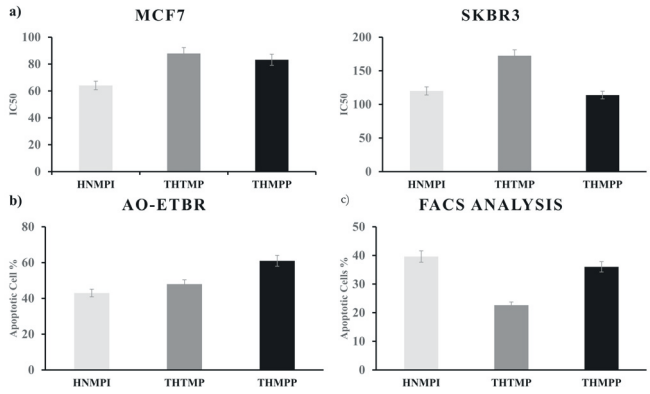

Figure 7: a) IC_{50} values of compounds: The graph compares the IC_{50} values of THMPP, THTMP, and HNPMI in MCF7 and SkBr3 cells. b) Morphological analysis of apoptosis induction by the drug candidates using AO/EtBr stain: The figure indicates the percentage of cells in the apoptotic condition after treatment with the drug candidates. c) FACS analysis of cells treated with compounds: Proportion of cells in different cell cycle phases analyzed using Annexin V/PI staining. The figure represents the percentage of cells in the apoptotic phase after HNPMI, THMPP, and THTMP treatment.

We performed a similar set of experiments with HNPMI, our third compound, with these results. The compound exhibits a different side chain from THMPP and THTMP, but it has the same indoline backbone. Following these results, our third publication reported the anticancer potential of HNPMI in MCF-7 and SkBr3 cells. Similar to the other two compounds, HNPMI showed cytotoxicity to cancer cells in a dose-dependent manner. The IC_{50} concentrations were found to be 64.10μM and 119.99μM (Figure 7a), respectively, the lowest among the three compounds studied. HNPMI was also nontoxic to the normal cell H9C2 at 10 μM and 100 μM.

The cytotoxicity in cells was due to the sensitization of apoptosis, which was confirmed by using apoptosis assays for the other two compounds. The activity of caspase-3 and caspase-9 increased by 0.218-fold and 0.478-fold in MCF-7 cells and by 0.098-fold and 0.269-fold in SkBr3 cells compared with untreated cells (Figure 8a). The genomic DNA fragments were also observed in HNPMI-treated cells when agarose gel electrophoresis was conducted. AV/PI staining and sorting by FACS revealed that around 40% of the cells underwent apoptosis upon treatment with HNPMI for 24 h (Figure 7c). Similarly, 43% of MCF-7 cells showed apoptotic induction when they were detected with fluorescent stains (Figure 7b). Morphological changes in the cells were also observed in HNPMI-treated cells.

As apoptosis induction is evident, the mechanism behind the cell's shift toward death was determined. It was confirmed from the results that the compound was responsible for the deregulation of PI3K and S6K1 in treated cellsHNPMI had a 0.4-fold and 0.3-fold effect on PI3K and S6K1 gene expression, respectively, although EGFR gene expression remained unchanged (Figure 8b). However, the computational analysis on EGFR protein and HNPMI showed that the compound interacts with the active site residue of EGFR (Gly 772 and Met 769). The interactions led to a docking score of -75.104[124]. According to the computational ADME/T study, HNPMI has good pharmacokinetic features and follows the drug-

likeliness principles. Furthermore, HNPMI does not induce carcinogenic effects on cells and has good oral bioavailability.

Furthermore, the QSAR model built using HNPMI predicts similar bioactive compounds in the future. The equation was built using IC_{50} values of known anticancer compounds; it also emphasized the presence of the indole ring, the aromaticity, and certain other substituents, such as nitrogen and oxygen, ascertainingthe biological activity of the compounds.

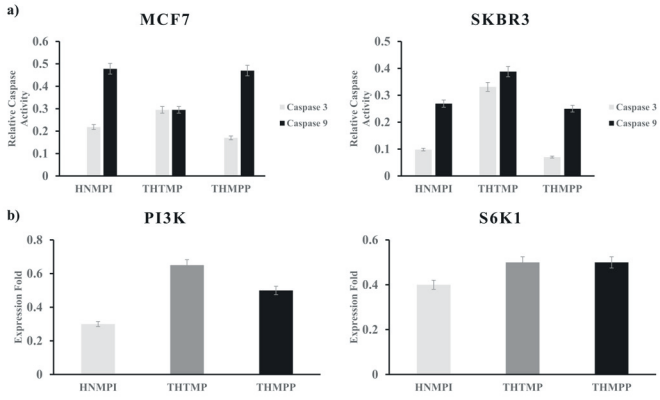

Figure 8: a) Caspase-3 and caspase-9 activation by the selected compounds. The graph illustrates the fold change in the caspases enzyme after treating THMPP, THTMP, and HNPMI in MCF7 and SkBr3 cells. b) Alteration of PI3K and S6K1 gene expression in MCF7 cells: The graph shows the fold change in PI3K and S6K1 genes after treating cells with HNPMI, THMPP, and THTMP.

We chose to perform a combined computational analysis to compare the activities of all three compounds and find the best among the three. The EGFR protein was considered for the study, the compounds' interaction with EGFR was studied in detail with a set of tools, and the results were published. Publication 4 provides insights into a comparative analysis of all three compounds: THMPP, THTMP, and HNPMI.

The compounds THMPP, THTMP, and HNPMI, were initially checked for drug-likeliness properties. The compounds had strong ADME/Tox characteristics, and the structure of the compounds obeyed Lipinski's rule of five for drug likeliness. In addition, the human oral absorption was also good, predicting the compound's ability to be used for human consumption.

A comprehensive computational study was done to understand further the interactions between the drugs and the EGFR receptor. The protein structure was downloaded from the PDB (1M17), and the experiments were performed. Initially, the interaction of the compounds with the tyrosine kinase domain of the EGFR protein was studied, and the Glide score was tabulated. The compounds showed hydrogen bond interaction, π–cation interaction, and hydrophobic interaction with the active site residues of EGFR. The score was compared with the well-known standard inhibitor, Gefitinib. The Glide score was -5.345Kcal/mol for HNPMI, -5.670 Kcal/mol for THTMP, -5.797Kcal/mol for THMPP, and -6.297Kcal/mol for Gefitinib (Table 2).

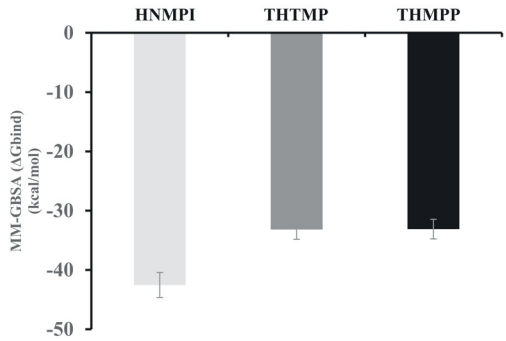

Figure 9: Interaction analysis of compounds with EGFR: The graph depicts the MM-GB/SA binding energy values of the compounds interacting with the EGFR kinase domain.

The interaction of the compounds with the key residues of the protein was also observed and tabulated. The key residues include Lys 21, Met 769, Asp 831, and Ala 719. Binding free energies were calculated after docking by using MM-GBSA analysis. The ΔG bind values for HNPMI, THTMP, and THMPP were -42.534 (Kcal/mol), -33.183 (Kcal/mol), and -33.108 (Kcal/mol), respectively (Figure 9).

Molecular dynamics simulation was subsequently performed to check the stability of the protein-ligand complex. The simulation was run for 100ns for this purpose; it was evident from the results that the complex was stable, and the interactions were intact for 30% of the simulation time in the selected trajectory. The RMSD was plotted, and the interactions of key residues were tracked cautiously. The residues in the binding pocket, Lys 721, Met 769, Asp 831, and Ala 719, interact with the compounds and are stable. The density functional theory was also applied to study the electron donor/acceptor property of HNPMI, THTMP, and THMPP. The HOMO and LUMO potential energy of the HNPMI, THTMP, and THMPP were detected to be -0.018 and -0.010, -0.018 and 0.009, and -0.19 -0.086, respectively[125].

Table 2: Molecular docking analysis and binding free energies (kcal/mol) of HNPMI, THTMP, and THMPP with EGFR

Ligand name	**Glide XP score (kcal/mol)**	**Glide energy (kcal/mol)**	**Interacting Residues**
HNPMI	-5.345	-63.170	Asp 831 Lys 721
THTMP	-5.670	-48.726	Lys 721 Ala 719
THMPP	-5.797	-54.810	Lys 721 Met 769
GEFITINIB	-6.297	-79.051	Lys 721

E-pharmacophore modeling was performed to enhance the compounds that are useful for further new drug-designing processes. The sites of HNPMI, THTMP, and THMPP were identified through this method, including an aromatic ring, an acceptor and a donor group, and a hydrogen bond donor group. The initial number of pharmacophore site generation was set to default; however, a five-pharmacophore site hypothesis ADHHR was generated. This is a powerful tool for lead hopping and enables the screening of hundreds of compounds per second.

It was observed from the data published in these four publications that the three compounds possessed the adequate anticancer potential to induce apoptosis by modulating EGFR signaling. Therefore, a comparative study on all the assays performed is exemplified here.

From the cytotoxic analysis, the IC_{50} values were compared and tabulated. The lowest IC_{50} value is for HNPMI in both MCF-7 and Skbr3 cells. In addition, the comparative results of caspase activity and gene expression analyses are tabulated. HNPMI was found to be the best of the three compounds in all the cases.

The computational analysis on docking scores, MMGBSA, and HOMO /LUMO scores is compared and tabulated. The results demonstrate that HNPMI is the best hit among the three, and it interacts with the EGFR tyrosine kinase domain. Apart from these, the RMSD of the protein-ligand complex was the lowest for HNPMI, the HNPMI–EGFR complex was more stable, and the interaction of ligands with the active site residues was stronger, making more than one specific contact with the ligand and occurring longer in the simulation time. The interactions will correlate with the docking results. The residues in the binding pocket, Lys 721, Met 769, Asp 831, and Ala 719, interact with the compounds even after simulation.

We conclude from all the cumulative results observed that the HNPMI is the best compound, and it exhibits better anticancer activity than THTMP and THMPP. The corresponding figures and tables of the results mentioned earlier are provided next in this thesis.

5 INFERENCE AND DISCUSSION

The earlier chapters describe the anticancer potential of the three indoline derivatives HNPMI, THTMP, and THMPP against breast cancer cells. On the whole, it was also found that the compound HNPMI proved to be the best of the three. Thus, this thesis also accomplished all the objectives stated in Chapter 1.

5.1 Cytotoxicity of the novel compounds HNPMI, THTMP, and THMPP

The cytotoxicity of the compounds against breast cancer cells was evaluated, and it was found that the IC_{50} concentration was the lowest for HNPMI. Many reports on the quantitative and qualitative analysis of phenolic compounds show cytotoxicity in breast cancer cells. A myriad of reports has also shown lower IC_{50} values of the phenolics from the plant and synthetic sources.

Doan et al.[126] reported earlier on the anticancer activity of our compounds of interest (HNPMI, THTMP, and THMPP) against osteosarcoma cells and brain tumor cells. The IC_{50} values for these compounds range from 64 to 172 μM, considering both the cell types. Compared with many dietary phenolic compounds such as Galic acid (IC_{50} 80.5μM*) and ϱ-coumaric acid (IC_{50} 1.2 Mm**), this range of IC_{50} against breast cancer (MCF7 cells) is promising and lower.[13] Though slightly more potent than curcumin, it is comparable to Resveratrol's IC_{50} values and is less potent than Capsaicin, a common phenolic studied for its anticancer activity.[127,128] Other phenolic compounds have been proven to trigger cell cycle arrest and apoptosis in

cancer cells than breast cancer. Chen et al. demonstrated that few compounds had IC_{50} values of 100 μM against HL60 cells, which are equivalent to those of the proposed compound.[129]

5.2 Apoptotic induction by the compounds in breast cancer cells by activation of caspase-3 and caspase-9

Our results show that the cytotoxicity in the cells is due to the compounds' potential to induce or initiate apoptosis in cancer cells.

Caspases are proteolytic enzymes that are key molecular players in apoptosis. They are called cysteine-dependent aspartate-directed proteases. They are produced as pro-caspases, which are inactive forms of caspases (zymogens). Their posttranslational modification is tightly regulated, and they are appropriately activated on selected stimuli. The active caspases exist as heterotetramers, resulting from the dimerization of pro-caspases. Caspases are grouped into three subclasses, namely initiator, executioner, and inflammatory caspases. The initiator caspases usually cleave themselves and are auto brutality, which includes caspase-2, caspase-8, caspase-9, and caspase-10; they are essential for the cleavage of executioner caspases caspase-3, caspase-6, and caspase-7 and activate them. The initiator caspases initiate the apoptotic signal in apoptosis, and the executioner caspases carry out the following proteolysis. These executioners cleave an array of target proteins, leading to the characteristic apoptotic breakdown of a cell.[97]

Breakdown of the cell includes the plasma membrane protrusion, and a portion of the cytoplasm is filled with it. As a result, the nuclear DNA fragments and is filled into blebs along with that. DNA fragmentation is when the DNA strand is broken down into pieces because of the formation of nicks by endonucleases. This fragmentation is an important hallmark of apoptosis, and the executioner caspases

mediate it. The role of caspases is in making the endonuclease active by caspases, and it is named after that function as a CAD (caspase-activated DNase). The CAD is usually translated as an inactive form bound to its inhibitor of CAD (ICAD/DFF45). The caspases, especially caspase 3, are responsible for removing its inhibitor ICAD from the complex. As a result, they make CAD active, which preferentially cleaves the double-stranded DNA to generate blunt ends or ends with single-base overhangs[130] (Figure 10).

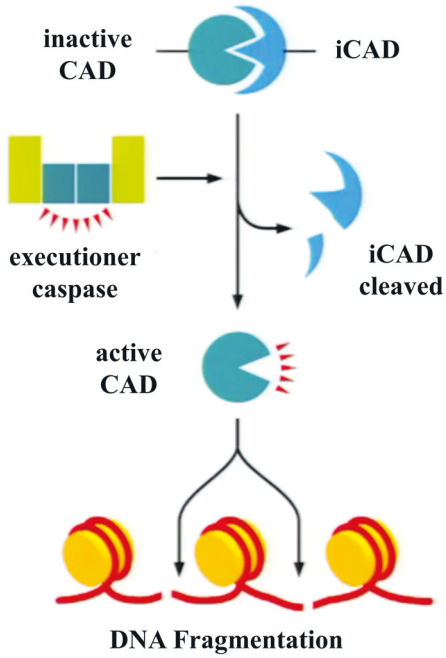

Figure 10: Activation of DNA fragmentation by caspases cascade.

Caspases have impending consequences in tumorigenesis, and the chemoresistance observed in human cancers. However, mutations in the caspase gene are found only in some cancers, such as hepatocellular carcinoma, colon cancer, and stomach cancer. On the other hand, Caspase-3 and caspase-9 are known to be expressed in

other cancers. Furthermore, it is noted that there is a decreased expression of caspases, whereas mutation or silencing is not so common. Despite these factors, caspases are found to be deficient in cancers because of certain factors, such as (1) the pathway upstream to caspase activation is abrogated; (2) some proteins specifically inhibit caspases in cancerous conditions; or (3) alternative splicing may generate dominant-negative caspase variants.[131] To summarize, it is also reported that 75% of breast cancer tissues either lack caspase-3 expression or are downregulated.

It has been reported in many studies that MCF-7 cells are devoid of caspase activity in the case of the breast cancer cell line. Furthermore, it was experimentally proved that, upon receiving apoptotic stimuli such as TNF β, MCF7 cells undergo cell death, but the fragmentation of DNA is not observed. One of the reasons for the deficiency of caspase-3 in MCF-7 cells is that exon 3 of the caspase gene has a deletion mutation.[132,133] The characteristics of MCF7 cells to resist apoptosis and be devoid of caspase activity are behind their unresponsiveness to chemo- and radiation therapy.[134] As a result, finding a novel drug with therapeutic effect through a caspase-3-independent mechanism is firmly recommended.

Our experimental results in the present study show that the compounds HNPMI, THTMP, and THMPP initiate apoptosis and cause cell death by activating caspase-9 (initiator) and caspase-3 (executioner), which cause DNA fragmentation in cancer cells after treatment.

5.3 Novel compounds downregulate the constitutive PI3K–S6K1 gene expression

The compounds HNPMI, THTMP, and THMPP effectively induce apoptosis in cancer cells. Furthermore, we focus on the compounds' use as targeted chemotherapy. The cancer cells are killed by inhibiting or activating a specific gene or protein involved in the cancer mechanism. Targeted therapy is favored because of its ability to kill cancer cells without affecting normal cells, thereby reducing the undesirable adverse effects of chemo drugs. Many signal pathways are distorted during the tumorigenic process. The upregulation of oncogenes and/or their products and the downregulation of tumor suppressors are commonly detected in cancer cells.

The phosphatidylinositol 3-kinases (PI3Ks) are constitutively activated in an exceptionally high percentage of breast cancer cases. The PI3Ks belong to the protein kinase family; they are activated by any growth factor and phosphorylate the substrate phosphatidylinositol 4,5-bisphosphate (PIP2). The phosphorylated PIP2 becomes PIP3, acts as a signal transducer and activates further downstream kinases, including AKT. The PI3K signaling cascade is controlled by the dual lipid and protein phosphatase PTEN, which negatively regulates the intracellular levels of PIP3.[135]

The deregulation of the PI3K signaling pathway is common in many cancers because of either a mutation in the catalytic subunit of PI3K or downregulation of the PTEN gene. The expression of the PI3K or AKT genes is controlled by various transcriptional factors such as FOXO, which are activated by these kinases themselves, which results in them being called "effector" molecules. The PI3K signaling pathway is implicated in cell cycle progression, tumor metastasis, and

enhanced chemotherapeutic resistance. AKT are effector molecules, so the gene expression is indirectly controlled by the amount of expression of PI3K proteins.[136]

Another major player in cancer progression is the 40S ribosomal S6 kinases (S6K). They exist as two structurally similar homologs, except at an ATP binding site. However, many reports have shed light on S6K1 predominantly, as they are found to be overexpressed in 20% of breast cancers.[137] It is necessary to understand that S6K1 is essential for the activation of the Estrogen Receptor. S6K1 phosphorylates ER, which is often expressed in breast cells and mediates cell proliferation.[138]

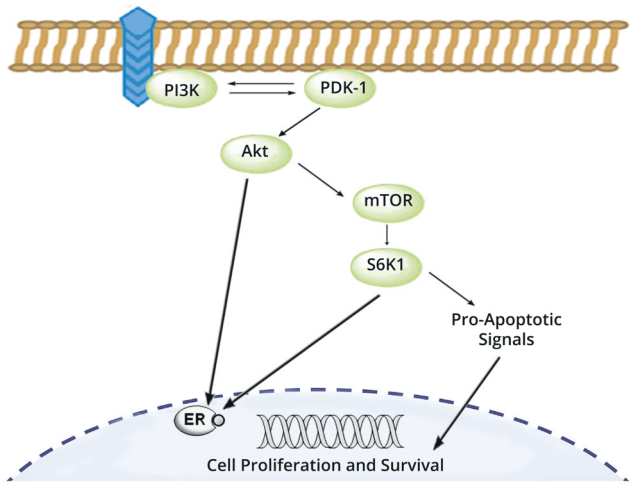

Figure 11: Schematic representation of the role of PI3K and S6K1 in cell proliferation.

The molecular-level link between PI3K and S6K1 is through the AKT-activating mTORC1, which, in turn, activates S6K1 (Figure 11). Studies have shown that the S6K proteins sensitize cells to apoptosis by altering the ratio of pro-and anti-apoptotic proteins.[139] Our results showed that, by using HNPMI, THMPP, and THTMP, the treatment of breast cancer cells has effectively downregulated the gene expression of PI3K and S6K1. This implies reduced PI3K-mediated signaling, which

appropriately responds to the cytotoxicity induced in the MCF-7 and SkBr3 cells and the apoptosis induction observed in them. There are many reports on the thriving chemo drugs in use that are targeted against these molecules. Wortmannin and LY294002 are the inhibitors of PI3K that were characterized first. They have been proved to inhibit PI3K and abort the activation of downstream effectors of PIK3CA in breast epithelial colorectal cancer cells.[140] PI3K delta-specific inhibitor idelalisib, the first PI3K compound approved by the U.S. FDA, proves to be effective in cancer treatment.[141] Very few reports exist on S6K1 inhibitors in breast cancer. Still, a novel inhibitor against cervical cancer has been reported: Rapamycin is widely studied as an mTOR/S6K1 inhibitor, and Rosmarinic acid methyl ester is recommended for cancer cases that are resistant to cisplatin.[142]

5.4 Compounds interact with EGFR, thereby downregulating PI3K and S6K1

Apart from PI3K and S6K1, many noteworthy signaling pathways are widely studied in cancerous conditions. The EGFR-mediated growth process is a significant cascade among them. Epidermal Growth Factor Receptor (EGFR) is a receptor tyrosine kinase enzyme that regulates cell proliferation, apoptosis, angiogenesis, and metastasis.

This extensive functionality of EGFR involves regulating the downstream signals of PI3K-AKT-mTOR, JAK-STAT, and ERK–MAPK pathways (Figure 12). The efficient and effective role in cell signaling makes it one of the key molecules often overexpressed in cancer cells, including breast cancer.

A myriad of small molecules is studied as inhibitors targeting EGFR. These molecules have produced promising therapeutic benefits to responsive types of cancers, namely Erlotinib, Gefitinib, and Lapatinib.[143,144] The inhibitors primarily targeting Tyrosine kinase activity of EGFR turned out to be successful in cancer

treatment.[145] This is primarily because the kinase activity of EGFR is predominantly involved in promoting cell proliferation compared with cell survival.[144]

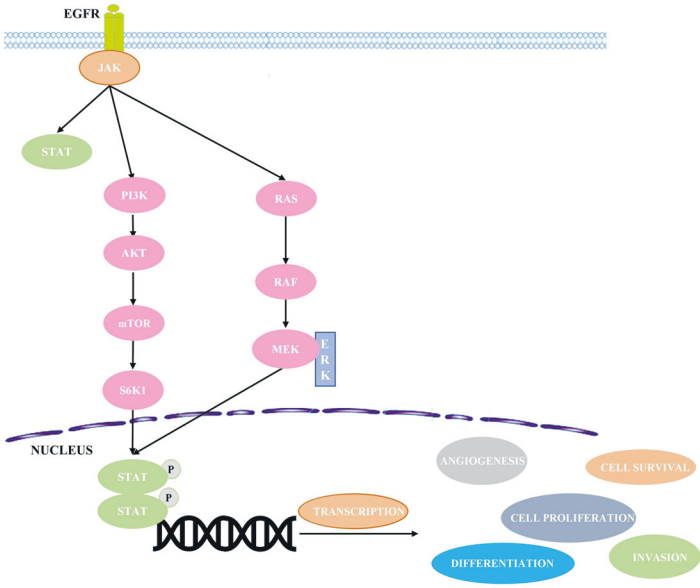

Figure 12: Representation of the multiple roles of EGFR in cell survival and proliferation.

The aggravating problem with the existing EGFR inhibitors as anticancer drugs is that the EGFR-overexpressing cancer cells do not respond to the EGFR–kinase domain inhibitors. It is undeniable that the emergence of novel drug molecules increases but demand always exists to anticipate molecules that overcome resistance in EGFR-overexpressing cancer cells.

There are different oncogenic pathways in tumors with high EGFR expression profiles, which may help understand resistance mechanisms. The initiation of the EGFR results in the activation of downstream signaling pathways, including the Ras-Raf-MKK extracellular signal-regulated kinase (ERK) and lipid kinase, phosphatidylinositol 3-kinase/Akt pathways[146]. The activation of the downstream molecules Akt and the Signal Transduction and Activator of Transcription (STAT),

which ensures cell survival, may be responsible for the resistance to apoptosis induced by therapies.

Thus, a need exists for a new drug to target multiple pathways that are involved in cancer progression and apoptosis hindrance. The results of this gene expression study reveal that the compounds THTMP, THMPP, and HNPMI downregulate PI3K and S6K1 genes without any effect on the expression of the EGFR gene. Therefore, a computational analysis to find the interaction of the compounds with the EGFR protein at its kinase domain was carried out to find answers to this ambiguous question. This was done and validated using MDS to confirm that HNPMI interacts with the EGFR protein as effectively as Gefitinib. This is evident from the ligand interaction profiles.

Similar studies have been performed in advanced research to find a new drug for cancer treatment. For example, quinazoline-based EGFR inhibitors were studied by a research group using *in-silico* methods. They utilized the QSAR model, molecular docking, and ADME prediction and used the Schrödinger suite in 2016.[141] The inhibitor for selectively mutated EGFR was studied *in-silico* through virtual screening followed by molecular docking analysis in curcumin derivatives.[147] Many reports depict the similar activity of various small molecules against EGFR kinase activity, including Benzothiazole derivatives,[148] 2, 7-diamino-thiazolo [4,5-d] pyrimidine analogs,[122] novel 5-Deazaalloxazine analogs,[149], and so on. There is also a report on Furanocoumarin derivatives against the multiple targets involved in breast cancer tumorigenesis.[150] They have performed a structure-based docking analysis.

To conclude, the compounds exhibit anticancer activity, conferring cytotoxicity on cancer cells. Cell death is not necrotic entirely, but it is mediated by apoptosis. The cancer cells gain this sensitivity to apoptosis triggered by the compound's ability to interact with the EGFR protein, thereby downregulating the gene expression of the downstream signal molecules PI3K and S6K1.

HNPMI invariably exhibits the best activity in all the studies after comparing the potential among the three compounds. Hence, it is emphasized that the novel

compound HNPMI is a potent drug against breast cancer. The importance of the study lies in its ultimate finding that the novel compound HNPMI can target ER+ breast cancer cells resistant to other chemotherapeutic drugs.

5.5 Strength and Limitations

In all four studies (I-IV), specific attention was given to analyses of the compound potentiality experimentally and validated computationally. The study is more reliable because of the use of different cell lines, and excellent controls for all the experiments. The methodologies involve multiple perspectives, including microscopic analysis, colorimetric tests, gene expression levels, and computational methods. The study's main limitation was that the research only expresses compound activity in the cultured cells. Therefore, it has to go through animal studies and clinical studies to confirm its activity as a potent drug. Furthermore, the compound's effectiveness is not studied in other cancers and does not focus on other hallmarks except apoptosis.

6 CONCLUSION

The heterogeneity of breast cancers remains a significant challenge for public health, and the tumor stands out as a common life-threatening disease. Breast cancer ranks as the first and most frequently diagnosed cancer in women, and it represents one in four cancers diagnosed among women globally.[151] Conventional treatments such as surgery, radiation therapy, chemotherapy, hormonal therapy, targeted therapy, and immunotherapy are used against breast cancer. However, the recurrence of the disease is immense, leading to a low survival rate. Currently, many bioactive chemical agents that have originated from natural sources or synthetic approaches compete for a significant role as potent anticancer agents against breast cancer. The synthetic compound engineered with targeted therapy can recognize and destroy specific cancer cells without affecting normal cells. In this study, we have performed the cytotoxic analysis of three chosen synthetic compounds and calculated their IC50 values. We also analyzed and evidenced that the compounds could induce apoptosis in breast cancer cells. Further, the interaction of the compounds with EGFR protein was also studied *in-silico*. Furthermore, the potential differential regulation of genes in the PI3K/S6K1 pathways was analyzed.

To sum up, this thesis concludes that out of the three alkylaminophenolic derivates analyzed, HNPMI is found to be the best compound with the highest toxicity toward breast cancer cells. HNPMI induces apoptosis by increasing caspase activity and downregulating the expression of PI3K and S6K1 genes. Also, HNPMI binds with the EGFR active site residues leading to the downregulation of these genes.

Nevertheless, the other two compounds, THMPP and THTMP, also possess cytotoxicity in cells and promote apoptosis. The compounds were shown to be non-toxic to normal cells. QSAR adds biological significance to the quantitative structural relationship. Additionally, considering the long-term administration of this drug as an anti-breast cancer agent, HNPMI's excellent safety profile has been indubitably proven with the help of ADME/T studies. The recommended drug targets in-vitro, the possibility of structure refinement of the compounds to increase their biological activity, the possibility to be used as a co-drug, the identification of precise delivery agents, etc., are considered significant values of the drug. Overall, HNPMI is a promising candidate for executing further phase clinical trials with pharmacological importance against breast cancer treatment.

7 REFERENCES

1. Ma, X. & Yu, H. Global burden of cancer. *Yale Journal of Biology and Medicine* **79**, 85–94 (2006).

2. Sung, H. *et al.* Global Cancer Statistics 2020: GLOBOCAN Estimates of Incidence and Mortality Worldwide for 36 Cancers in 185 Countries. *CA. Cancer J. Clin.* **71**, 209–249 (2021).

3. Siegel, R. L., Miller, K. D. & Jemal, A. Cancer statistics, 2016. *CA. Cancer J. Clin.* **66**, 7–30 (2016).

4. Tong, C. W. S., Wu, M., Cho, W. C. S. & To, K. K. W. Recent Advances in the Treatment of Breast Cancer. *Front. Oncol.* **8**, 227 (2018).

5. Navya, V., Pavan, S. & Swami, A. Recent Advances in the Chemotherapy of Breast Cancer. *Adv. Cancer Prev.* **03**, 1–4 (2018).

6. Chia, S. K. *et al.* The impact of new chemotherapeutic and hormone agents on survival in a population-based cohort of women with metastatic breast cancer. *Cancer* **110**, 973–979 (2007).

7. Gravanis, I., Vleminckx, C., Jonsson, B. & Pignatti, F. The changing world of cancer drug development: the regulatory bodies' perspective. *Chinese Clin. Oncol.* **3**, 11 (2014).

8. Liu, J. *et al.* Current research on anti-breast cancer synthetic compounds. *RSC Adv.* **8**, 4386–4416 (2018).

9. LS, R., NJA, S., NCP, S., MC, M. & AJ, T. Anticancer Properties of Phenolic Acids in Colon Cancer – A Review. *J. Nutr. Food Sci.* **06**, 1–7 (2016).

10. Kampa, M. *et al.* Antiproliferative and apoptotic effects of selective phenolic acids on T47D human breast cancer cells: potential mechanisms

of action. *Breast Cancer Res.* **6**, R63-74 (2004).

11. Kampa, M. *et al.* Introduction Antiproliferative and apoptotic effects of selective phenolic acids on T47D human breast cancer cells: potential mechanisms of action. (2004). doi:10.1186/bcr752

12. Foti, M. C. Antioxidant properties of phenols. *J. Pharm. Pharmacol.* **59**, 1673–1685 (2007).

13. Anantharaju, P. G., Gowda, P. C., Vimalambike, M. G. & Madhunapantula, S. V. An overview on the role of dietary phenolics for the treatment of cancers. *Nutr. J.* **15**, 99 (2016).

14. Roy, M., Chakraborty, S., Siddiqi, M. & Bhattacharya, R. K. Induction of apoptosis in tumor cells by natural phenolic compounds. *Asian Pac J Cancer Prev* **3**, 61–67 (2002).

15. Beltz, L. A., Bayer, D. K., Moss, A. L. & Simet, I. M. Mechanisms of cancer prevention by green and black tea polyphenols. *Anticancer. Agents Med. Chem.* **6**, 389–406 (2006).

16. Sinha, D., Sarkar, N., Biswas, J. & Bishayee, A. Resveratrol for breast cancer prevention and therapy: Preclinical evidence and molecular mechanisms. *Semin. Cancer Biol.* **40_41**, 209–232 (2016).

17. Lee, M. F., Pan, M. H., Chiou, Y. S., Cheng, A. C. & Huang, H. Resveratrol modulates MED28 (magicin/EG-1) expression and inhibits epidermal growth factor (EGF)-induced migration in MDA-MB-231 human breast cancer cells. *J. Agric. Food Chem.* **59**, 11853–11861 (2011).

18. Jung, K. H. *et al.* EGF receptor stimulation shifts breast cancer cell glucose metabolism toward glycolytic flux through PI3 kinase signaling. *PLoS One* **14**, 1–14 (2019).

19. Ferlay, J. *et al.* Estimating the global cancer incidence and mortality in 2018: GLOBOCAN sources and methods. *Int. J. Cancer* **144**, 1941–1953 (2019).

20. Parise, C. A. & Caggiano, V. Breast Cancer Survival Defined by the ER/PR/HER2 Subtypes and a Surrogate Classification according to Tumor Grade and Immunohistochemical Biomarkers. *J. Cancer Epidemiol.*

2014, 469251 (2014).

21. Perou, C. M. *et al.* Molecular portraits of human breast tumours. *Nature* **406**, 747–752 (2000).

22. Bauer, K., Parise, C. & Caggiano, V. Use of ER/PR/HER2 subtypes in conjunction with the 2007 St Gallen Consensus Statement for early breast cancer. *BMC Cancer* **10**, 228 (2010).

23. Sørlie, T. *et al.* Gene expression patterns of breast carcinomas distinguish tumor subclasses with clinical implications. *Proc. Natl. Acad. Sci.* **98**, 10869–10874 (2001).

24. Hussain, S. A. *et al.* Role of chemotherapy in breast cancer. *Expert Review of Anticancer Therapy* **5**, 1095–1110 (2005).

25. Goldhirsch, A. *et al.* Meeting highlights: updated international expert consensus on the primary therapy of early breast cancer. *J. Clin. Oncol.* **21**, 3357–3365 (2003).

26. Abe, O. *et al.* Effects of chemotherapy and hormonal therapy for early breast cancer on recurrence and 15-year survival: An overview of the randomised trials. *Lancet* **365**, 1687–1717 (2005).

27. Henderson, I. C. *et al.* Improved outcomes from adding sequential paclitaxel but not from escalating doxorubicin dose in an adjuvant chemotherapy regimen for patients with node-positive primary breast cancer. *J. Clin. Oncol.* **21**, 976–983 (2003).

28. Pinto, A. C., Ades, F., de Azambuja, E. & Piccart-Gebhart, M. Trastuzumab for patients with HER2 positive breast cancer: Delivery, duration and combination therapies. *Breast* **22**, (2013).

29. Pegram, M. D. & Slamon, D. J. Combination therapy with trastuzumab (Herceptin) and cisplatin for chemoresistant metastatic breast cancer: evidence for receptor-enhanced chemosensitivity. in *Seminars in oncology* **26**, 89–95 (1999).

30. Pfeffer, C. M. & Singh, A. T. K. Apoptosis: A target for anticancer therapy. *International Journal of Molecular Sciences* **19**, (2018).

31. Hensley, P., Mishra, M. & Kyprianou, N. Targeting caspases in cancer therapeutics. *Biological Chemistry* **394**, 831–843 (2013).

32. Olsson, M. & Zhivotovsky, B. Caspases and cancer. *Cell Death and Differentiation* **18**, 1441–1449 (2011).

33. Ke, X. & Shen, L. Molecular targeted therapy of cancer: The progress and future prospect. *Front. Lab. Med.* **1**, 69–75 (2017).

34. Smith, C. Drug target validation: Hitting the target. *Nature* **422**, 341–347 (2003).

35. Xu, J. & Hagler, A. Chemoinformatics and drug discovery. *Molecules* **7**, 566–600 (2002).

36. Baig, M. H. *et al.* Drug Discovery and In Silico Techniques: A Mini-Review Mohd Hassan Baig1, Khurshid Ahmad1, Mohd Adil2, Zainul A Khan3, Mohd Imran Khan4, *. (2014). doi:10.4172/2329-6674.1000123

37. Méry, B. *et al.* In Vitro Cell Death Determination for Drug Discovery: A Landscape Review of Real Issues. *J. Cell Death* **10**, 117967071769125 (2017).

38. Yang, Wang, Zang, Tang & Li. Cell-Based Assays in High-Throughput Screening for Drug Discovery. *Int. J. Biotechnol. Wellness Ind.* (2012). doi:10.6000/1927-3037.2012.01.01.02

39. Miller, T. W., Rexer, B. N., Garrett, J. T. & Arteaga, C. L. Mutations in the phosphatidylinositol 3-kinase pathway: Role in tumor progression and therapeutic implications in breast cancer. *Breast Cancer Research* **13**, 224 (2011).

40. Miller, T. W. *et al.* Hyperactivation of phosphatidylinositol-3 kinase promotes escape from hormone dependence in estrogen receptor-positive human breast cancer. *J. Clin. Invest.* **120**, 2406–2413 (2010).

41. Blackwell, K. *et al.* Phase I/II dose-escalation study of PI3K inhibitors pilaralisib or voxtalisib in combination with letrozole in patients with hormone-receptor-positive and HER2-negative metastatic breast cancer refractory to a non-steroidal aromatase inhibitor. *Breast Cancer Res. Treat.* **154**, 287–297 (2015).

42. Xu, H. *et al.* Recent advances of highly selective CDK4/6 inhibitors in breast cancer. *Journal of Hematology and Oncology* **10**, (2017).

43. Shah, A. N. & Cristofanilli, M. The Growing Role of CDK4/6 Inhibitors in Treating Hormone Receptor-Positive Advanced Breast Cancer. *Current Treatment Options in Oncology* **18**, (2017).

44. Finn, R. S. *et al.* Palbociclib and Letrozole in Advanced Breast Cancer. *N. Engl. J. Med.* **375**, 1925–1936 (2016).

45. Robson, M. *et al.* Olaparib for Metastatic Breast Cancer in Patients with a Germline *BRCA* Mutation. *N. Engl. J. Med.* **377**, 523–533 (2017).

46. Brown, J. S., Kaye, S. B. & Yap, T. A. PARP inhibitors: The race is on. *British Journal of Cancer* **114**, 713–715 (2016).

47. Keen, J. C. *et al.* A novel histone deacetylase inhibitor, Scriptaid, enhances expression of functional estrogen receptor α (ER) in ER negative human breast cancer cells in combination with 5-aza 2'-deoxycytidine. *Breast Cancer Res. Treat.* **81**, 177–186 (2003).

48. Munster, P. N. *et al.* A phase II study of the histone deacetylase inhibitor vorinostat combined with tamoxifen for the treatment of patients with hormone therapy-resistant breast cancer. *Br. J. Cancer* **104**, 1828–1835 (2011).

49. Nahta, R. & Esteva, F. J. HER2 therapy: Molecular mechanisms of trastuzumab resistance. *Breast Cancer Research* **8**, (2006).

50. Chan, A. *et al.* Neratinib after trastuzumab-based adjuvant therapy in patients with HER2-positive breast cancer (ExteNET): A multicentre, randomised, double-blind, placebo-controlled, phase 3 trial. *Lancet Oncol.* **17**, 367–377 (2016).

51. Graul, A. I. Promoting, improving and accelerating the drug development and approval processes. *Drug News Perspect.* **22**, 30–38 (2009).

52. Livshits, Z., Rao, R. B. & Smith, S. W. An approach to chemotherapy-associated toxicity. *Emergency Medicine Clinics of North America* **32**, 167–203 (2014).

53. Sun, J. *et al.* A systematic analysis of FDA-approved anticancer drugs. *BMC Syst. Biol.* **11**, (2017).

54. Ghodsi, R., Azizi, E. & Zarghi, A. Design, Synthesis and Biological Evaluation of4-(Imidazolylmethyl)-2-(4-methylsulfonyl phenyl)-Quinoline Derivatives as Selective COX-2 Inhibitors and In-vitro Anti-breast Cancer Agents. *Iran. J. Pharm. Res. IJPR* **15**, 169–177 (2016).

55. Mohammadhosseini, N. *et al.* Novel N-2-(Furyl)-2-(chlorobenzyloxyimino) Ethyl Piperazinyl Quinolones: Synthesis, Cytotoxic Evaluation and Structure-Activity Relationship. *Iran. J. Pharm. Res. IJPR* **14**, 1095–1103 (2015).

56. Ahmed, M. F., Belal, A. & Youns, M. Design, synthesis, molecular modeling and anti-breast cancer activity of novel quinazolin-4-one derivatives linked to thiazolidinone, oxadiazole or pyrazole moieties. *Med. Chem. Res.* **24**, 2993–3007 (2015).

57. Yin, S. *et al.* Design, synthesis and biological evaluation of novel EGFR/HER2 dual inhibitors bearing a oxazolo[4,5-g]quinazolin-2(1H)-one scaffold. *Eur. J. Med. Chem.* **120**, 26–36 (2016).

58. Yellapu, N. K. *et al.* Design, synthesis, in silico, and in vitro evaluation of novel pyrimidine phosphonates with cytotoxicity against breast cancer cells. *Med. Chem. Res.* **23**, 317–328 (2014).

59. Kostakis, I. K. *et al.* Design, synthesis and cell growth inhibitory activity of a series of novel aminosubstituted xantheno[1,2-d]imidazoles in breast cancer cells. *Bioorganic Med. Chem.* **16**, 3445–3455 (2008).

60. Basli, A., Belkacem, N. & Amrani, I. Health Benefits of Phenolic Compounds Against Cancers. in *Phenolic Compounds - Biological Activity* (InTech, 2017). doi:10.5772/67232

61. Huang, W. Y., Cai, Y. Z. & Zhang, Y. Natural phenolic compounds from medicinal herbs and dietary plants: Potential use for cancer prevention. *Nutrition and Cancer* **62**, 1–20 (2010).

62. Aires, A. Phenolics in Foods: Extraction, Analysis and Measurements. in *Phenolic Compounds - Natural Sources, Importance and Applications* (InTech, 2017). doi:10.5772/66889

63. Vogt, T. Phenylpropanoid biosynthesis. *Molecular Plant* **3**, 2–20 (2010).

64. Ghasemzadeh, A. & Jaafar, H. Z. E. Profiling of phenolic compounds and their antioxidant and anticancer activities in pandan (Pandanus amaryllifolius Roxb.) extracts from different locations of Malaysia. *BMC Complement. Altern. Med.* **13**, (2013).

65. Zhang, X. *et al.* Ferulic acid exerts antitumor activity and inhibits metastasis in breast cancer cells by regulating epithelial to mesenchymal transition. *Oncol. Rep.* **36**, 271–278 (2016).

66. De, P., Baltas, M. & Bedos-Belval, F. Cinnamic Acid Derivatives as Anticancer Agents-A Review. *Curr. Med. Chem.* **18**, 1672–1703 (2011).

67. Hundsdörfer, C. *et al.* Indeno[1,2-b]indole derivatives as a novel class of potent human protein kinase CK2 inhibitors. *Bioorg. Med. Chem.* **20**, 2282–2289 (2012).

68. Du, L. *et al.* New alkaloids and diterpenes from a deep ocean sediment derived fungus Penicillium sp. *Tetrahedron* **65**, 1033–1039 (2009).

69. Takahashi, N., Honda, T. & Ohba, T. Anticancer and superoxide scavenging activities of p-alkylaminophenols having various length alkyl chains. *Bioorganic Med. Chem.* **14**, 409–417 (2006).

70. Lin, P. Y. *et al.* Anti-cancer effects of 3,5-dimethylaminophenol in A549 lung cancer cells. *PLoS One* **13**, (2018).

71. Wang, H. *et al.* N-(4-Hydroxyphenyl)retinamide increases dihydroceramide and synergizes with dimethylsphingosine to enhance cancer cell killing. *Mol. Cancer Ther.* **7**, 2967–2976 (2008).

72. Tulipani, S. *et al.* Antioxidants, phenolic compounds, and nutritional quality of different strawberry genotypes. in *Journal of Agricultural and Food Chemistry* **56**, 696–704 (2008).

73. Ratnam, D. V., Ankola, D. D., Bhardwaj, V., Sahana, D. K. & Kumar, M. N. V. R. Role of antioxidants in prophylaxis and therapy: A pharmaceutical perspective. *Journal of Controlled Release* **113**, 189–207 (2006).

74. Huang, W. Y., Zhang, H. C., Liu, W. X. & Li, C. Y. Survey of antioxidant capacity and phenolic composition of blueberry, blackberry, and strawberry in Nanjing. *Journal of Zhejiang University: Science B* **13**, 94–102 (2012).

75. Liu, M. *et al.* Antioxidant and antiproliferative activities of raspberries. *J. Agric. Food Chem.* **50**, 2926–2930 (2002).

76. Losada-Echeberría, M., Herranz-López, M., Micol, V. & Barrajón-Catalán, E. Polyphenols as promising drugs against main breast cancer signatures. *Antioxidants* **6**, (2017).

77. Soule, H. D., Vazquez, J., Long, A., Albert, S. & Brennan, M. A human cell line from a pleural effusion derived from a breast carcinoma. *J. Natl. cancer Inst.* **51**, 1409–1416 (1973).

78. Dai, X., Cheng, H., Bai, Z. & Li, J. Breast cancer cell line classification and Its relevance with breast tumor subtyping. *Journal of Cancer* **8**, 3131–3141 (2017).

79. Palanivel, S., Murugesan, A., Yli-Harja, O. & Kandhavelu, M. Anticancer activity of THMPP: Downregulation of PI3K/ S6K1 in breast cancer cell line. *Saudi Pharm. J.* **28**, 495–503 (2020).

80. Baguley, B. C. & Leung, E. Breast Cancer Cell Lines. **2**, (1995).

81. Garbar, C., Mascaux, C., Giustiniani, J., Merrouche, Y. & Bensussan, A. Chemotherapy treatment induces an increase of autophagy in the luminal breast cancer cell MCF7, but not in the triple-negative MDA-MB231. *Sci. Rep.* **7**, 1–11 (2017).

82. Fogh, J. & Trempe, G. New Human Tumor Cell Lines. in *Human Tumor Cells in Vitro* 115–159 (Springer US, 1975). doi:10.1007/978-1-4757-1647-4_5

83. SK-BR-3: Human Breast Cancer Cell Line (ATCC HTB-30) | Memorial Sloan Kettering Cancer Center. Available at: https://www.mskcc.org/research-advantage/support/technology/tangible-material/human-breast-cell-line-sk-br-3. (Accessed: 2nd July 2021)

84. Suvarna, V., Murahari, M., Khan, T., Chaubey, P. & Sangave, P. Phytochemicals and PI3K inhibitors in cancer-An insight. *Frontiers in Pharmacology* **8**, 916 (2017).

85. Dua, R. *et al.* EGFR over-expression and activation in high HER2, ER negative breast cancer cell line induces trastuzumab resistance. *Breast Cancer Res. Treat.* **122**, 685–697 (2010).

86. Brigger, D., Schläfli, A. M., Garattini, E. & Tschan, M. P. Activation of RARα induces autophagy in SKBR3 breast cancer cells and depletion of key autophagy genes enhances ATRA toxicity. *Cell Death Dis.* **6**, e1861–e1861 (2015).

87. Zordoky, B. N. M. & El-Kadi, A. O. S. H9c2 cell line is a valuable in vitro model to study the drug metabolizing enzymes in the heart. *J. Pharmacol. Toxicol. Methods* **56**, 317–322 (2007).

88. Peng, K. *et al.* Novel EGFR inhibitors attenuate cardiac hypertrophy induced by angiotensin II. *J. Cell. Mol. Med.* **20**, 482–494 (2016).

89. Cell line profile MDA-MB-231 (ECACC catalogue no. 92020424).

90. Guo, Y. & Pei, X. Tetrandrine-Induced Autophagy in MDA-MB-231 Triple-Negative Breast Cancer Cell through the Inhibition of PI3K/AKT/mTOR Signaling. *Evidence-based Complement. Altern. Med.* **2019**, (2019).

91. Meerloo, J. Van, Cloos, J., Van Meerloo, J. & Kaspers, G. J. L. Cell sensitivity assays: The MTT assay IN2016 View project RNA profiling in liquid biopsies to predict MTX efficacy in Rheumatoid Arthritis and Acute Lymphoblastic Leukemia. View project Chapter 20 Cell Sensitivity Assays: The MTT Assay. *Artic. Methods Mol. Biol.* (2011). doi:10.1007/978-1-61779-080-5_20

92. Berridge, M. V. & Tan, A. S. Characterization of the Cellular Reduction of 3-(4,5-dimethylthiazol-2- yl)-2,5-diphenyltetrazolium bromide (MTT): Subcellular Localization, Substrate Dependence, and Involvement of Mitochondrial Electron Transport in MTT Reduction. *Arch. Biochem. Biophys.* **303**, 474–482 (1993).

93. Mosmann, T. Rapid colorimetric assay for cellular growth and survival:

application to proliferation and cytotoxicity assays. *J. Immunol. Methods* **65**, 55–63 (1983).

94. Wong, R. S. Y. Apoptosis in cancer: from pathogenesis to treatment. *J. Exp. Clin. Cancer Res.* **30**, 87 (2011).

95. Thornberry, N. A. The caspase family of cysteine proteases. *British Medical Bulletin* **53**, 478–490 (1997).

96. Chang, H. Y. & Yang, X. Proteases for Cell Suicide: Functions and Regulation of Caspases. *Microbiol. Mol. Biol. Rev.* **64**, 821–846 (2000).

97. Martin, S. J. Caspases: Executioners of Apoptosis. in *Pathobiology of Human Disease: A Dynamic Encyclopedia of Disease Mechanisms* 145–152 (Elsevier Inc., 2014). doi:10.1016/B978-0-12-386456-7.01411-8

98. Goldberg, Y. P. *et al.* Cleavage of huntingtin by apopain, a proapoptotic cysteine protease, is modulated by the polyglutamine tract. *Nat. Genet.* **13**, 442–449 (1996).

99. Bradford, M. A Rapid and Sensitive Method for the Quantitation of Microgram Quantities of Protein Utilizing the Principle of Protein-Dye Binding. *Anal. Biochem.* **72**, 248–254 (1976).

100. Kitazumi, I. & Tsukahara, M. Regulation of DNA fragmentation: the role of caspases and phosphorylation. *FEBS J.* **278**, 427–441 (2011).

101. Saadat, Y. R., Saeidi, N., Vahed, S. Z., Barzegari, A. & Barar, J. An update to DNA ladder assay for apoptosis detection. *BioImpacts* **5**, 25–28 (2015).

102. Koopman, G. *et al.* Annexin V for flow cytometric detection of phosphatidylserine expression on B cells undergoing apoptosis. *Blood* **84**, 1415–20 (1994).

103. Rieger, A. M., Nelson, K. L., Konowalchuk, J. D. & Barreda, D. R. Modified annexin V/propidium iodide apoptosis assay for accurate assessment of cell death. *J. Vis. Exp.* 2597 (2011). doi:10.3791/2597

104. Ribble, D., Goldstein, N. B., Norris, D. A. & Shellman, Y. G. A simple technique for quantifying apoptosis in 96-well plates. *BMC Biotechnol.* **5**, 12 (2005).

105. Liu, K., Liu, P. cheng, Liu, R. & Wu, X. Dual AO/EB staining to detect apoptosis in osteosarcoma cells compared with flow cytometry. *Med. Sci. Monit. Basic Res.* **21**, 15–20 (2015).

106. CHOMZYNSKI, P. & Sacchi, N. Single-Step Method of RNA Isolation by Acid Guanidinium Thiocyanate–Phenol–Chloroform Extraction. *Anal. Biochem.* **162**, 156–159 (1987).

107. Malik, A., Singh, H., Andrabi, M., Husain, S. A. & Ahmad, S. Databases and QSAR for cancer research. *Cancer Inform.* **2**, 99–111 (2007).

108. Wildman, S. A. & Crippen, G. M. Three-dimensional molecular descriptors and a novel QSAR method. *J. Mol. Graph. Model.* **21**, 161–70 (2002).

109. Roy, K. *et al.* Validation of QSAR Models. *Underst. Basics QSAR Appl. Pharm. Sci. Risk Assess.* 231–289 (2015). doi:10.1016/B978-0-12-801505-6.00007-7

110. Hoelder, S., Clarke, P. A. & Workman, P. Discovery of small molecule cancer drugs: Successes, challenges and opportunities. *Molecular Oncology* **6**, 155–176 (2012).

111. Sliwoski, G., Kothiwale, S., Meiler, J. & Lowe, E. W. Computational methods in drug discovery. *Pharmacol. Rev.* **66**, 334–395 (2014).

112. Kitazaki, T. *et al.* Gefitinib, an EGFR tyrosine kinase inhibitor, directly inhibits the function of P-glycoprotein in multidrug resistant cancer cells. *Lung Cancer* **49**, 337–343 (2005).

113. Sigismund, S., Avanzato, D. & Lanzetti, L. Emerging functions of the EGFR in cancer. *Molecular Oncology* **12**, 3–20 (2018).

114. Maennling, A. E. *et al.* Molecular targeting therapy against egfr family in breast cancer: Progress and future potentials. *Cancers (Basel).* **11**, (2019).

115. Bethune, G., Bethune, D., Ridgway, N. & Xu, Z. Epidermal growth factor receptor (EGFR) in lung cancer: An overview and update. *Journal of Thoracic Disease* **2**, 48–51 (2010).

116. Madhavi Sastry, G., Adzhigirey, M., Day, T., Annabhimoju, R. &

Sherman, W. Protein and ligand preparation: Parameters, protocols, and influence on virtual screening enrichments. *J. Comput. Aided. Mol. Des.* **27**, 221–234 (2013).

117. Choowongkomon, K., Sawatdichaikul, O., Songtawee, N. & Limtrakul, J. Receptor-based virtual screening of EGFR kinase inhibitors from the NCI diversity database. *Molecules* **15**, 4041–4054 (2010).

118. Friesner, R. A. *et al.* Extra precision glide: Docking and scoring incorporating a model of hydrophobic enclosure for protein-ligand complexes. *J. Med. Chem.* **49**, 6177–6196 (2006).

119. Jacobson, M. P. *et al.* A Hierarchical Approach to All-Atom Protein Loop Prediction. *Proteins Struct. Funct. Genet.* **55**, 351–367 (2004).

120. Verma, G. *et al.* Pharmacophore modeling, 3D-QSAR, docking and ADME prediction of quinazoline based EGFR inhibitors. *Arab. J. Chem.* **12**, 4815–4839 (2019).

121. Cho, A. E., Guallar, V., Berne, B. J. & Friesner, R. Importance of accurate charges in molecular docking: Quantum Mechanical/Molecular Mechanical (QM/MM) approach. *J. Comput. Chem.* **26**, 915–931 (2005).

122. Liao, Q.-H., Gao, Q.-Z., Wei, J. & Chou, K.-C. Docking and Molecular Dynamics Study on the Inhibitory Activity of Novel Inhibitors on Epidermal Growth Factor Receptor (EGFR). *Med. Chem. (Los. Angeles).* **7**, 24–31 (2010).

123. Palanivel, S., Yli-Harja, O. & Kandhavelu, M. Alkylamino Phenol Derivative Induces Apoptosis by Inhibiting EGFR Signaling Pathway in Breast Cancer Cells. *Anticancer. Agents Med. Chem.* **20**, 809–819 (2020).

124. Palanivel, S., Murugesan, A., Subramanian, K., Yli-Harja, O. & Kandhavelu, M. Antiproliferative and apoptotic effects of indole derivative, N-(2-hydroxy-5-nitrophenyl (4'-methylphenyl) methyl) indoline in breast cancer cells. *Eur. J. Pharmacol.* **881**, 173195 (2020).

125. Palanivel, S., Yli-Harja, O. & Kandhavelu, M. Molecular interaction study of novel indoline derivatives with EGFR-kinase domain using multiple computational analysis. *J. Biomol. Struct. Dyn.* **0**, 1–10 (2021).

126. Karjalainen, A. *et al.* Synthesis of Phenol-derivatives and Biological Screening for Anticancer Activity. *Anticancer. Agents Med. Chem.* **17**, 1710–1720 (2018).

127. Kolahi, M., Tabandeh, M., Saremy, S., Hosseini, S. & Hashemitabar, M. The Study of Apoptotic Effect of p-Coumaric Acid on Breast Cancer Cells MCF-7. *SSU_Journals* **24**, 211–221 (2016).

128. Wang, K., Zhu, X., Zhang, K., Zhu, L. & Zhou, F. Investigation of Gallic acid induced anticancer effect in human breast carcinoma MCF-7 cells. *J. Biochem. Mol. Toxicol.* **28**, 387–393 (2014).

129. Chen, C.-J. *et al. (2E)-N,N-dibutyl-3-(4-hydroxy-3-methoxyphenyl) acrylamide induces apoptosis and cell cycle arrest in HL-60 cells. Anticancer research* **27**, (2007).

130. Collins, J. A., Schandl, C. A., Young, K. K., Vesely, J. & Willingham, M. C. Major DNA fragmentation is a late event in apoptosis. *J. Histochem. Cytochem.* **45**, 923–934 (1997).

131. Jäger, R. & Zwacka, R. M. The enigmatic roles of caspases in tumor development. *Cancers* **2**, 1952–1979 (2010).

132. Jänicke, R. U., Sprengart, M. L., Wati, M. R. & Porter, A. G. Caspase-3 is required for DNA fragmentation and morphological changes associated with apoptosis. *J. Biol. Chem.* **273**, 9357–9360 (1998).

133. Kagawa, S. *et al.* Deficiency of Caspase-3 in MCF7 Cells Blocks Bax-mediated Nuclear Fragmentation but not Cell Death. *Clin. Cancer Res.* **7**, 1474 LP – 1480 (2001).

134. Yang, X.-H. *et al.* Reconstitution of Caspase 3 Sensitizes MCF-7 Breast Cancer Cells to Doxorubicin- and Etoposide-induced Apoptosis. *Cancer Res.* **61**, 348 LP – 354 (2001).

135. Liu, P., Cheng, H., Roberts, T. M. & Zhao, J. J. Targeting the phosphoinositide 3-kinase pathway in cancer. *Nature Reviews Drug Discovery* **8**, 627–644 (2009).

136. Fruman, D. A. *et al.* The PI3K Pathway in Human Disease. *Cell* **170**, 605–635 (2017).

137. Bärlund, M. *et al.* Detecting activation of ribosomal protein S6 kinase by complementary DNA and tissue microarray analysis. *J. Natl. Cancer Inst.* **92**, 1252–1259 (2000).

138. Holz, M. K. The role of S6K1 in ER-positive breast cancer. *Cell Cycle* **11**, 3159–65 (2012).

139. Sridharan, S. & Basu, A. Distinct roles of mTOR targets S6K1 and S6K2 in breast cancer. *International Journal of Molecular Sciences* **21**, (2020).

140. Wang, Y. *et al.* PI3K inhibitor LY294002, as opposed to wortmannin, enhances AKT phosphorylation in gemcitabine-resistant pancreatic cancer cells. *Int. J. Oncol.* **50**, 606–612 (2017).

141. Yang, Q., Modi, P., Newcomb, T., Quéva, C. & Gandhi, V. Idelalisib: First-in-class PI3K delta inhibitor for the treatment of chronic lymphocytic leukemia, small lymphocytic leukemia, and follicular lymphoma. *Clin. Cancer Res.* **21**, 1537–1542 (2015).

142. Nam, K. H. *et al.* Identification of a novel S6K1 inhibitor, rosmarinic acid methyl ester, for treating cisplatin-resistant cervical cancer. *BMC Cancer* **19**, (2019).

143. Singh, D., Kumar Attri, B., Kaur Gill, R. & Bariwal, J. Review on EGFR Inhibitors: Critical Updates. *Mini-Reviews Med. Chem.* **16**, 1134–1166 (2016).

144. Xu, X. *et al.* Research and development of anticancer agents under the guidance of biomarkers. *Cancer Transl. Med.* **5**, 17 (2019).

145. Ayati, A. *et al.* A review on progression of epidermal growth factor receptor (EGFR) inhibitors as an efficient approach in cancer targeted therapy. *Bioorg. Chem.* **99**, 103811 (2020).

146. Dobashi, Y. *et al.* Critical and diverse involvement of Akt/mammalian target of rapamycin signaling in human lung carcinomas. *Cancer* **115**, 107–118 (2009).

147. Shaik, N. A., Al-Kreathy, H. M., Ajabnoor, G. M., Verma, P. K. & Banaganapalli, B. Molecular designing, virtual screening and docking study of novel curcumin analogue as mutation (S769L and K846R) selective inhibitor for EGFR. *Saudi J. Biol. Sci.* **26**, 439–448 (2019).

148. Shahare, H. V. & Talele, G. S. Designing of benzothiazole derivatives as promising EGFR tyrosine kinase inhibitors: a pharmacoinformatics study. *J. Biomol. Struct. Dyn.* **38**, 1365–1374 (2020).

149. Mahmoud, S. *et al.* Design, Synthesis, Antitumor Activity and Molecular Docking Study of Novel 5-Deazaalloxazine Analogs. *Molecules* **25**, (2020).

150. Acharya, R., Chacko, S., Bose, P., Lapenna, A. & Pattanayak, S. P. Structure Based Multitargeted Molecular Docking Analysis of Selected Furanocoumarins against Breast Cancer. *Sci. Rep.* **9**, (2019).

151. GLOBOCAN 2020: New Global Cancer Data | UICC. Available at: https://www.uicc.org/news/globocan-2020-new-global-cancer-data. (Accessed: 25th August 2021)

PUBLICATIONS

I

Anticancer activity of THMPP: Downregulation of PI3K/ S6K1 in breast cancer cell line

Palanivel S, Murugesan A, Yli-Harja O, and Kandhavelu M

Saudi Pharmaceutical Journal, Volume 28(4), 19 March 2020, Pages 495-503.

doi.org: 10.1016/j.jsps.2020.02.015

Saudi Pharmaceutical Journal 28 (2020) 495–503

Contents lists available at ScienceDirect

Saudi Pharmaceutical Journal

journal homepage: www.sciencedirect.com

Original article

Anticancer activity of THMPP: Downregulation of PI3K/ S6K1 in breast cancer cell line

Suresh Palanivel [a,b], Akshaya Murugesan [a,b,c], Olli Yli-Harja [b,d,e], Meenakshisundaram Kandhavelu [a,b,*]

[a] Molecular Signaling Lab, Faculty of Medicine and Health Technology, Tampere University and BioMediTech, Tays Cancer Center, Tampere University Hospital, P.O. Box 553, 33101 Tampere, Finland
[b] Institute of Biosciences and Medical Technology, 33101 Tampere, Finland
[c] Department of Biotechnology, Lady Doak College, Thallakulam, Madurai 625002, India
[d] Computaional Systems Biology Group, Faculty of Medicine and Health Technology, Tampere University and BioMediTech, Tays Cancer Center, Tampere University Hospital, P.O. Box 553, 33101 Tampere, Finland
[e] Institute for Systems Biology, 1441N 34th Street, Seattle, WA 98103-8904, USA

ARTICLE INFO

Article history:
Received 15 January 2020
Accepted 29 February 2020
Available online 19 March 2020

Keywords:
Tetrahydroquinoline
Apoptosis
Gene expression
EGFR
Docking
ADME
QSAR

ABSTRACT

Breast cancer is the most common cancer that majorly affects female. The present study is focused on exploring the potential anticancer activity of 2-((1, 2, 3, 4-Tetrahydroquinolin-1-yl) (4 methoxyphenyl) methyl) phenol (THMPP), against human breast cancer. The mechanism of action, activation of specific signaling pathways, structural activity relationship and drug-likeness properties of THMPP remains elusive. Cell proliferation and viability assay, caspase enzyme activity, DNA fragmentation and FITC/Annexin V, AO/EtBr staining, RT-PCR, QSAR and ADME analysis were executed to understand the mode of action of the drug. The effect of THMPP on multiple breast cancer cell lines (MCF-7 and SkBr3), and non-tumorigenic cell line (H9C2) was assessed by MTT assay. THMPP at IC_{50} concentration of 83.23 μM and 113.94 μM, induced cell death in MCF-7 and SkBr3 cells, respectively. Increased level of caspase-3 and -9, fragmentation of DNA, translocation of phosphatidylserine membrane and morphological changes in the cells confirmed the effect of THMPP in inducing the apoptosis. Gene expression analysis has shown that THMPP was able to downregulate the expression of PI3K/S6K1 genes, possibly via EGFR signaling pathway in both the cell lines, MCF-7 and SkBr3. Further, molecular docking also confirms the potential binding of THMPP with EGFR. QSAR and ADME analysis proved THMPP as an effective anti-breast cancer drug, exhibiting important pharmacological properties. Overall, the results suggest that THMPP induced cell death might be regulated by EGFR signaling pathway which augments THMPP being developed as a potential candidate for treating breast cancer.

1. Introduction

Breast cancer is the most challenging type of cancer worldwide. In 2018, about 2.1 million new breast cancer cases have been diagnosed. In over 100 countries, it ranks as the leading causes of cancer death (Bray et al., 2018). Estrogen receptors (ER) are responsible for approximately 70–75% of inter-tumor heterogeneic nature of breast cancer. Estrogens on binding to ER is responsible for the transcription/expression of many growth factors involving cellular proliferation (Sun et al., 2001). Apart from estrogens, there are many non-steroidal growth factors including EGF and IGF1, that can bind to ER and stimulate proliferation via signal transduction pathways like MAPK pathway (Kato et al., 1995). Progesterone receptor (PR) also plays an equal importance in cancer development and progression as ER.

Abbreviations: THMPP, 2-((1, 2, 3, 4-Tetrahydroquinolin-1-yl) (4 methoxyphenyl) methyl) phenol; IC_{50}, The half maximal inhibitory concentration; FITC, Fluorescein isothiocyanate; AO/EtBr, Acridine orange/ethidium bromide; RTPCR, Reverse Transcriptase PCR; QSAR, Quantitative structure activity relationship; ADME-Absorption, Distribution, Metabolism, and Excretion; MCF-7, Michigan Cancer Foundation-7; SkBr3, Sloan–Kettering Cancer Center; EGFR, Epidermal Growth Factor Receptor; ER, Estrogen Receptor; PR, Progesterone Receptor; PI3K, Phosphoinositide 3-kinase; FACS, Fluorescence-activated cell sorting.

* Corresponding author.
E-mail addresses: suresh.palanivel@tuni.fi (S. Palanivel), akshaya.murugesan@tuni.fi (A. Murugesan), olli.yli-harja@tuni.fi (O. Yli-Harja), meenakshisundaram.kandhavelu@tuni.fi (M. Kandhavelu).

Peer review under responsibility of King Saud University.

ELSEVIER Production and hosting by Elsevier

https://doi.org/10.1016/j.jsps.2020.02.015
1319-0164/

The treatment regimens followed in ER+/PR+ breast cancer cases are mostly hormonal/endocrine therapy. It is done by blocking the ER, in-turn controlling the growth promoting effects on the cell. Though, it is recognized as an effective treatment for ER+/PR+ patients, most of the patience develops resistance to such therapies. There is a vital need for the novel therapies over the existing hormonal therapies, thereby extending the progression period, eliminating or reducing the resistance and postpone the chemotherapy (Ciruelos Gil, 2014).

In accordance with this, our research group indulges in synthesis of novel small molecule drugs for multiple cancer treatments. One such phenolic derivatives is, 2-((1, 2, 3, 4-Tetrahydroquinolin-1-yl) (4 methoxyphenyl) methyl) phenol (THMPP), found to have good cytotoxicity activity against bone carcinoma cells (Karjalainen et al., 2017). We hypothesize that THMPP might have anticancer activity against breast cancer and hence we wish to explore the mechanism of its action of the compound THMPP against breast cancer cells.

The present study also signifies that THMPP can induce cell death in breast cancer cells via EGFR signaling pathway. The EGFR overexpressed in metastatic breast cancer cells that influences the downstream signaling pathways such as the ERK MAPK, PI3K-AKT, SRC, PLC-γ1-PKC, JNK, and JAK-STAT pathways. The PI3K/AKT/mTOR pathway is the well-known signaling pathway involved in cell proliferation and survival. In tumorigenesis, this signal cascade is continuously activated even in the absence of any growth factors/ligands. Inhibition of this pathway can suppress the tumor growth and eventually benefit the ER+ patient through endocrine therapy (Martelli et al., 2010). Hence, we also propose to investigate the effect of THMPP in the regulation of PI3K signaling pathway genes in combination with computational analysis.

2. Materials and methods

2.1. Cell lines and culture

Human breast adenocarcinoma cell lines, MCF-7, SkBr3; Triple negative breast cancer cells, MDAMB-231; and rat myoblast cells, H9C2, were obtained from NCCS, Pune. All the cell lines used in the study was EGFR (+). Cells were cultured in Dulbecco's Modified Eagle Medium (DMEM), supplemented with 10% Fetal Bovine Serum (FBS), maintained at 37 °C humidified with 5% CO_2 (Vaiyapuri et al., 2015). THMPP (Fig. 1a) was synthesized by our research group as previously described. Untreated cells were used as a negative control with cyclophosphamide, as a positive control (Fig. 1b). The characterization of the chemical compound and the preparation of THMPP was described in the previously established procedure (Doan et al., 2019, 2017). NMR spectroscopic data of the compound was included as the supplementary file (Supplementary file 1).

2.2. Cytotoxicity assay

The cytotoxicity potential of THMPP against the growth of breast cancer cells were analyzed using MTT assay (Mosmann, 1983). The cell density of 1.2×10^4 cells/well were plated in 96 well plates and maintained at 37 °C overnight. Cells were treated with varying concentrations of the samples (10, 25, 50, 75 and 100 μM) for 24 h, followed by the addition of 100 μl medium with 10 μl of MTT (5 mg/ml). As a comparative study, MDAMB-231 cells were also treated with 10 μM concentration of THMPP. H9C2, non-tumorous cells were used as a control cell line and treated with the lower concentration of 10 μM and higher concentration of 100 μM THMPP. The medium was discarded after 4 h of treatment and the formazan crystals was dissolved using 100 μl of DMSO. The purple color developed was read using microtiter plate reader at 570 nm. Cyclophosphamide was used as the positive control and the cells with the medium (untreated) serves as a control. Cell viability was calculated using the following formula:

$$\text{Viability } \% = \left(\frac{\text{Test OD}}{\text{Control OD}}\right) \times 100; \text{ Cytotoxicity } \% = 100 - \text{Viability}\%.$$

2.3. Caspases 3 and 9 activity

Caspase-3 and -9 activities were measured by colorimetric assay kit, following the manufacturer's protocol (Calbiochem, Merck). Treated cells were lysed using the buffer containing 50 mM HEPES, 100 mM NaCl, 0.1% CHAPS, 1 mM DTT, 100 mM EDTA and centrifuged at 10000 rpm for 1 min. The extracts were carefully collected, and the protein concentration was estimated by Bradford's assay. Approximately, 100–200 μg of protein for each assay was prepared by lysing the cell with 50 μl cell lysis buffer and incubated in 96-well plates with 5 μl of the 4 mM p-nitroanilide (pNA) substrates, DEVD-pNA for 2 h at 37 °C. The Caspase-3 and -9 activities were analysed by measuring the cleaved substrate to free pNA at 405 nm in a microplate reader. The relative level of Caspase-3 and -9 were quantified using the ratio of the absorbance of THMPP treated to untreated cells.

2.4. DNA fragmentation

To study the effect of the compound in apoptosis induction in breast cancer cells, DNA of MCF-7 cells were subjected to electrophoresis. Briefly, MCF-7 cells were lysed using 100 μl of cell lysis buffer for one hour at room temperature, and the cell debris was removed by centrifugation for 15 min at 3000 rpm at 4° C. The supernatant was then mixed with equal volume of phenol: chloroform: isoamyl alcohol mixture, and then centrifuged at 5000 rpm for 15 min. The DNA was precipitated on adding 40 μl of 3.5 M ammonium acetate and ice-cold isopropanol to the aqueous phase and incubated at −20 °C for 1 h. The sample was centrifuged at 10000 rpm for 15 min and the pellet was washed with 70% ethanol and stored in 20–50 μl of TE buffer. DNA samples were electrophoresed at 50 V in 2% agarose gel (*w*/*v*). DNA was detected using EtBr staining under UV light along with DNA ladder (1 kb) as control (Basnakian and James, 1994).

2.5. RNA extraction and CDNA synthesis

Total cellular RNA from both the untreated and treated MCF-7 cells were extracted using ONE STEP-RNA Reagent (Bio Basic Canada Inc.). This method is an improved version of single-step RNA isolation using phenol and guanidine isothiocyanate (Chomzynski and Sacchi, 1987). RNA pellet was extracted and vacuum dried for 5–10 min, dissolved in DEPC treated water and stored at −20 °C. The isolated RNA (1–2 μg) was immediately reverse transcribed using EasyScript Plus™ Reverse Transcriptase primed using oligo-dT. The reaction mixture consists of 1–2 μg of RNA, 2 μl oligo-dT (stock 10 μM), with the total volume of 12.5 μl with DEPC-treated water. The mixture was incubated at 65 °C for 5 min and 1X reverse transcriptase buffer, 2.5 mM of dNTP mix, and 40 U/μl of RNase inhibitor were added in specified order. Finally, 1 μl of Easy Script reverse transcriptase (200 U/μl) was added after 5 min of incubation at 42 °C. The final reaction was set up at 42 °C for 50 min, heated up to 70 °C for 10 min and chilled on ice (Chomzynski and Sacchi, 1987).

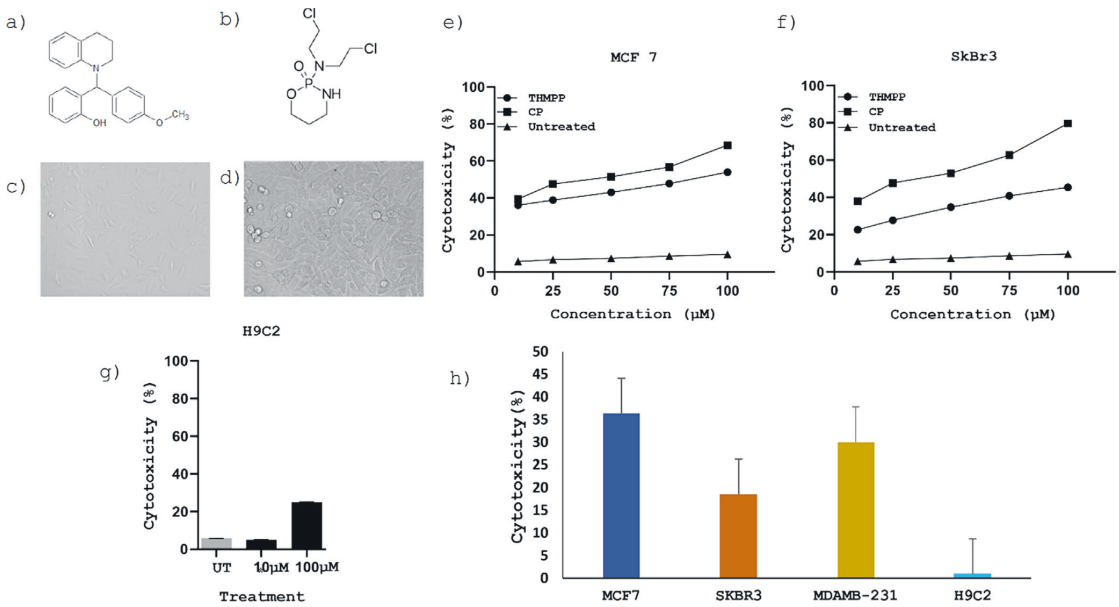

Fig. 1. Cytotoxicity effect of THMPP in different breast cancer cell lines. (a) and (b)- Ligand structure: 2D structure of THMPP and CP. IUPAC: – 2-((1, 2, 3, 4-Tetrahydroquinolin-1-yl) (4 methoxyphenyl) methyl) phenol and N,N-bis(2-chloroethyl)-2-oxo-1,3,2λ^5-oxazaphosphinan-2-amine, respectively; M. wt – 329.443 and 261.083. The phase contrast microscopic images of MCF-7 cell line (c) untreated and (d) treated. Cell cytotoxicity of THMPP in different cell lines by MTT assay (e) MCF-7 cells (f) SkBr3 cells at different concentration (10 μM, 25 μM, 50 μM, 75 μM and 100 μM) and (g) Treatment of H9C2 cells with10μM and 100 μM of THMPP. Cyclophosphamide was used as a positive control; (h) Percentage of growth inhibition in multiple breast cancer cell lines and non-tumorous cells treated with 10 μM THMPP. Data points and error bars represent mean ± S.E.M (n = 3 per group). Statistical significance was assumed for p-values *P < 0.0001.

2.6. Reverse transcription polymerase chain reaction (RT-PCR) analysis

Amplification of the target genes *EGFR*, *PI3K*, *S6K1* and β-actin were achieved using specific forward and reverse primers. β- actin, that shows the constitutive expression was used as a control for the gene expression analysis. The primers for the target mRNA were used as follows: *EGFR*, Fw: 5′- TCCCCGTAATTATGTGGT GACA GATC-3′ and Rv: 5′-ACCCCTAAATGCCACCGGC-3′ with the amplicon size 250 bp; *PI3K*, Fw: 5′-AACACAGAAGACCAATACTC-3′ and Rv: 5′-TTCGCCATCTACCACTAC-3′ with the amplicon size of 195 bp; *S6K1*, Fw: 5′-CACATAACCTGTGGTCTGTTGCTG-3′ and Rv: 5′- AGA TGCA AAGCGAACTTGGGATA-3′ with the amplicon size of 180 bp; and for reference gene *β- actin*, Fw: 5′-CACCCGCGAGTACAACCTT-3′ and Rv: 5′-CCCATACCCACCATCACACC-3′ with the amplicon size of 204 bp, were synthesized and used further for PCR reactions.

The PCR reaction was setup using the following reagents: 1X Taq Buffer (with $MgCl_2$), 0.2 mM dNTPs, 2.5 mM $MgCl_2$, 0.3 μM forward and reverse primer, template cDNA (10% of the reaction) and 1U Taq Polymerase. Amplification was performed with the following PCR conditions: initial denaturation at 94° C for 2 min and 32 cycles of 94° C for 30 s, T_a for 1 min, 72° C for 1 min 20 s with the final extension at 72° C for 7 min. T_a was specifically optimized for each gene such as 56° C for *EGFR*, 54° C for *PI3K*, 56° C for *S6K1* and 54° C for β- actin. The amplicons were separated on 1.5% agarose gel with 100 bp ladder was as a marker at 50 V for 90 min. Image J software was used to quantify the band intensity.

2.7. FACS analysis

FACS analysis was performed to check the apoptotic induction in MCF-7 cells after treatment with THMPP using FITC Annexin V (Vermes et al., 1995). FITC Annexin V stained cells negative to propidium iodide (PI) represents apoptotic cells, FITC Annexin V/PI stained cells represents late apoptosis/ necrotic cells, whereas FITC Annexin V/PI negative cells represents live cells (Koopman et al., 1994). MCF-7 cells (1×10^5 cells/sample) were treated with the IC_{50} concentration of THMPP and 5 μl of FITC Annexin V and 5 μl PI were added and then incubated for 15 min at 25° C in the dark. Binding buffer (1X) was added to each sample and subjected to flow cytometry analysis. The cells were acquired and gated by FITC-A and PE-A. All the measurements were performed within 1 h under similar settings in the equipment.

2.8. ACRIDINE orange/ethidium bromide (AO/ETBR) staining

Apoptosis induction by THMPP in MCF-7 was identified by AO/EtBr dual staining. As explained previously, MCF-7 cells were treated with varying concentrations of THMPP, 78.23 μM, 83.23 μM and 88.23 μM with the control well left untreated. The cells were incubated for 24 h and trypsinised. It was centrifuged, and the pellet was suspended in PBS. To 25 μl of the supernatant solution, 25 μl of staining solution containing 1:1 mixture of 100 μg/ml AO and 100 μg/ml EB was added. The cell suspension (10 μl) was observed under fluorescent microscope using blue (420–495 nm) and green filter (510–560 nm) and at least 300 cells/well was used for quantification in different fields (Basikc et al., 2006; Chowdhury et al., 2012).

2.9. Molecular docking using gold

Automated docking for THMPP against EGFR was performed using the genetic algorithm GOLD (Version 3.2 CCDC, Cambridge,

UK) (Jones et al., 1997b). It has been validated earlier with a data set containing 300 protein-ligand complexes retrieved from PDB (Manikandan and Malik, 2008). To explore the ligand conformation and rotational flexibility of selected receptor, GOLD program makes use of genetic algorithm (GA). Grid box not exceeding 10 Å in size was chosen and the coordinates of the enclosing box (x = 121 Å; y = 87 Å; z = 45 Å) were also described from the active residues. Maximum of 10 different structural conformations for docking was examined and the highest binding conformers were selected for further analysis (Nissink et al., 2002).

2.10. QSAR analysis of THMPP

A quantitative structure-biological activity-property relationship (QSAR) approach was performed to quantitatively depict and provide mechanistic insights into interactions between the chemical structures of THMPP by considering the compounds with similar structures. QSAR is used for testing the relationship between the molecular descriptors of the set of compounds of interest with their respective biological activity (Roy et al., 2015). Here, 32 compounds were selected which share a significant structural similarity with the THMPP. In addition, biological activity in terms of IC_{50} were also collected from the literature (Table 1). The Dragon software calculates the descriptors for the compounds, which has about 1497 descriptors, that are classified into 18 groups. Each molecule in the training set were found to have set of 18 descriptors (Todeschini and Gramatica, 1997). Set of descriptors that are most appropriate to the IC_{50} of the compounds were selected for further analysis, and the MLR models were built and QSAR equations eliminating the variables were established using BUILDQSAR software.

2.11. ADMET analysis

The various pharmacokinetics properties and physiochemical properties of the compound, THMPP were calculated using ADMET descriptors. ADMET can provide metabolic interactions of the drug by profiling its Absorption, Distribution, Metabolism, Excretion and Toxicity properties. The prediction will contain the following important ADMET descriptors such as Blood-Brain Barrier penetration, Human Intestinal Absorption, CYP450 2C9, Caco-2 cell permeability and Ames test. The drug likeliness score of the compound determines the potentiality of the compound.

3. Results

3.1. THMPP induced cytotoxicity effect

To evaluate the effect of THMPP against the human breast cancer cell lines MCF-7 and SkBr3 and the non-cancerous mouse myoblast cells H9C2, the percentage of cell proliferation/cell viability was measured using MTT assay. The phase contrast microscopic images of the treated and untreated MCF-7 cells are represented in Fig. 1c and d. THMPP showed a dose-dependent increase in the cytotoxicity against MCF-7 cells and SkBr3 (Fig. 1e and f). The toxicity of THMPP against MCF-7 and SkBr3 cells was found to be 36.47%, 53.98% and 18.86%, 40.47% at 10 μM and 100 μM, respectively. The IC_{50} concentration of THMPP against was less in MCF-7 with 83.23 μM than SkB3 cells with 113.94 μM (Fig. 1e and f). Cyclophosphamide was used as a positive control, where its cytotoxicity against MCF-7 and SkBr3 was significantly high. The IC_{50} value of CP against MCF-7 and SkBr3 was found to be 42.79 μM and 38.34 μM, respectively (Fig. 1e and f). Also, THMPP

Table 1
List of training set and test set compounds with its IC_{50} values.

Training Set			
S.No	Compound Name	IC_{50}	References
1	2-((1,2,3,4-tetrahydroquinolin-1-yl)(4-methoxyphenyl)methyl)phenol	83.23	Present Study
2	Curcusone B	0.2	Sawadogo et al., 2012
3	Curcusone C	0.08	
4	Curcusone D	0.1	
5	voruscarin	4	
6	Uscharin	4	
7	2-Hydroxy-isojatrogrossidion	0.2	
8	2-epi-hydroxyisojatrogrossidion	0.2	
9	Multidione	5.5	
10	4Z jatrogrossidentadion	0.6	
11	4E jatrogrossidentadion	2.1	
12	Pinostrobin	10.2	
13	Balanitin-6/7	2.6	
14	Jatropholone	7.5	
15	Multi-substituent phenyl derivatives 1	1.38	Tao et al., 2010
16	Multi-substituent phenyl derivatives 4	11.74	
17	Mangrove-derived quinones 7	0.17	
18	Mangrove-derived quinones 8	2.53	
19	Mangrove-derived quinones 9	1.43	
20	Mangrove-derived quinones 11	13.23	
21	Mangrove-derived quinones 13	16.32	
Test Set			
S.No	Compound Name	IC_{50}	References
1	Mangrove-derived quinones 14	35.23	Tao et al., 2010
2	Mangrove-derived quinones 18	17.22	
3	Isoflavone analog 78	19.77	
4	Fatty acid derivatives 81	0.41	
5	Phytol	34	Malek et al., 2008
6	phenolic constituents 4	62.9	El Molla et al., 2016
7	phenolic constituents 6	63.8	

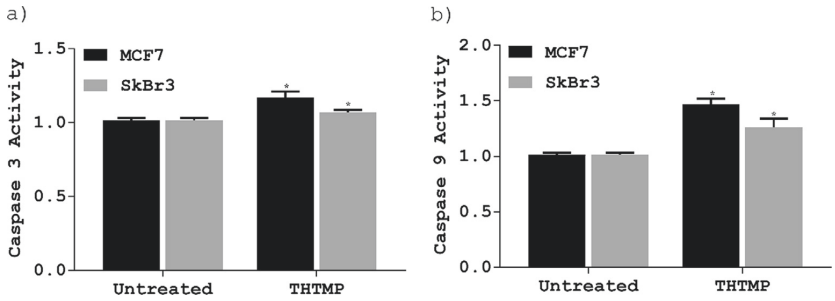

Fig. 2. Caspase-3 and Caspase-9 activity in THMPP treated MCF-7 and SkBr3 cell lines. (a) Relative caspase-3 activity of THMPP treated MCF-7 and SkBr3 compared with the untreated cells. The results were considered significant (two way ANOVA) in comparison with the untreated group (*, $P \leq 0.007$). (b) Relative caspase-9 activity of THMPP treated MCF-7 and SkBr3 compared with the untreated cells. The results were considered significant (two way ANOVA) in comparison with the untreated group (*, $P < 0.0001$). Data represents Mean ± SEM (n = 3 experiment).

has least percentage of cytotoxicity to non-cancerous cells, H9C2 (0.91%) when compared with other breast cancer cell lines such as MCF-7(36%), SkBr3(18%) and MDAMB-231(30%) upon treatment with 10 μM of THMPP (Fig. 1g and h). These results suggested that THMPP has the ability to specifically target breast cancer cell lines than the normal cells. The differences in the treated conditions was found to be statistically significant as per two-way ANOVA (P-val ue < 0.0001).

3.2. Caspase-3 and caspase-9 induction

To clarify whether THMPP could induce apoptosis, caspase-3 and -9 activities were measured in MCF-7 and SkBr3. The cells were treated with the respective IC_{50} concentration of THMPP. In both the cell lines, there was significant fold change in the enzyme activity after the treatment. In MCF-7 cells, it was found that the caspase-3 and -9 activities were increased by a fold level of 0.17 and 0.47, whereas in SkBr3, fold change of 0.07 and 0.25 was observed respectively, when compared to the untreated cells (Fig. 2a and b). Thus, THMPP could activate caspase enzyme activity, thereby induces apoptosis in both the cell lines. The values were statistically significant, as per two-way ANOVA test ($P < 0.0001$).

3.3. Induction of DNA strand break by THMPP

To further substantiate the ability of THMPP in inducing apoptosis, the cells were subjected for DNA fragmentation assay. The DNA fragmentation is a sign of apoptosis, which causes nicks in genomic DNA of the cells (Eastman and Barry, 1992). The genomic DNA from THMPP treated MCF-7 cells was isolated and analysed by agarose gel electrophoresis. The result shows that untreated cells have intact DNA with no laddering whereas treated cells showed a characteristic ladder of inter-nucleosomal fragmentation, confirming the induction of apoptosis (Fig. 3a).

3.4. Analysis of apoptosis induction by THMPP using Annexin V/PI

The phosphatidylserine externalization in MCF-7 cells stained with Annexin V-FITC/PI was quantified by flow cytometry to assess the apoptotic cell death. The analysis showed that THMPP could induce apoptosis in a concentration-dependent manner (Fig. 3). The untreated cells were mostly viable. The cells with compromised membrane were analysed by staining using membrane impermeable dye, PI. Thus the counter staining with PI and Annexin V delineates the cells at different cell phase. The cells treated with THMPP showed 3.21% of early apoptotic cells, 36.02% of late apoptotic cells and 59.7% viable cells (Fig. 3d). This substantiates the effect of THMPP in apoptosis mediated cell death (Fig. 3b and c).

MCF-7 cells were treated with a varying doses of THMPP for 24 h, as described in the method section. Apoptotic cell death causing nuclear fragmentation was assessed upon treatment with varying concentration of THMPP and the cells were observed under flourescent microscope (Fig. 4). The dual AO/EB fluorescent staining qualitatively and quantitatively reveals the morphological

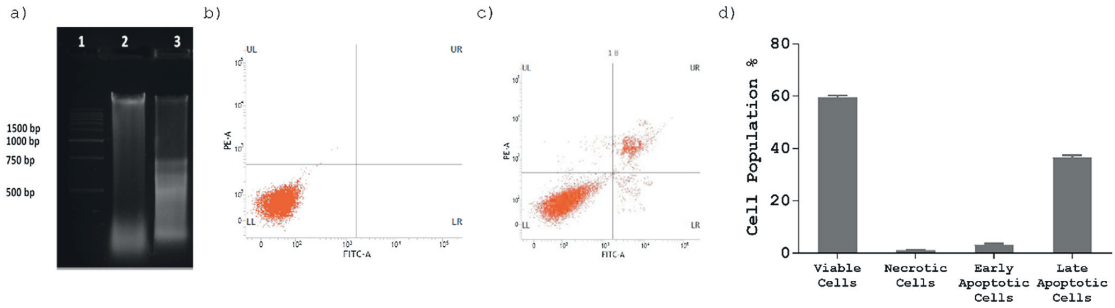

Fig. 3. DNA fragmentation of MCF-7 cells exposed to THMPP (a) DNA gel electrophoresis of internucleosomal DNA fragmentation in 1.5% Agarose gel upon treatment with THMPP in MCF-7 cell lines (lane 1) Marker-1 Kb ladder; (lane 2) negative control without treatment; (lane 3) DNA of cells treated with THMPP. Assessment of apoptosis by FACS of apoptosis in THMPP (IC_{50} – 83.23 μM) treated MCF-7 cells measured using FITC-labelled annexin V/PI (b) untreated cells; (c) THMPP treated MCF-7 cells. UL- necrotic cells, UR- late apoptotic cells, LL - viable cells, LR – early apoptotic cells. (d) Quantitative analysis on the percentage of viable, apoptotic, or necrotic cells by FACS analysis.

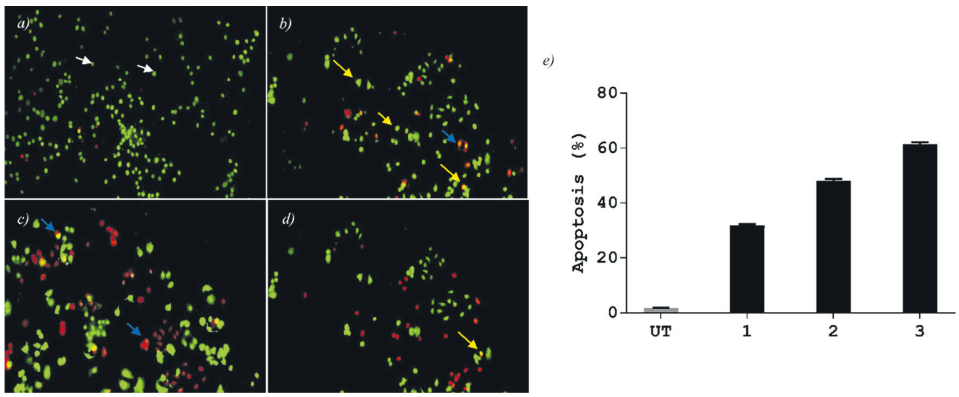

Fig. 4. Fluorescence microscopy images of AO-EtBr stained MCF-7 cells after treatment with THMPP. (a) Untreated cells; MCF-7 cells treated with THMPP at different concentrations (b) 78.23 μM, (c) 83.23 μM and (d) 88.23 μM. The white, yellow and blue arrows are representing viable, early apoptotic, and late apoptotic cells respectively. (e) percentage of apoptosis at different concentrations, where treatment 1 is 78.23 μM; treatment 2 is 83.23 μM; and treatment 3 is 88.23 μM.

changes in apoptotic cells, with clear distinction between normal cells, apoptotic cells, and necrotic cells.

The Fig. 4a–d showed the mode of cell death by dual AO/EB staining. Control cells (untreated MCF-7 cells) are normal healthy cells with green fluorescent cells having normal cytoplasm and nuclei morphology, and represents only less than 2% cells in apoptotic stage. The cells entering early apoptosis appears yellowish green fluorescence with membrane blebbing and those cells in late apoptosis appeared orange/red fluorescence. It is observed that 48% of the cells were in apoptotic stage upon treatment with 83.23 μM of THMPP, 61% cells at 88.23 μM and 32% cells at 78.23 μM of THMPP treatment. As the concentration of the compound increases, there is a significant increase in the apoptosis induction and thus THMPP induces cell death through apoptosis pathway (Fig. 4e).

3.5. Effect of THMPP on the expression of PI3K and S6K1 genes

To further understand the mechanism of action of THMPP, we examined the influence of THMPP in PI3K signaling pathway.

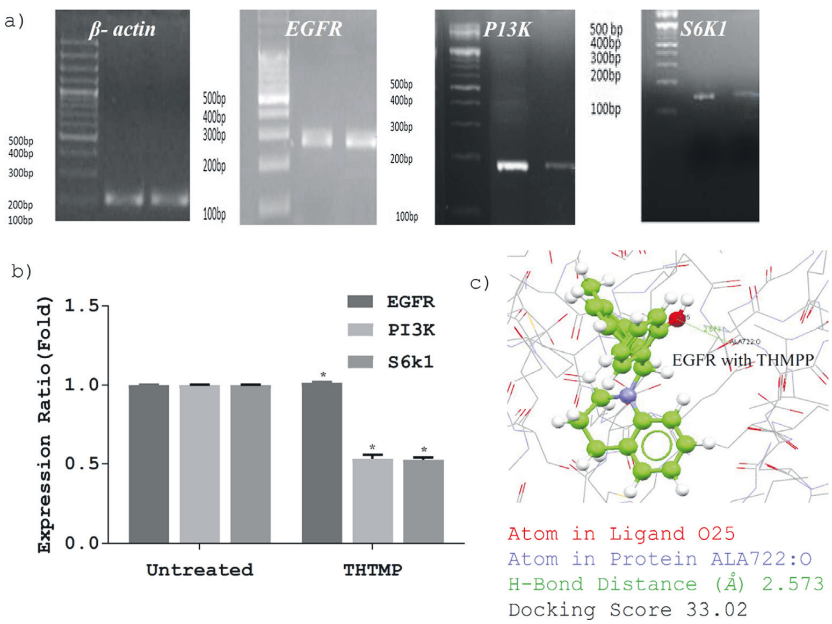

Fig. 5. Gene expression analysis in MCF-7 cell upon THMPP treatment. (a) RT-PCR amplification of *β- actin* (204 bp), *EGFR* (250 bp), *P13K* (195 bp) and *S6K1* genes (180 bp). (Lane 1: 100 bp DNA marker, Lane 2: control (untreated) Lane 3: (PCR amplicon treated with THMPP); (b) Optical density was measured to evaluate the mRNA expression of *EGFR; S6K1; PI3K*, with the housekeeping gene *β-actin* serving as the normalization control. The fold change represented as the expression ratio of the genes. Data points and error bars represent mean ± S.E.M (n = 3 per group). Statistical significance was assumed for p-values *P < 0.0001. (c) Molecular docking analysis of THMPP with EGFR. The surface-docking model of THMPP in the EGFR active site. The ligand is represented as sticks; and the protein active sites as lines, hydrogen bond interaction are shown in dotted lines (Red) and the interacting residues are labelled.

Semi-quantitative RT-PCR was carried out using primers specific for *EGFR, PI3K and S6K1* genes with β-actin as the reference control. The genes with respective band size of 204 bp (β-*actin*), 250 bp (*EGFR*), 195 bp (*PI3K*) and 180 bp (*S6K1*) were observed clearly in agarose gel (Fig. 5a). The ImageJ was used to calculate the expression fold of each gene. EGFR gene expression was not altered upon THMPP treatment when compared with the untreated cell lines. But, there occurs a reduced level of altered gene expression level with 0.5 fold change in both *PI3K* and *S6K1* (Fig. 5b). These results suggest that the THMPP could induce apoptosis by down regulating the expression of genes, *PI3K* and *S6KI* involved in PI3K/AKT signalling pathway (Fig. 5b). The values were found to be statistically significant, as per two way ANOVA test (P-value < 0.0001).

3.6. Molecular docking of THMPP with EGFR

Molecular docking was performed using GOLD (Jones et al., 1997b). The 3D structure of EGFR was availed from protein data bank with the PDB ids: 2RGP. Binding compatibility was evaluated based on the docked energy in kcal/mol (Fig. 5c). The active sites present in the crystal structure of the five receptors were obtained from the pdbsum database which was further used for the docking analysis. The following amino acids are present in the 32 active sites of EGFR receptors, ie., Leu718, Gly719, Ala722, Val726, Ala743, Lys745, Met766, Cys775, Arg776, Leu777, Leu788, Thr790, Gln791, Leu792, Met793, Pro794, Phe795, Gly796, Asp800, Arg803, Arg832, Leu833, Val834, His835, Arg836, Asp837, Leu844, Leu862, His888, Lys913, Lys970, Arg977. Many significant interactions were predicted between the ligand (THMPP) and the receptor (EGFR). The best docking score of 33.02 determines the best interaction. The Fig. 5c represents the docking score and residual values of the interaction.

3.7. THMPP structure activity relationship and its pharmacokinetics properties

BUILDQSAR was used to predict the anti-cancer potential of the compound, THMPP. Based on the compounds selected (Table 1), a QSAR model was built. The regression line was plotted and the compounds that significantly deviate away were considered as outliers and excluded from the modelling procedure. The QSAR model was tested against the compounds in the test set and the predictability of the QSAR model was validated (Fig. 6) using the correlation coefficient value, (r) 0.970 for training set (Fig. 6a) and 0.985 for the test set (Fig. 6b). This shows the efficiency of the model generated and the results clearly indicated that the compound was predicted to be a potent anti-cancer agent. In particular, THMPP correlates well with the equation, which substantiates its toxic effect against cancer cells.

Table 2
ADME and drug likeness properties of the ligand THMPP.

End Points	HTS Data	Accuracy
Blood-Brain Barrier	BBB+	0,8003
Human Intestinal Absorption	HIA+	0,9971
Caco-2 Permeability	Caco2+	0,5375
P-glycoprotein Substrate	Non-substrate	0,7583
P-glycoprotein Inhibitor	Non-inhibitor	0,6068
	Non-inhibitor	0,9278
Renal Organic Cation Transporter	Non-inhibitor	0,8148
Subcellular localization	Mitochondria	0,6819
CYP450 2C9 Substrate	Non-substrate	0,6246
CYP450 2D6 Substrate	Non-substrate	0,8092
CYP450 3A4 Substrate	Substrate	0,6311
CYP450 1A2 Inhibitor	Inhibitor	0,7358
CYP450 2C9 Inhibitor	Inhibitor	0,651
CYP450 2D6 Inhibitor	Non-inhibitor	0,8645
CYP450 2C19 Inhibitor	Non-inhibitor	0,5508
CYP450 3A4 Inhibitor	Non-inhibitor	0,7413
CYP Inhibitory Promiscuity	High CYP Inhibitory Promiscuity	0,7253
Human Ether-a-go-go-Related Gene Inhibition	Strong inhibitor	0,5167
	Non-inhibitor	0,7336
AMES Toxicity	AMES toxic	0,9402
Carcinogens	Non-carcinogens	0,6772
Fish Toxicity	High FHMT	0,9583
Tetrahymena Pyriformis Toxicity	High TPT	0,9846
Honey Bee Toxicity	Low HBT	0,513
Biodegradation	Not ready biodegradable	0,9604
Acute Oral Toxicity	Category III	0,7048
Carcinogenicity (Three-class)	Warning	0,4551

Further, the results of the ADMET analysis are shown in the Table 2. The oral bioavailability and ADMET risk profiling were within their acceptable limit for THMPP. It obeyed Lipinski rule of five and had good absorption properties. Also, it is predicted to cross the Blood Brain Barrier and has Caco-2 permeability and good intestinal absorption and predicted to be localized in mitochondria of the cell. The metabolism and toxicity parameters are also acceptable for THMPP. The complete endpoints prediction concludes that the compound THMPP, exhibits good drug likeliness properties.

4. Discussion

Several studies are reported on various natural and synthetic phenolics to have cytotoxic effect on cancer cells. (Liu et al., 2018; LS et al., 2016; Spatafora and Tringali, 2012). Reports on

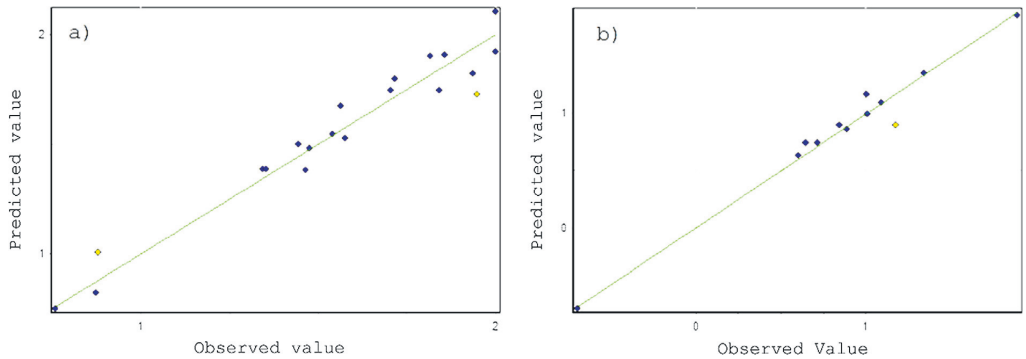

Fig. 6. QSAR Correlation plot. (a) Training set correlation coefficient (R2 = 0.970). (b) Test set correlation coefficient (R2 = 0.985).

phenolic derivative like phenolic acids are available which deal with anti-oxidant property and their action on cancer cell proliferation. Many dietry phenolic acids have also been tested. In particular, the well known phenolics, caffeic acid when treated with breast cancer cells, T47D showed good growth inhibition with the IC_{50} of 2.17×10^{-9} M (Kampa et al., 2004b). Phenolic compounds which are structurally related have been also shown to induce cell cycle arrest and apoptosis of cancer cells(Ahmad et al., 2011) (Amawi et al., 2017).

The susceptible nature of tumor cells to apoptosis is the vital determinant of chemotherapy efficacy (Stumm et al., 2004). Thus, an effective anti-cancer drugs, which can target breast cancer cells by inducing apoptosis is needed for efficient treatment. We determined the ability of THMPP to induce apoptosis in breast cancer cells using DNA fragmentation analysis, Caspase3/9 activity assay, FITC/Annexin staining and AO/EtBr fluorescent staining procedures. It is evident that, THMPP induced apoptosis via caspase 3/9 activation, but then other signaling pathways might also be induced along with caspase 3/9 activation. Therefore, further analysis of apoptosis and/or autophagy signaling pathway on multiple cancer cell types should be implemented for anticancer development.

On the other hand, expression of genes involved in the tumor progression is altered in cancer conditions. PI3K/AKT/S6K1/mTOR pathway promotes cell survival and cell proliferation, which is continuously over-expressed in breast cancer cells. In this study, the newly synthesized THMPP was able to down regulate *PI3K* and *S6K1* genes, which could suppress proliferation and induce apoptosis. Also, decrease in the *S6K1* expression reduces the risk of radiation resistance of cancer cells(Tandon et al., 2011). This attribute reduces the risk of side effects which are common in chemotherapeutic agents. Similar researches were also carried out in the well known polyphenols of green and black tea and were reported to have anti-cancer properties by up- or down-regulating a number of key enzymes (Beltz et al., 2006). Overall, THMPP was identified to be a candidate drug to treat multiple breast cancer and further clinical trials in animal model is essential to verify the antitumor activity.

5. Conclusion

The present investigation revealed that THMPP can act as a potential drug for treating breast cancer. This study demonstrated that THMPP has cytotoxic activity on MCF-7 and SkBr3 breast cancer cell line. THMPP was determined to be apoptosis induced, triggering DNA fragmentation as well as caspase 3/9 in human breast cancer cell lines. Additionally, molecular docking of THMPP with EGFR identified that the can potentially interact with EGFR and activate its downstream signaling pathway. Gene expression analysis also confirms the downregulation of *PI3K*, suggesting that THMPP might de-regulate the EGFR signaling pathway in breast cancer cells. The QSAR and ADMET analysis also proves that THMPP as non carcinogenic and a good drug-like candidate for breast cancer treatment. Overall, we anticipate that THMPP can be technically exploited further for the development of an effective anti-breast cancer agents.

Author contributions

SP executed the experiments and data analysis. AK involved in technical discussion and management. OY and MK conceived and managed all studies. All the authors contributed to writing the manuscript.

Ethical approval

This article does not contain any studies with human participants performed by any of the authors.

Acknowledgement

We would like to thank Prof. Nuno R. Candeias, Faculty of Engineering and Natural Sciences, Tampere University for gift of synthesized compounds.

Declaration of Competing Interest

The authors declare that they have no known competing financial interests or personal relationships that could have appeared to influence the work reported in this paper.

References

Ahmad, A., Sakr, W.A., Rahman, K.W., 2011. Mechanisms and therapeutic implications of cell death induction by indole compounds. Cancers (Basel) 3, 2955. https://doi.org/10.3390/CANCERS3032955.

Amawi, H., Ashby, C.R., Samuel, T., Peraman, R., Tiwari, A.K., Tiwari, A.K., 2017. Polyphenolic nutrients in cancer chemoprevention and metastasis: role of the epithelial-to-mesenchymal (EMT) pathway. Nutrients 9. https://doi.org/10.3390/nu9080911.

Basikc, D., Papovic, S., Ristic, P., Arsenijevic, N., 2006. Analysis of cycloheximide-induced apoptosis in human leukocytes: fluorescence microscopy using annexin V/propidium iodide versus acridin orange/ethidium bromide. Cell Biol. Int. 30, 924–932. https://doi.org/10.1016/j.cellbi.2006.06.016.

Basnakian, A.G., James, S.J., 1994. A rapid and sensitive assay for the detection of DNA fragmentation during early phases of apoptosis. Nucleic Acids Res. 22, 2714–2715.

Beltz, L.A., Bayer, D.K., Moss, A.L., Simet, I.M., 2006. Mechanisms of cancer prevention by green and black tea polyphenols. Anticancer. Agents Med. Chem. 6, 389–406.

Bray, F., Ferlay, J., Soerjomataram, I., Siegel, R.L., Torre, L.A., Jemal, A., 2018. Global cancer statistics 2018: GLOBOCAN estimates of incidence and mortality worldwide for 36 cancers in 185 countries. CA Cancer J. Clin. 68, 394–424. https://doi.org/10.3322/caac.21492.

Chomzynski, P., Sacchi, N., 1987. Single-step method of RNA isolation by acid guanidinium thiocyanate–phenol–chloroform extraction. Anal. Biochem. 162, 156–159. https://doi.org/10.1006/abio.1987.9999.

Chowdhury, S., Kandhavelu, M., Yli-Harja, O., Ribeiro, A.S., 2012. An interacting multiple model filter-based autofocus strategy for confocal time-lapse microscopy. J. Microsc. https://doi.org/10.1111/j.1365-2818.2011.03568.x.

Ciruelos Gil, E.M., 2014. Targeting the PI3K/AKT/mTOR pathway in estrogen receptor-positive breast cancer. Cancer Treat. Rev. 40, 862–871. https://doi.org/10.1016/j.ctrv.2014.03.004.

Doan, P., Musa, A., Candeias, N.R., Emmert-Streib, F., Yli-Harja, O., Kandhavelu, M., 2019. Alkylaminophenol induces G1/S phase cell cycle arrest in glioblastoma cells through p53 and cyclin-dependent kinase signaling pathway. Front. Pharmacol. https://doi.org/10.3389/fphar.2019.00330.

Doan, P., Nguyen, T., Yli-Harja, O., Candeias, N.R., Kandhavelu, M., 2017. Effect of alkylaminophenols on growth inhibition and apoptosis of bone cancer cells. Eur. J. Pharm. Sci. 107, 208–216. https://doi.org/10.1016/j.ejps.2017.07.016.

El Molla, S.G., Motaal, A.A., El Hefnawy, H., El Fishawy, A., 2016. Cytotoxic activity of phenolic constituents from Echinochloa crus-galli against four human cancer cell lines. Brazilian J. Pharmacogn. https://doi.org/10.1016/j.bjp.2015.07.026.

Jones, G., Willett, P., Glen, R.C., Leach, A.R., Taylor, R., 1997b. Development and validation of a genetic algorithm for flexible docking. J. Mol. Biol. https://doi.org/10.1006/jmbi.1996.0897.

Kampa, M., Alexaki, V.-I., Notas, G., Nifli, A.-P., Nistikaki, A., Hatzoglou, A., Bakogeorgou, E., Kouimtzoglou, E., Blekas, G., Boskou, D., Gravanis, A., Castanas, E., 2004b. Introduction Antiproliferative and apoptotic effects of selective phenolic acids on T47D human breast cancer cells: potential mechanisms of action. https://doi.org/10.1186/bcr752.

Karjalainen, A., Yli-Harja, O., Kandhavelu, M., Doan, P., Candeias, N.R., Sandberg, O., Chandraseelan, J.G., 2017. Synthesis of phenol-derivatives and biological screening for anticancer activity. Anticancer. Agents Med. Chem. 17, 1710–1720. https://doi.org/10.2174/1871520617666170327142027.

Kato, S., Endoh, H., Masuhiro, Y., Kitamoto, T., Uchiyama, S., Sasaki, H., Masushige, S., Gotoh, Y., Nishida, E., Kawashima, H., Metzger, D., Chambon, P., 1995. Activation of the estrogen receptor through phosphorylation by mitogen-activated protein kinase. Science 270, 1491–1494.

Koopman, G., Reutelingsperger, C.P., Kuijten, G.A., Keehnen, R.M., Pals, S.T., van Oers, M.H., 1994. Annexin V for flow cytometric detection of phosphatidylserine expression on B cells undergoing apoptosis. Blood 84, 1415–1420.

Liu, J., Ming, B., Gong, G.-H., Wang, D., Bao, G.-L., Yu, L.-J., 2018. Current research on anti-breast cancer synthetic compounds. https://doi.org/10.1039/c7ra12912b.

Ls, R., Nja, S., Ncp, S., Mc, M., Aj, T., 2016. Anticancer properties of phenolic acids in colon cancer – a review. J. Nutr. Food Sci. 06, 1–7. https://doi.org/10.4172/2155-9600.1000468.

Malek, S.N.A., Wahab, N.A., Yaacob, H., Shin, S.K., Lai, H.S., Serm, L.G., Rahman, S.N.S. A., 2008. Cytotoxic Activity of Pereskia bleo (Cactaceae) Against Selected Human Cell Lines. Int. J. Cancer Res. 4, 20–27. https://doi.org/10.3923/ijcr.2008.20.27.

Manikandan, S., Malik, B.K., 2008. Modeling of human CCR5 as target for HIV-I and virtual screening with marine therapeutic compounds. Bioinformation 3, 89–94.

Martelli, A.M., Chiarini, F., Evangelisti, C., Grimaldi, C., Ognibene, A., Manzoli, L., Billi, A.M., McCubrey, J.A., 2010. The phosphatidylinositol 3-kinase/AKT/mammalian target of rapamycin signaling network and the control of normal myelopoiesis. Histol. Histopathol. 25, 669–680. https://doi.org/10.14670/HH-25.669.

Mosmann, T., 1983. Rapid colorimetric assay for cellular growth and survival: application to proliferation and cytotoxicity assays. J. Immunol. Methods 65, 55–63.

Nissink, J.W.M., Murray, C., Hartshorn, M., Verdonk, M.L., Cole, J.C., Taylor, R., 2002. A new test set for validating predictions of protein-ligand interaction. Proteins Struct. Funct. Bioinforma. 49, 457–471. https://doi.org/10.1002/prot.10232.

Roy, K., Kar, S., Das, R.N., Roy, K., Kar, S., Das, R.N., 2015. Validation of QSAR models. Underst. Basics QSAR Appl. Pharm. Sci. Risk Assess., 231–289 https://doi.org/10.1016/B978-0-12-801505-6.00007-7.

Sawadogo, W.R., Le Douaron, G., Maciuk, A., Bories, C., Loiseau, P.M., Figadère, B., Guissou, I.P., Nacoulma, O.G., 2012. In vitro antileishmanial and antitrypanosomal activities of five medicinal plants from Burkina Faso. Parasitol. Res. 110, 1779–1783. https://doi.org/10.1007/s00436-011-2699-3.

Spatafora, C., Tringali, C., 2012. Natural-derived polyphenols as potential anticancer agents. Anticancer. Agents Med. Chem. 12, 902–918. https://doi.org/10.2174/187152012802649996.

Stumm, S., Meyer, A., Lindner, M., Bastert, G., Wallwiener, D., Gückel, B., 2004. Paclitaxel treatment of breast cancer cell lines modulates fas/fas ligand expression and induces apoptosis which can be inhibited through the CD40 receptor. Oncology 66, 101–111. https://doi.org/10.1159/000077435.

Sun, M., Paciga, J.E., Feldman, R.I., Yuan, Z., Coppola, D., Lu, Y.Y., Shelley, S.A., Nicosia, S.V., Cheng, J.Q., 2001. Phosphatidylinositol-3-OH kinase (PI3K)/AKT2, activated in breast cancer, regulates and is induced by estrogen receptor (ER) via interaction between ER and PI3K 1. Cancer Res. 61, 5985–5991.

Tandon, P., Gallo, C.A., Khatri, S., Barger, J.F., Yepiskoposyan, H., Plas, D.R., 2011. Requirement for ribosomal protein S6 kinase 1 to mediate glycolysis and apoptosis resistance induced by Pten deficiency. Proc. Natl. Acad. Sci. U.S.A. 108, 2361–2365. https://doi.org/10.1073/pnas.1013629108.

Tao, L.Y., Zhang, J.Y., Liang, Y.J., Chen, L.M., Zheng, L.S., Wang, F., Mi, Y.J., She, Z.G., To, K.K.W., Lin, Y.C., Fu, L.W., 2010. Anticancer effect and structure-activity analysis of marine products isolated from metabolites of mangrove fungi in the South China Sea. Mar. Drugs. https://doi.org/10.3390/md8041094.

Todeschini, R., Gramatica, P., 1997. 3D-modelling and Prediction by WHIM descriptors. Part 6. Application of WHIM descriptors in QSAR studies. Quant. Struct. Relationships 16, 120–125. https://doi.org/10.1002/qsar.19970160204.

Vaiyapuri, P.S., Ali, A.A., Mohammad, A.A., Kandhavelu, J., Kandhavelu, M., 2015. Time lapse microscopy observation of cellular structural changes and image analysis of drug treated cancer cells to characterize the cellular heterogeneity. Environ. Toxicol. 30, 724–734. https://doi.org/10.1002/tox.21950.

Vermes, I., Haanen, C., Steffens-Nakken, H., Reutelingsperger, C., 1995. A novel assay for apoptosis. Flow cytometric detection of phosphatidylserine expression on early apoptotic cells using fluorescein labelled Annexin V. J. Immunol. Methods 184, 39–51.

PUBLICATIONS

II

Alkylamino phenol derivative induces apoptosis by inhibiting EGFR signaling pathway in breast cancer cells

Palanivel S, Yli-Harja O, and Kandhavelu M

Anticancer Agents in Medicinal Chemistry; Volume 20(7):03 July 2020, Pages 809-819.

doi.org: 10.2174/1871520620666200213101407

Alkylamino phenol derivative induces apoptosis by inhibiting EGFR signaling pathway in breast cancer cells

Suresh PALANIVEL[a,b], , Olli YLI-HARJA[b,c,d], and Meenakshisundaram KANDHAVELU[a,b*]

[a]*Molecular Signaling Lab, Faculty of Medicine and Health Technology, Tampere University and BioMediTech, P.O. Box 553, 33101 Tampere, Finland.*

[b]*Institute of Biosciences and Medical Technology, Tampere, Finland*

[c]*Computational Systems Biology Group, Faculty of Medicine and Health Technology, Tampere University and BioMediTech, P.O. Box 553, 33101 Tampere, Finland.*

[d]*Institute for Systems Biology, 1441N 34th Street, Seattle, WA 98103-8904, USA*

Kandhavelu M

Abstract: Background and Objective: *The present study was carried out to evaluate the anticancer property of an alkylamino phenol derivative –2-((3,4-Dihydroquinolin-1(2H)-yl)(p-tolyl)methyl)phenol) (THTMP) against human breast cancer cells. The cytotoxicity of the THTMP was assessed to know its specificity towards breast cancer cells without affecting the normal cells.* ***Methods:*** *The THTMP was synthesized and the cytotoxicity was assessed by MTT assay, Caspases enzyme activity, DNA fragmentation and FITC/Annexin V, AO/EtBr staining, RT-PCR and QSAR. In addition, ADME analysis were executed to understand the mode of action of THTMP.* ***Results:*** *THTMP showed potential cytotoxic activity against the growth of MCF7 and SK-BR3 cells with the IC_{50} values of 87.92 µM and 172.51 µM, respectively. Interestingly, THTMP found to activate caspase 3 and caspase 9 enzymes in cancer cells, which are the key enzymes implicated in apoptosis. THTMP induced apoptosis in which 33 % of the cells entered the late apoptotic stage after 24h of treatment. Thus, the results revealed that the apoptotic response could be influenced by the association of THTMP with the Epidermal Growth Factor Receptor (EGFR) mediated inhibition of the phosphatidylinositol 3-kinase (PI3K)/S6K1 signaling pathway. In addition, docking was performed to study the binding mode of the THTMP, which shows better interaction with EGFR. The structural elucidation of THTMP by quantitative structure–activity relationship model (QSAR) and ADMET screening suggested, THTMP as an effective anticancer compound.* ***Conclusion****: This work strengthens the potential of being a promising drug-like compound, THTMP, for the discovery of anticancer drug against breast cancer.*

Keywords: Phenol derivative, breast cancer cells, apoptosis, PI3K/AKT pathway, ADME.

1. INTRODUCTION

It is anticipated that nearly one million women are diagnosed to be victims of breast carcinoma every year [3], making it the most prevalent cancer among women [1], [2]. It is the most common cancer in Southeast Asian women and among East Asian women, it is the second common cancer following gastric cancer [3]. The FDA approved drugs approved for the treatment of breast cancer include lapatinib, eribulin, fulvestrants, pertuzumab, mesylate, everolimus and many other agents[4]. The major problem is that the cancer cells develop resistance to many chemo drugs, which arises the need to search for new group of anticancer agents targeting breast cancer cells specifically [5].

Previous evidence emphasizing the importance of apoptosis in the development of new therapeutic agents and in the treatment of cancer [6]–[8]. The apoptotic mechanism is frequently used to detect new cancer agents because failure to cause apoptosis is a key factor which causes cancer[9], [10].

*Address correspondence to this author at the Molecular Signaling Lab, Faculty of Medicine and Health Technology, Tampere University, Finland, P.O.Box 553, 33101 Tampere, Finland; E.mail: * meenakshisundaram.kandhavelu@tuni.fi.

Cellular morphological and biochemical changes include the recession of cells, nuclear condensation and DNA fragmentation, dynamic membrane blebbing and cell adhesion loss, externalisation of phosphatidylserin, and intracellular specific proteolysis.[11]. Thus, an effective anticancer drug which can target breast cancer cells by inducing apoptosis in these cells is needed for curing this disease.

In the past decade, there are myriad studies on phenolic compounds and their ability to control tumour progression. The main basis of these compounds' activity was due to their anti-oxidant properties. The main activity was based on the number and length of the ester in caffeic esters as well as hydroxyl groups. In many plant species, phenolic compounds occur naturally and consist mainly of single or multiple aromatic rings with hydroxylic residues. As reported by many researchers, the presence and ability of phenol moieties to act like free radical scavengers shows that natural compounds, such as quinones, flavonoids, lignans, coumarins, stilbenes, and tannins have broad biological properties.[12]–[15]. Although phenols are abundant in nature, certain chemically synthesized derivatives such as eugenol dimmers have shown

stronger anti - cancer activities.[16]. In the present research, we report the apoptosis-inducing potential of a chemically synthesized alkylaminophenols - 2-((3,4-Dihydroquinolin-1(2H)-yl)(p-tolyl)methyl)phenol (THTMP). In the previous report, our group have studied the anticancer property of this compound against bone cancer cells [17]. However, the study on the compound's activity against breast cancer has not studied and hence the present study aims to explore the mechanism behind the action of the compound at a molecular level in breast cancer cells.

Approximately 45% of breast cancers express the epidermal growth factor receptor (EGFR), ranging from 14% to 91% of expression in breast carcinomas[18]. One of the a critical intracellular signaling system for cell growth and survival is PI3K / AKT / mTOR pathway which is known to be involved in ER+ tumorigenesis and in endocrine therapy resistance.[19]. The PI3K pathway is commonly altered in ER+/HER2− breast cancer. The integrated analysis of the molecular pathway informs a synergistic combination therapy for basal breast cancer targeting PTEN/PI3 K and EGFR.[20]. In this report, the study pays attention to the alteration in the expression of EGFR, PI3Kand S6K1genes in the breast cancer cell lines after treating with the synthesized compound.

2. MATERIALS AND METHODS

2.1 Cells, materials and compounds:

The breast cancer cells MCF-7, SK-BR3, MDA-MB-231 [21], Human Embryonic Kidney cells (HEK293T, immortal cells) (ATCC, crl-3216, Sigma-Aldrich, UK) and, the non-tumorigenic cells, cardiomyocyte cells H9C2 [22] (NCCS, Pune, India) were routinely maintained in DMEM high glucose media (Invitrogen) supplemented with 10% FBS along with 100 U/ml Penicillin plus 100µg/µl Streptomycin incubated at 37˚C in a humidified CO^2 incubator [23]. Alkylamino phenol derivative –2-((3,4-Dihydroquinolin-1(2H)-yl)(p-tolyl)methyl)phenol), THTMP (Figure 1a), was synthesized by our group. Its preparation and spectral characterization were previously reported [24], [25]. The NMR structure of elemental analysis is given in the supplementary file.

2.2 Cytotoxicity assay:

The cytotoxicity of THTMP was evaluated using MTT method as prescribed by Mossman, 1983. MTT assay was carried out for both the normal and cancer cells. All the three cell lines viz. MCF-7, SK-BR3 and H9C2 cells (20000 cells) were seeded on a 96-well plate. After adherence of cells, a varying concentration of the THTMP was added (10, 25, 50, 75, and 100 µM) and incubated for 24 hrs. To the cells, MTT solution (10 µL of 5 mg/ml) was added and left for 4hrs. DMSO was used to dissolve the formazan crystals and absorbance was read at 570 nm in a microtitre plate reader. A known chemotherapeutic agent Cyclophosphamide was used as a positive control. Cells without sample (untreated) served as a control [26]. From the results of this cytotoxic assay, IC_{50} value of THTMP against breast cancer cell lines was determined and the same concentration was used for further analysis. In addition, HEK293 cells were treated with 100 µM concentration of THTMP for 48 hours and cell death percentage was measure using trypan blue method as described previously.

2.3 CASPASEs quantification assay:

Casp-3 and Casp-9 were quantified by chromogenic assays using readymade kits and carried out as per the manufacturer's protocol (Calbiochem, Merck). The THTMP (IC_{50}) treated cells (MCF7 and SK-BR3 cells) were lysed using buffer consisting of 50 mM HEPES, 100 mM NaCl, 0.1% CHAPS, 1mM DTT, 100 mM EDTA. The protein from the lysates was determined using Bradford method. In 50 µL of buffer mentioned, 200 µg of protein from the cell extracts was diluted and used for each assay. This protein solution was incubated with p-nitroanilide (pNA) substrates, DEVD-pNA (casp- 3 activity) for 2 h at 37° C. Caspase activity was expressed as the free pNA cleaved which was measured by absorbance at 405 nm in a microtiter plate reader. Relative Casp-3 and 9 activities were calculated by comparing the absorbance in the untreated and treated wells.

2.4 DNA fragmentation analysis:

The treated THTMP (at IC_{50} Conc.) and untreated MCF7 cells ($1*10^6$ cells) were digested with 100µl of cell lysis buffer constituting of Tris-EDTA-SDS at room temperature for one hour. The DNA was extracted from the lysates as described previously [27], [28]. Briefly, cell lysate was then subjected to phenol: chloroform: isoamylalcohol (25:24:1) extraction and ethanol precipitation. Subsequently, it was centrifuged at 16000 g, 4˚ C for15 min and the DNA pellet was obtained. It was then stored in 25 µl of 0.1 M Tris–EDTA (pH 8.5). The isolated genomic DNA was run on 1 % agarose gel for 2 h voltage set at 50 V using TBE as running buffer (40 mM Tris–borate, 1 mM EDTA) containing 0.5 µg/ml ethidium bromide and visualized under UV light [29]. A DNA ladder size ranging from 250 kb – 3000 Kb was loaded in the first well to understand the size of fragments formed.

2.5 Annexin/PI Assay:

FACS analysis was executed to check the apoptotic induction in MCF-7 cells after treatment with THTMP.FITC Annexin V Apoptosis Detection Kit I of BD Pharmingen (BD Biosciences) was used for the study and the protocol was followed as described by the manufacturer. Briefly, MCF7 cells were grown on a 6 well plate in complete DMEM media for 18 hrs, allowing the cells to adhere to the surface of the plate. After attaining uniform confluence of 75 %, the cells were treated with THTMP (IC_{50}). The cells were incubated for 24 hrs and then trypsinised. It was then centrifuged, and the pellet was suspended in PBS. The cells were washed with 1X Binding Buffer and 100 µl of the solution (with 1×10^5 cells) was transferred to a 5 ml culture tube. To this suspension, 5 µl of FITC Annexin V and 5 µl PI were added and vortexed gently. It was then incubated for 15 min at 25° C in the dark.400 µl of 1X Binding Buffer was added to each tube and analyzed by flow cytometry within 1 hr [30], [31].

2.6 Acrydine orange / Ethidium Bromide dual staining:

The fluorescent dual staining was performed to determine if exposure to THTMP would cause cell death by apoptosis in MCF-7. The cells were grown, treated with THTMP and collected as explained in section 2.5. To avoid minor errors in microscopic examinations, THTMP was added to cells in three different concentrations – at IC_{50}, a slight below and a higher concentration of IC_{50}.To the cell suspension, equal volume of staining solution (1:1) mixture of 100 µg/ml AO and 100 µg/ml EB were added. 10µl of the suspension was placed on a clean microscopic slide and observed under fluorescent microscope 20X magnification using a blue filter (420-495 nm) and a green filter (510-560 nm). The cells were viewed in different fields and quantified after counting at least 300 cells per well.

2.7 Total RNA isolation and cDNA synthesis:

Total RNA from treated and untreated MCF7 cells were isolated using ONE STEP-RNA Reagent (BiobasicInc) which is a monophasic solution of phenol and guanidine isothiocyanate. This method is an improvement to the single-step RNA isolation method developed by Chomczynski and Sacchi (1987). In brief, the cells (approximately $5*10^6$) were lysed by adding 1ml of ONE STEP-RNA reagent and centrifuged. To dissociate nucleoprotein complexes 200µl of chloroform was added and incubated for 5 min at 15-30˚ C. After vigorous shaking, the samples were centrifuged at 12,000 g for 15 minutes at 2~8° C. The upper aqueous layer formed was precipitated by mixing isopropyl alcohol. The mixture was allowed to stand for 15 min. The RNA precipitates and forms as a pellet when centrifuged. The pellet was washed again with 75 % ethanol and centrifuged at 7,500 g for 5 minutes at 2~8° C. The ethanol was removed completely and dissolved in DEPC treated water and stored in -20° C [32].

RNA isolated from the cells was reverse transcribed using oligo-dTas a primer. In a 1.5 ml Eppendorf PCR tube, 1-2 µg of RNA, 2 µl of 10µM oligo-dT was added and the total volume was made up to 20µl using DEPC treated water. The tube was incubated at 65º C for 5 min (Water Bath) and chilled immediately on ice. Then, 4 µl of 5X reverse transcriptase buffer, 2 µl of 25 mM dNTP mix and 0.5 µl of RNase inhibitor (40 U/µl) were added in the same order. After incubating at 42ºC for 5 min, 1 µl of Easy Script reverse transcriptase (200 U/µl) was added and the reaction was carried out at 42º C for 50 min. Finally, the tube was heated up to 70º C for 10 min and chilled on ice. The samples were stored at -20º C until further use.

2.8 Reverse transcriptase PCR:

To amplify the cDNA, PCR ready mix was used according to the manufacturer's instruction. Primers specific for EGFR, PI3K and S6K1 genes were designed. The primer sequence and the PCR conditions are tabulated below. β- actin was used as an endogenous control to check for equal loading. After PCR reaction, to confirm the amplification, it was loaded in an agarose gel and the bands were analyzed. The primers for the target mRNA were EGFR (Forward: 5'TCCCCGTAATTATGTGGTGACAGATC 3' and Reverse: ACCCCTAAATGCCACCGGC), with the amplicon length 250 bp;PI3K (Forward: 5'AACACAGAAGACCAATACTC 3' and Reverse: 5' TTCGCCATCTACCACTAC), with the amplicon length 195 bp; S6K1 (Forward: 5'CACATAACCTGTGGTCTGTTGCTG 3' and Reverse: 5' AGATGCAAAGCGAACTTGGGATA3'), with the amplicon length 180 bp; and for reference gene β- actin (Forward: 5'CACCCGCGAGTACAACCTT 3' and Reverse: 5' CCCATACCCACCATCACACC 3'), with the amplicon length 204 bp, were synthesized and used for PCR. The PCR was setup with the following reagents: 1X Taq Buffer (with MgCl2), 0.2 mM dNTPs, 2.5 mM MgCl2, 0.3 µM forward and reverse Primer, Template cDNA (10% of the reaction) and 1U Taq Polymerase. The PCR was run with the following conditions upto 32 cycles: Initial denaturation - 94˚ C for 2 min, denaturation - 94˚ C for 30 s, Annealing - Ta for 1min, Extension - 72˚ C for 1 min 20 s, Final extension - 72˚ C for 7 min, and Hold at 4˚ C. Ta specifically optimized for each gene viz.56˚ C for EGFR, 54˚ C for PI3K, 56˚ C for S6K1 and 54˚ C for β- actin.

2.9 Molecular docking:

To understand the mechanism of action of the synthesized compound THTMP, a combined computational analysis was made. The structure of the THTMP was drawn using ACD/Chemsketch. The Epidermal Growth Factor receptor protein structure was retrieved from PDB database (https://www.rcsb.org/). Molecular docking of the THTMP was performed against target Epidermal Growth Factor receptor. Here, GOLD software was used for docking [33]. GOLD calculates mode for docking small molecules in a protein binding site and provides a package of structure - visualization and manipulation programs (Hermes), the protein - leaning - docking (GOLD) and post - processing programs (GoldMine) and docking results visualization programs as part of the GOLD Suite.

2.10 ADME/Tox properties:

The pharmacokinetic properties of the THTMP were evaluated using ADMETSAR[34]. AdmetSAR is the latest tool to study the ADME properties of any chemical based on its structure. Studying the ADMET properties provide the drug-likeliness property of the THTMP.

2.11 Quantitative structure–activity relationship models (QSAR):

QSAR analysis was carried out with an attempt to derive and understand the relationship between biological activity and molecular descriptors [35]. In the present study, we have collected 32 structurally similar compounds (Table 1) along with their biological activity (expressed as IC_{50}) from the earlier researches and reports. To calculate the molecular descriptors, we have used Dragon software. It contains 1497 descriptors as 18 groups [33]. The set of 18 descriptors was calculated for each molecule in the training set using the

DRAGON software. Based on the IC_{50} values, descriptor set was chosen, MLR models were built. Following that, the relevant variables were selected or eliminated to frame the QSAR equation which was performed using BUILDQSAR software. The goodness of the correlation is tested by the square of coefficient regression (R2), square of cross regression (q2), the F-test (F), and the standard deviation (S). The number of compounds is represented as "n" and the correlation coefficient as "r".

Training Set			
No	**Compound Name**	**IC_{50} (µM)**	**Ref**
1	2-((3,4-dihydroquinolin-1(2H)-yl) (p-tolyl)methyl)phenol	87.92	Present study
2	Curcumin	7.6	[36]
3	THMPP	50.5	[37]
4	alkylaminophenols1	88.4	
5	alkylaminophenols3	86	
6	alkylaminophenols8	69.4	
7	alkylaminophenols9	65.5	
8	2-(4-methyl-6-(1- methyl-1Hbenzo[d]imidazol-2- yl)-2-propyl-1Hbenzo[d]imidazol-1- yl)-N-phenylacetamide	52.09	[38]
9	2-(4-methyl-6-(1-methyl-1Hbenzo[d]imidazol-2-yl)-2-propyl-1Hbenzo[d]imidazol-1-yl)-N-o-tolylacetamide	100	
10	N-(2-methoxyphenyl)-2-(4-methyl-6-(1-methyl-1Hbenzo[d]imidazol-2-yl)-2-propyl-1Hbenzo[d]imidazol-1-yl)acetamide	100	
11	thieno [2, 3-d] pyrimidine derivatives -9	27.83	[39]
12	thieno [2, 3-d] pyrimidine derivatives -10	34.64	
13	thieno [2, 3-d] pyrimidine derivatives -11	37.78	
14	thieno [2, 3-d] pyrimidine derivatives -12	29.22	
15	thieno [2, 3-d] pyrimidine derivatives -13	22.52	
16	thieno [2, 3-d] pyrimidine derivatives -14	22.12	
17	Dihydroactinidiolide	30	[40]
18	Beta-sitosterol	72	
19	2,4-di tert butylphenol	5.75	
20	Alpha-Tocopherol	7.5	

Test Set			
No	**Compound Name**	**IC_{50} (µM)**	**Ref**
1	Doxorubicin	12.355	[41]
2	Artemisinin 8	7	
3	Artemisinin 14	22	
4	Artemisinin 15	15	[42]
5	Artemisinin 20	10.1	
6	Artemisinin 24	4	
7	Oblongifolin C (OC)	7.7	[43]
8	Kurubasch aldehyde	78	
9	Longistylin A	5.2	
10	Longistylin C	4.4	[44]
11	Pinostrobin	10.2	
12	Curcusone A	0.2	

Table 1: List of training and test set of compounds used for QSAR model.

3. RESULTS

3.1 Cytotoxicity of THTMP in normal and cancer cell lines:

The toxicity of THTMP was tested on three cell lines- MCF7, SK-BR3 and H9C2 cells. The viability was determined by using MTT analysis. As shown in Figure 1b-1d, THTMP was toxic to cancer cells MCF7 and SK-BR3 cells whereas, in normal H9C2 cells, the toxicity was found to be too low. THTMP showed a dose-dependent increase in cytotoxicity against MCF7 cells with 35.03 % and 54.29 % toxicity at 10 µM and 100 µM respectively. The IC_{50} was calculated to be 87.92 µM (Figure 1 b). Similarly, toxicity increased in a dose-dependent manner against SK-BR3 cells with 14.68 % and 35.14 % toxicity at 10 µM and 100 µM, respectively. The IC_{50} was calculated to be 172.51 µM (Figure 1 c). THTMP did not show significant cytotoxicity against H9C2 cells, 22.04 % toxicity was observed at 100 µM concentration. The IC_{50} was calculated to be 255.91 µM (Figure 1 d). Based on these results, further experiments were carried out by treating cells with THTMP at this IC_{50} concentration.

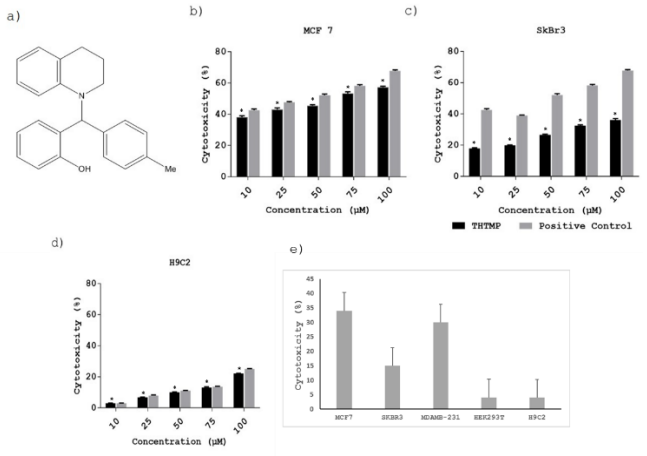

Figure 1: a) - Chemical structure of the investigative drug, THTMP. IUPAC: 2-((3,4-Dihydroquinolin-1(2H)-yl)(p-tolyl)methyl)phenol; MW-329.443. Cell cytotoxicity was determined by MTT assay for THTMP; the percentage of cell viability was calculated relative to control (untreated) in b) MCF7 cells, c) SK-BR3 cells and d) H9C2 cells. e) Percentage of cytotoxicity in multiple breast cancer (MCF7, SK-BR3, MDA-MB-231) and non-tumorous (HEK293T, H9C2) cell lines treated with 10 µM of THTMP. Data points and error bars represent mean ± S.E.M (n=3 per group) with the statistical significance, p-values (*, P<0.05).

The comparative analysis of cytotoxic effect of THTMP at 10 µM confirm its ability to induce the cell death only in breast cancer cells (MCF7, SK-BR3, MDA-MB-231) and not in any other normal cells (H9C2 and HEK293). MCF7 has the maximum growth inhibition of about 34 %, MDAMB-231 with 30 % followed by SK-BR3 with 15 %, and the least

cytotoxic effect on control cell, HEK293 and H9C2 (Figure 1 e). Thus, THTMP specifically targets breast cancer cells which makes it as a potent cytotoxic agent.

3.2 CASPASEs quantification assay:

Caspase 3 and 9 play a vital role in the cascade of signals inducing apoptosis of cells [45]. The capacity of any small molecule to induce the caspase activation is considered to be a demanding matter of its cytotoxicity effect on cancer cells. To ascertain apoptosis induced by THTMP, caspase 3 and caspase 9 activities were determined in both the breast cancer cell lines – MCF7 and SK-BR3 after treatment with our compound at their respective IC_{50} values (87.92 µM and 172.51 µM). In MCF7 cells, it was found that the activities of both Casp 3 & 9 were increased by a fold of 0.295 when treated with THTMP compared to untreated cells. In the case of SK-BR3, the level of Casp 3 was 0.331-fold higher in treated cells compared to untreated cells (Figure 2a). The Casp 9 level was increased by 0.388-fold in THTMP treated cells (Figure 2b). This shows that THTMP induces apoptosis in cancer cells through caspase activation.

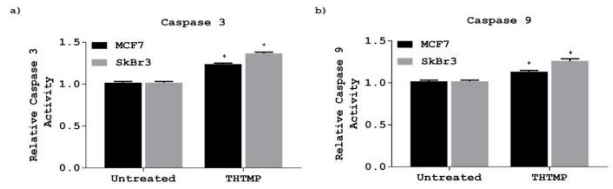

Figure 2: Caspase 3 and Caspase 9 activity in THTMP treated MCF7 cells and SKBR3 cells. a) Relative caspase 3 activity of THTMP treated MCF7 cells and SK-BR3 cells. b) relative caspase 9 activity of THTMP in MCF7 cells and SK-BR3 cells. All the datasets are composed of an n=3 experiment and compared by two-way ANOVA tests revealed significantly more relative caspase 9 activity of THTMP treated cells in comparison with the untreated cells (*, $P<0.05$). Data represents Mean ± SEM of two individual experiments (n=3).

3.3 Induction of DNA fragmentation by THTMP:

Following caspases quantification, DNA fragmentation in the cells was studied to detect the breaks and nicks formed in the DNA strand during apoptosis. The fragments in the DNA were formed due to the activation of endonucleases while cell undergoes apoptosis, which can be examined using electrophoresis [46]. Genomic DNA fragmentation was analyzed in MCF7 cells to determine the induction of apoptosis. The fragmentation was not observed in untreated cells (Figure 3 a). Cells treated with THTMP at the IC_{50} concentration showed DNA fragmentation. This internucleosomal DNA fragmentation supported the progression of apoptosis in THTMP treated MCF-7 cells. DNA fragmentation during necrosis appears to be less extensive and reflected as a minor decrease in the cellular DNA content. Thus, the occurrence of laddering of DNA provides evidence that THTMP mediates apoptosis in breast cancer cells (Figure3 a).

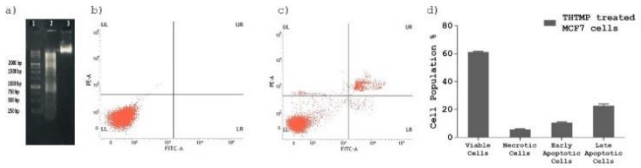

Figure 3: a) DNA extracted from MCF7 cells viewed on ethidium bromide stained agarose gel. Lane 1- 1Kb Ladder; Lane 2 - DNA of cells treated with THTMP; Lane 3- DNA of untreated cells. b) FACS analysis of the effect of THTMP on MCF7 cell lines at 87.92 µM concentration. Annexin/PI staining followed by FACS analysis in MCF7 cells, Untreated and c) THTMP treated. UL- Necrotic cells, UR- Late apoptotic cells, LL - Viable cells, LR – Early apoptotic cells. d) Percentage of viable, necrotic and apoptotic cells treated by THTMP in MCF7 cells.

3.4 THTMP induced apoptosis in MCF-7 cells

The monitoring of phosphatidylserine (PS) translocations using the V-FITC / PI annexin was conducted to investigate the cell death induced by THTMP. The analysis of flow cytometry relies on the ability of the protein Annexin V to bind to PS, which is externalized in the external membrane after the induction of apoptosis. PS is located in the internal membrane in viable cells, but it is translocated on the external membrane when apoptosis is induced and available for binding with Annexin V. In addition to PI it was possible to distinguish viable (AnnV / PI), early apoptotic (AnnV+/PI), late apoptotic (AnnV plus / PI+) and necrotic cells (AnnV / PI+); [47]. The flow cytometry analysis of MCF-7 cells showed THTMP treatment shifted the population of viable cells to the apoptotic stage (Figure 3 b and c). After treatment with IC_{50} of THTMP for 24 hrs, the late apoptotic cellswere22.62% and there was a non-significant change in the percentage of early stage apoptotic cells which was 10.57 % (Figure3 d). These results demonstrate the ability of the compound to exert apoptosis, particularly in late stage apoptosis in MCF-7 cells.

3.5 Morphological observation of apoptosis by AO/EtBr staining:

To detect the tumor cell apoptosis the cells were treated with AO/EtBr and visualized under fluorescence microscope. Figure 3 shows the MCF-7 cells stained with AO/EtBr together. The control cells show the appearance of green fluorescence with normal nuclear morphology (Figure 4 a). The treated cells exhibit bright yellow-green color and orange staining represents the cells at early and late apoptotic stage respectively (Figure 4a-d). Treating cells with 82.86 µM THTMP showed 8.23 % cells were in early apoptotic stage and 3.76 % cells were in late apoptotic stage; 87.90 µM of THTMP showed 11.63 % cells were in early apoptotic stage and 22.96 % cells were in late apoptotic stage; 92.34 µM THTMP exhibited 28.4 % cells were in early apoptotic stage and 31.5 % cells were in late apoptotic stage (Figure 4 e). This finding was characterized by membrane blebbing, nuclear shrinkage, and significant DNA fragmentation. Necrotic cells were stained uniform orange. The clear evidence of apoptosis

induction in the cells was visualized in all three concentrations of THTMP.

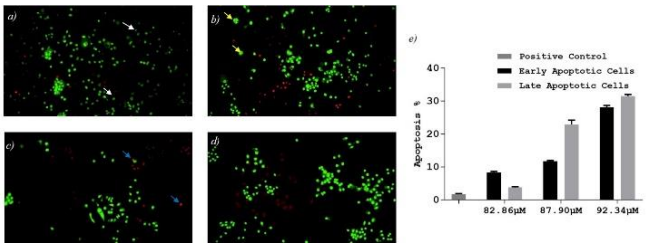

Figure 4: Apoptotic morphology detection by acridine orange-ethidium bromide (AO/EB) fluorescent staining in MCF7 cell line treated with THTMP. a) Untreated cells; treated with THTMP at different concentrations b) 82.86 µM; c) 87.90 µM; d) 92.34 µM. Appearance of green fluorescence (white arrow) in untreated control cells represents viable cells with normal morphology whereas visualization of bright yellow green color (yellow arrow) and reddish yellow/orange staining (blue arrow) in the treated cells shows the presence of early and late apoptotic cells. Necrotic cells will stain uniform orange. e) the percentage of apoptosis population stained with AO/EtBr at different concentrations.

3.6 Alteration in the expression of genes related to apoptosis:

It is apparent from the above-said experiments that THTMP triggers cell death in cancer cells. To understand the mechanism of action of THTMP led us to study the alteration in the expression of various genes involved in apoptosis. The cDNA was amplified by using primers specific for EGFR, PI3K and S6K1 genes along with an endogenous control β-actin as described in method section. The results suggest that the expression EGFR did not alter in the cells after treatment with THTMP whereas there was a significant reduction in the expression of PI3K and S6K1genes. The gel pictures and the expression ratio (in folds) are represented in Figure5 a. Both the expression of the genes was decreased by nearly 0.5-fold when treated with THTMP. This paves us the way to understand that THTMP shuts off overexpression of PI3K and S6K1in ER+ cancer cells.

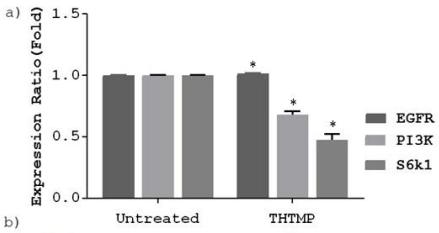

c)

Receptor name	Atom in ligand	Atom in protein	H-Bond Distance (Å)	Docking Score
EGFR	H41	LEU862:O	2.603	37.25

Figure 5: Reverse transcript PCR analysis of β-actin, EGFR, S6K1 and PI3K mRNA expression in MCF7 cell lines treated with THTMP. Gene expression is normalized with housekeeping gene β-actin expression. The fold change in the expression ratio of the genes a) EGFR; S6K1; PI3K. b) Molecular docking analysis of EGFR with THTMP ligand. The figure shows the docked ligand in the binding cavity of the receptor protein. The ligand is represented as sticks; and the protein active sites are represented as lines. Respective hydrogen bond interaction is marked as dotted lines (Red) and the interacting residues are labelled. c) The table shows the interaction properties of THTMP with the receptors EGFR. Data represents Mean ± SEM of two individual experiments (n=3) with the statistical significance, p-values (*, P<0.05).

3.7 THTMP binds to EGFR:

To substantiate that THTMP acts at a molecular level in the cancer cells and prevents tumor survival and growth, a combined computational approach was carried out. At first, the protein structure of the targets was retrieved from PDB database - EGFR (2RGP) (Figure 5 b). The active site residues were obtained from PDB Sum. For EGFR following active residues were identified:LEU718, GLY719, ALA722, VAL726, ALA743, LYS745, MET766, CYS775, ARG776, LEU777, LEU788, THR790, GLN791, LEU792, MET793, PRO794, PHE795, GLY796, ASP800, ARG803, ARG832, LEU833, VAL834, HIS835, ARG836,ASP837, LEU844, LEU862, HIS888, LYS913, LYS970, ARG977[48]. The molecular docking of the ligand THTMP against the receptor's EGFR showed significant interaction (Figure 5.2). The best interaction was seen with EGFR receptor with a score of 37.25. The docking score and the residues involved in the interaction are tabulated in Figure 5 C.

In addition to the docking study, it is also confirmed from the cytotoxicity analysis, THTMP could induce the cell death only in EGFR(+) breast cancer cells (MCF7, SK-BR3, MDAMB-231) whereas, its effect is nullified in EGFR(+) (H9C2) and EGFR(-) (HEK293) normal cells. This substantiates that, THTMP has no off target effects other than EGFR(+) breast cancer cells. The difference in the mechanism of cytotoxicity by THTMP against EGFR(+) breast cancer cells and EGFR(+) normal cells requires detailed investigation.

3.8 Pharmacokinetic studies of bioavailability:

The computational analysis predicted the compound's oral bioavailability (rule of five) and its ADMET properties [48] and the relevant individual descriptors are tabulated (Table 2). THTMP has a good Human Intestinal Absorption (HIA) and penetrates through blood-brain barrier. Its subcellular localization is mitochondria. In terms of metabolism, it is found that THTMP acts as a substrate and non-inhibitor of CYP450. The compound by itself has no carcinogenicity property. The result elucidates that THTMP has good drug likeliness property.

Endpoints	HTS Data	Accuracy
Blood-Brain Barrier	BBB+	0,8003
Human Intestinal Absorption	HIA+	0.9335
Caco-2 Permeability	Caco2+	0.9734
P-glycoprotein Substrate	Non-substrate	0.508
P-glycoprotein Inhibitor	Inhibitor	0.5403
	Non-inhibitor	0.5825
Renal Organic Cation Transporter	Inhibitor	0.5268
Subcellular localization	Mitochondria	0,7583
CYP450 2C9 Substrate	Non-substrate	0.7122
CYP450 2D6 Substrate	Substrate	0.7675
CYP450 3A4 Substrate	Substrate	0.6655
CYP450 1A2 Inhibitor	Inhibitor	0.6832
CYP450 2C9 Inhibitor	Non-inhibitor	0.591
CYP450 2D6 Inhibitor	Inhibitor	0.7657
CYP450 2C19 Inhibitor	Non-inhibitor	0.6266
CYP450 3A4 Inhibitor	Non-inhibitor	0.5106
CYP Inhibitory Promiscuity	High CYP Inhibitory Promiscuity	0.774
Human Ether-a-go-go-Related Gene Inhibition	Strong inhibitor	0.653
	Inhibitor	0.5874
AMES Toxicity	AMES toxic	0.905
Carcinogens	Non-carcinogens	0.8348
Fish Toxicity	High FHMT	0.8033
Tetrahymena Pyriformis Toxicity	High TPT	0.9816
Honey Bee Toxicity	Low HBT	0.626
Biodegradation	Not readily biodegradable	0.729
Acute Oral Toxicity	Category III	0.6572
Carcinogenicity (Three-class)	Non-required	0.4476

Table 2: Compliance of THTMP to ADMET prediction and drug likeliness properties

3.9. Chemical structure–activity relationship:

The biological potential of the compound was tested using the built QSAR model as described in method section. The compounds which well correlates with the QSAR model was considered to have good biological activity, which is the IC_{50} value against cancer cells (Table 1). The compounds that deviate from the regression line was considered as outliers and removed from the model (Figure 6). The validity and predictability of the QSAR model for the anticancer activity was cross validated by correlation coefficient value (r) of 0.970. The predicted model was further validated on the test set which showed a (r) value of 0.985. The result shows the efficiency of the predicted model, proving the compounds to possess anticancer activity. Specifically, THTMP well correlates with the equation which demonstrates the anticancer potential of the compound.

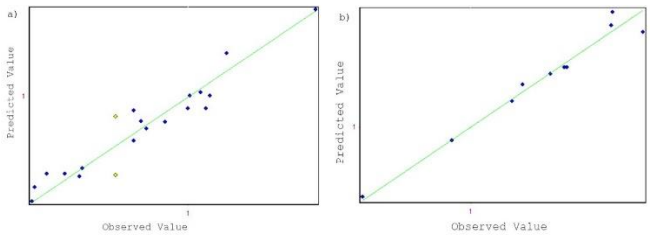

Figure 6: Correlation of biological activity and physicochemical parameters of a) training set and b) test set.

4. DISCUSSION

THTMP, a novel phenolic compound was synthesized and characterized, was already reported to have anticancer properties against Osteosarcoma [37]. In this study, it aims to expound in detail, the ability of the compound to inhibit tumor growth and induce apoptosis, especially in breast cancer cells.

Breast cancers possess heterogeneity due to the production of different hormone receptors. Previous studies have used two major breast cancer cell lines, MCF7 and SKBR3, to address the heterogeneity of cancer and to find whether the synthetic compound has effective or not. MCF7 is ER+/PR+/ HER2- whereas SK-BR3 is ER-/PR-/ HER2+. To determine the cytotoxicity of the compound THTMP, MTT assay was performed on theses cell lines. The IC_{50} values in MCF7 cells and SK-BR3 cells were determined. It was found to be 87 µM and 172 µM respectively. The THTMP is not toxic to normal cells – H9C2 while it decreases the growth the breast cancer cells. This shows the specificity of THTMP to only cancer cells without killing normal cells. The IC_{50} in case of normal cells is around 250 µM which is significantly higher concentration when compared to the cancer cell lines. Thus, it can be hypothesized that even higher dose administration will not affect the normal cells. However, this has to be evaluated in animal models to explore the potentially of the THTMP. This promising IC_{50} is comparatively lower than many other dietary phenolic like Galic acid, ρ-coumaric acid [49] against breast cancer cells. Though a bit higher than curcumin, it is in accordance with IC_{50} values of Resveratrol and lower than that of Capsaicin, which is common phenolic studied for anticancer activity [50].

There are myriads of a report on phenolic derivatives like phenolic acids which deal with anti-oxidant property and their action on cancer cell proliferation [51]. Many dietary phenolic acids have also been tested. Specifically, the well-known phenolic, Caffeic acid when treated with breast cancer cells T47D has shown a good growth inhibition with the IC_{50} of about 2.17×10^{-9} M. Few other phenolic compounds which are structurally related have been shown to induce cell cycle arrest and apoptosis of cancer cells other than breast cancer. In a study conducted by Chen et al., have shown a few compounds with IC_{50} values against HL60 cells. Nearly 100 µM, which are comparable to that of proposed compound[52].

The proposed compound has shown considerable control in tumor progression and the cells are shifted towards apoptosis. The results of Caspase 3 & 9 activation, FACS – Annexin V/PI staining and AO/EtBr staining and DNA fragmentation analysis have shown that THTMP induces apoptosis in MCF 7 cells. MCF 7 cells are caspase 3 deficient and are resistant to apoptotic stimuli [53]. This makes them unresponsive to chemotherapy and radiotherapy [49]. It is also reported that 75 % of breast cancer tissues lack caspase 3 expressions or it is down-regulated. Thus, developing a new drug which exhibits therapeutic action through caspase-3 independent pathway is strongly recommended. In the present study, induction of apoptosis by THTMP was further substantiated by the alteration in the caspase's activity in the MCF 7 cells. There is an increase in the fold of caspases after treating cells with THTMP.

Notably, the expression of genes involved in the tumor progression is altered in cancer conditions. Especially, PI3K/AKT signaling pathway is known to function as crucial

components of cell proliferation in cancer cells. PI3K over-expression promotes cell survival and cell proliferation. Similarly, high expression of SPK-1 (sphingosine kinase-1) and increased levels of its product, S1P are associated with aggressive tumor growth and radiation resistance. An elevated level of SPK1 is implicated in proliferation and anti-apoptotic activity in a variety of human cancers. In the present study, the newly synthesized THTMP is able to downregulate PI3K and S6K1 genes which suppress proliferation and induce apoptosis. Also, a decrease in the SPK1 expression reduces the risk of radiation resistance of cancer cells. Thus, the compound down-regulated the genes, which are anti-apoptotic and do not alter the expression of the receptor involved in the prognosis of cancer – EGFR. This attribute reduces the risk of side effects, which are common in chemotherapeutic agents. Similar researches have been carried out in the well-known polyphenols of green and black tea and have reported having anticancer properties by up or down-regulating a number of key enzymes, including mitogen-activated protein kinases and protein kinase C, and increased or decreased protein/mRNA levels, including that of cyclins, oncogenes, and tumor suppressor genes in cancer cells [53].

Following the *in vitro* studies, to understand the molecular interaction of THTMP in the cells, a combined computational study has been carried out including molecular docking and ADME/Tox analysis. Always computational analysis reduces the cost and time in screening the compounds and to get a clue if the expected activity is present in the selected compound. In this study, the compound is carefully drawn and docked against multiple targets, which are involved in the apoptosis. The potential of the compound to bind to the target, EGFR, implies that the compound can effectively regulate the downstream signaling pathway genes of this receptor and inhibit the anti-apoptotic proteins and induce the cells towards apoptosis. This docking result can be added evidence to THTMP for having anti-apoptotic activity. Hence, THTMP can be a potent novel chemotherapeutic agent targeting breast cancer.

5. CONCLUSIONS

Our study has demonstrated that the newly synthesized alkylaminophenolic compound THTMP has a strong cytotoxic effect on breast cancer cell lines. The bio-chemical assays such as MTT assay, Caspase assay (3 & 9), FACS, AO/EtBr and DNA fragmentation confirm that THTMP induces apoptosis at IC_{50}=87.92±1.7 µM. The gene expression analysis identified the downregulation of PI3K and S6K1 genes, which also confirms that THTMP can affect the EGFR signaling pathway. Further, *in silico* study, molecular docking predicts the interaction between the THTMP and the EGFR receptor. The QSAR and ADMET also confirm the potentiality of the compound as an anticancer agent. Overall, THTMP has a significant cytotoxic effect and plays a vital role in the induction of apoptosis and should have a potential effect in the treatment of cancer.

AUTHOR CONTRIBUTIONS

SP executed the experiments and data analysis. OY and MK conceived and managed all studies. All the authors contributed to writing the manuscript.

AUTHOR INFORMATION

Corresponding Author:
*meenakshisundaram.kandhavelu@tuni.fi; Phone: (+358)417488772

AUTHOR CONTRIBUTIONS

SP and KS executed the experiments and data analysis. OY and MK conceived and managed all studies. All the authors contributed to writing the manuscript.

CONFLICT OF INTEREST

There exists no conflict of interest between authors.

ACKNOWLEDGEMENT

We would like to thank Prof. Nuno R. Candeias, Faculty of Engineering and Natural Sciences, Tampere University for gift of synthesized compounds. Also, we would like thank Dr. Kumar SUBRAMANIAN (Oncology Division, Department of Internal Medicine, Faculty of Health Sciences, University of the Witwatersrand) who has been involved in the execution of experiments and manuscript revision.

ABBREVIATIONS

MCF-7 and Skbr3, Human breast adenocarcinoma epithelial cells, H9C2 - Rat cardiac myoblasts cell lines; IC_{50}, The half maximal inhibitory concentration; PI, Propidium Iodide; FACS- Fluorescence-activated cell sorting; AO/EtBr- Acridine Orange/Ethidium Bromide; QSAR- Quantitative Structural-Activity Relationship; Rt-PCR- Reverse transcript polymerase chain reaction;

REFERENCES

[1] F. Bray, J.-S. Ren, E. Masuyer, and J. Ferlay, "Global estimates of cancer prevalence for 27 sites in the adult population in 2008," *Int. J. Cancer*, vol. 132, no. 5, pp. 1133–1145, Mar. 2013.

[2] R. Siegel, D. Naishadham, and A. Jemal, "Cancer statistics, 2013," *CA. Cancer J. Clin.*, vol. 63, no. 1, pp. 11–30, Jan. 2013.

[3] T. The Lancet, "Breast cancer in developing countries," *Lancet*, vol. 374, no. 9701, p. 1567, Nov. 2009.

[4] J. Liu, B. Ming, G.-H. Gong, D. Wang, G.-L. Bao, and L.-J. Yu, "Current research on anti-breast cancer synthetic compounds," 2018.

[5] A. Mullard, "2017 FDA drug approvals.," *Nat. Rev. Drug Discov.*, vol. 17, no. 2, p. 150, Feb. 2018.

[6] R. Gerl and D. L. Vaux, "Apoptosis in the development and treatment of cancer," *Carcinogenesis*, vol. 26, no. 2, pp. 263–270, Sep. 2004.

[7] R. S. Y. Wong, "Apoptosis in cancer: from pathogenesis to treatment.," *J. Exp. Clin. Cancer Res.*, vol. 30, no. 1, p. 87, Sep. 2011.

[8] Y. P. Kwan *et al.*, "Evaluation of the cytotoxicity, cell-cycle arrest, and apoptotic induction by *Euphorbia hirta* in MCF-7 breast cancer cells," *Pharm. Biol.*, pp. 1–14, Jul. 2015.

[9] N. Zhang, X. Kong, S. Yan, C. Yuan, and Q. Yang, "Huaier aqueous extract inhibits proliferation of breast cancer cells by inducing apoptosis," *Cancer Sci.*, vol. 101, no. 11, pp. 2375–2383, Nov. 2010.

[10] Y. S. Tor *et al.*, "Induction of Apoptosis in MCF-7 Cells via Oxidative Stress Generation, Mitochondria-Dependent and Caspase-Independent Pathway by Ethyl Acetate Extract of Dillenia suffruticosa and Its Chemical Profile.," *PLoS One*, vol. 10, no. 6, p. e0127441, Jun. 2015.

[11] G. Mariño, M. Niso-Santano, E. H. Baehrecke, and G. Kroemer, "Self-consumption: the interplay of autophagy and apoptosis," *Nat. Rev. Mol. Cell Biol.*, vol. 15, no. 2, pp. 81–94, Feb. 2014.

[12] N. Cotelle, J. L. Bernier, J. P. Catteau, J. Pommery, J. C. Wallet, and E. M. Gaydou, "Antioxidant properties of hydroxy-flavones.," *Free Radic. Biol. Med.*, vol. 20, no. 1, pp. 35–43, 1996.

[13] R. A. Larson, "The antioxidants of higher plants," *Phytochemistry*, vol. 27, no. 4, pp. 969–978, Jan. 1988.

[14] Y. S. Velioglu, G. Mazza, L. Gao, and B. D. Oomah, "Antioxidant Activity and Total Phenolics in Selected Fruits, Vegetables, and Grain Products," *J. Agric. Food Chem.*, vol. 46, no. 10, pp. 4113–4117, Oct. 1998.

[15] W. Zheng and S. Y. Wang, "Antioxidant activity and phenolic compounds in selected herbs.," *J. Agric. Food Chem.*, vol. 49, no. 11, pp. 5165–70, Nov. 2001.

[16] S. K. Jaganathan and E. Supriyanto, "Antiproliferative and Molecular Mechanism of Eugenol-Induced Apoptosis in Cancer Cells," *Molecules*, vol. 17, no. 6, pp. 6290–6304, May 2012.

[17] P. Doan *et al.*, "Synthesis and biological screening for cytotoxic activity of N-substituted indolines and morpholines.," *Eur. J. Med. Chem.*, vol. 120, pp. 296–303, Sep. 2016.

[18] J. G. M. KLIJN, P. M. J. J. BERNS, P. I. M. SCHMITZ, and J. A. FOEKENS, "The Clinical Significance of Epidermal Growth Factor Receptor (EGF-R) in Human Breast Cancer: A Review on 5232 Patients*," *Endocr. Rev.*, vol. 13, no. 1, pp. 3–17, Feb. 1992.

[19] E. M. Ciruelos Gil, "Targeting the PI3K/AKT/mTOR pathway in estrogen receptor-positive breast cancer," *Cancer Treat. Rev.*, vol. 40, no. 7, pp. 862–871, Aug. 2014.

[20] Q.-B. She *et al.*, "Integrated molecular pathway analysis informs a synergistic combination therapy targeting PTEN/PI3K and EGFR pathways for basal-like breast cancer," *BMC Cancer*, vol. 16, no. 1, p. 587, Dec. 2016.

[21] K. Subik *et al.*, "The expression patterns of ER, PR, HER2, CK5/6, EGFR, KI-67 and AR by immunohistochemical analysis in breast cancer cell lines," *Breast Cancer Basic Clin. Res.*, 2010.

[22] K. Peng *et al.*, "Novel EGFR inhibitors attenuate cardiac hypertrophy induced by angiotensin II," *J. Cell. Mol. Med.*, 2016.

[23] P. S. Vaiyapuri, A. A. Ali, A. A. Mohammad, J. Kandhavelu, and M. Kandhavelu, "Time lapse microscopy observation of cellular structural changes and image analysis of drug treated cancer cells to characterize the cellular heterogeneity," *Environ. Toxicol.*, vol. 30, no. 6, pp. 724–734, May 2015.

[24] Í. Neto *et al.*, "Multicomponent Petasis-borono Mannich Preparation of Alkylaminophenols and Antimicrobial Activity Studies.," *ChemMedChem*, vol. 11, no. 18, pp. 2015–23, Sep. 2016.

[25] P. Doan, A. Musa, N. R. Candeias, F. Emmert-Streib, O. Yli-Harja, and M. Kandhavelu, "Alkylaminophenol induces G1/S phase cell cycle arrest in glioblastoma cells through p53 and cyclin-dependent kinase signaling pathway," *Front. Pharmacol.*, 2019.

[26] T. Mosmann, "Rapid colorimetric assay for cellular growth and survival: application to proliferation and cytotoxicity assays.," *J. Immunol. Methods*, vol. 65, no. 1–2, pp. 55–63, Dec. 1983.

[27] M. Herrmann, H. M. Lorenz, R. Voll, M. Grünke, W. Woith, and J. R. Kalden, "A rapid and simple method for the isolation of apoptotic DNA fragments.," *Nucleic Acids Res.*, vol. 22, no. 24, pp. 5506–7, Dec. 1994.

[28] A. S. Soror, A. S. Alla, Y. M. E.- Ayouty, and H. A. Gehan, "Cytotoxicity, DNA Fragmentation and Histological Analysis of MCF-7 Cells Treated with Acetylspermine," *Int. J. Pharmacol.*, vol. 11, no. 7, pp. 712–718, Jul. 2015.

[29] A. G. Basnakian and S. J. James, "A rapid and sensitive assay for the detection of DNA fragmentation during early phases of apoptosis.," *Nucleic Acids Res.*, vol. 22, no. 13, pp. 2714–5, Jul. 1994.

[30] I. Vermes, C. Haanen, H. Steffens-Nakken, and C. Reutelingsperger, "A novel assay for apoptosis. Flow cytometric detection of phosphatidylserine expression on early apoptotic cells using fluorescein labelled Annexin V.," *J. Immunol. Methods*, vol. 184, no. 1, pp. 39–51, Jul. 1995.

[31] G. Koopman, C. P. Reutelingsperger, G. A. Kuijten, R. M. Keehnen, S. T. Pals, and M. H. van Oers, "Annexin V for flow cytometric detection of phosphatidylserine expression on B cells undergoing apoptosis.," *Blood*, vol. 84, no. 5, pp. 1415–20, Sep. 1994.

[32] P. CHOMZYNSKI and N. Sacchi, "Single-Step Method of RNA Isolation by Acid Guanidinium Thiocyanate–Phenol–Chloroform Extraction," *Anal. Biochem.*, vol. 162, no. 1, pp. 156–159, Apr. 1987.

[33] G. Jones, P. Willett, R. C. Glen, A. R. Leach, and R. Taylor, "Development and validation of a genetic algorithm for flexible docking 1 1Edited by F. E. Cohen," *J. Mol. Biol.*, vol. 267, no. 3, pp. 727–748, Apr. 1997.

[34] F. Cheng *et al.*, "admetSAR: A Comprehensive Source and Free Tool for Assessment of Chemical ADMET Properties," *J. Chem. Inf. Model.*, vol. 52, no. 11, pp. 3099–3105, Nov. 2012.

[35] S. Kim *et al.*, "PubChem Substance and Compound databases," *Nucleic Acids Res.*, vol. 44, no. D1, pp. D1202–D1213, Jan. 2016.

[36] B. J. Cridge, L. Larsen, and R. J. Rosengren, "Curcumin and its derivatives in breast cancer: Current developments and potential for the treatment of drug-resistant cancers," *Oncol. Discov.*, vol. 1, no. 1, p. 6, Sep. 2013.

[37] P. Doan, T. Nguyen, O. Yli-Harja, N. R. Candeias, and M. Kandhavelu, "Effect of alkylaminophenols on growth inhibition and apoptosis of bone cancer cells.," *Eur. J. Pharm. Sci.*, vol. 107, pp. 208–216, Sep. 2017.

[38] P. S. Sukhramani, P. S. Sukhramani, S. A. Desai, and M. P. Suthar, "In-vitro cytotoxicity evaluation of novel N-substituted bis-benzimidazole derivatives for anti-lung and anti-breast cancer activity," *Ann. Biol. Res.*, vol. 2, no. 1, pp. 51–59.

[39] M. M. Ghorab and M. S. Alsaid, "Anticancer activity of some novel thieno [2, 3-d] pyrimidine derivatives.," *Biomed. Res.*, vol. 27, no. 1.

[40] S. N. A. Malek *et al.*, "Cytotoxic Activity of Pereskia bleo (Cactaceae) Against Selected Human Cell Lines," *Int. J. Cancer Res.*, vol. 4, no. 1, pp. 20–27, Jan. 2008.

[41] L. Vairavelu and M. V. and K. R. Prasad, "Synthesis, Biological Evaluation and Structure Activity Relationship of Substituted pyrazolo-, isoxazolo-, pyrimido- and mercaptopyrimidocycloocta[b]indoles," *Med. Chem. (Los. Angeles).*, vol. 06, no. 05, May 2016.

[42] R. Gaur, A. S. Pathania, F. A. Malik, R. S. Bhakuni, and R. K. Verma, "Synthesis of a series of novel dihydroartemisinin monomers and dimers containing chalcone as a linker and their anticancer activity.," *Eur. J. Med. Chem.*, vol. 122, pp. 232–246, Oct. 2016.

[43] C. Feng *et al.*, "A new anticancer compound, oblongifolin C, inhibits tumor growth and promotes apoptosis in HeLa cells through Bax activation.," *Int. J. cancer*, vol. 131, no. 6, pp. 1445–54, Sep. 2012.

[44] W. R. Sawadogo *et al.*, "In vitro antileishmanial and antitrypanosomal activities of five medicinal plants from Burkina Faso.," *Parasitol. Res.*, vol. 110, no. 5, pp. 1779–83, May 2012.

[45] J. G. Walsh, S. P. Cullen, C. Sheridan, A. U. Lüthi, C. Gerner, and S. J. Martin, "Executioner caspase-3 and caspase-7 are functionally distinct proteases.," *Proc. Natl. Acad. Sci. U. S. A.*, vol. 105, no. 35, pp. 12815–9, Sep. 2008.

[46] A. Eastman and M. A. Barry, "The origins of DNA breaks: a consequence of DNA damage, DNA repair, or apoptosis?," *Cancer Invest.*, vol. 10, no. 3, pp. 229–40, 1992.

[47] D. Basikc, S. Papovic, P. Ristic, and N. Arsenijevic, "Analysis of cycloheximide-induced apoptosis in human leukocytes: Fluorescence microscopy using annexin V/propidium iodide versus acridin orange/ethidium bromide," *Cell Biol. Int.*, vol. 30, no. 11, pp. 924–932, Nov. 2006.

[48] R. A. Laskowski, "PDBsum: summaries and analyses of PDB structures.," *Nucleic Acids Res.*, vol. 29, no. 1, pp. 221–2, Jan. 2001.

[49] P. G. Anantharaju, P. C. Gowda, M. G. Vimalambike, and S. V. Madhunapantula, "An overview on the role of dietary phenolics for the treatment of cancers," *Nutr. J.*, vol. 15, no. 1, p. 99, Dec. 2016.

[50] B. B. Aggarwal, A. Kumar, and A. C. Bharti, "Anticancer potential of curcumin: preclinical and clinical studies.," *Anticancer Res.*, vol. 23, no. 1A, pp. 363–98.

[51] M. Kampa *et al.*, "Antiproliferative and apoptotic effects of selective phenolic acids on T47D human breast cancer cells: potential mechanisms of action.," *Breast Cancer Res.*, vol. 6, no. 2, pp. R63-74, 2004.

[52] C.-J. Chen, H. Mei Hua, S.-C. Kuo, Y.-Y. Lai, J.-G. Chung, and W. Liu, *(2E)-N,N-dibutyl-3-(4-hydroxy-3-methoxyphenyl)*

acrylamide induces apoptosis and cell cycle arrest in HL-60 cells, vol. 27. 2007.

[53] L. A. Beltz, D. K. Bayer, A. L. Moss, and I. M. Simet, "Mechanisms of cancer prevention by green and black tea polyphenols.," *Anticancer. Agents Med. Chem.*, vol. 6, no. 5, pp. 389–406, Sep. 2006.

PUBLICATIONS

III

Antiproliferative and apoptotic effects of indole derivative, N-(2-hydroxy-5-nitrophenyl (4'-methylphenyl) methyl) indoline in breast cancer cells

Palanivel S, Murugesan A, Subramanian K, Yli-Harja O, and Kandhavelu M

European Journal of Pharmacology; Volume 881:15 August 2020, Pages 173-195.

doi.org: 10.1016/j.ejphar.2020.173195

European Journal of Pharmacology 881 (2020) 173195

Contents lists available at ScienceDirect

European Journal of Pharmacology

journal homepage: www.elsevier.com/locate/ejphar

Full length article

Antiproliferative and apoptotic effects of indole derivative, N-(2-hydroxy-5-nitrophenyl (4′-methylphenyl) methyl) indoline in breast cancer cells

Suresh Palanivel[a,b], Akshaya Murugesan[a,b,c], Kumar Subramanian[d], Olli Yli-Harja[b,e,f], Meenakshisundaram Kandhavelu[a,b,*]

[a] Molecular Signaling Lab, Faculty of Medicine and Health Technology, Tampere University and BioMediTech, Tays Cancer Center, Tampere University Hospital, P.O. Box 553, 33101, Tampere, Finland
[b] Institute of Biosciences and Medical Technology, Tampere, Finland
[c] Department of Biotechnology, Lady Doak College, Thallakulam, Madurai, 625002, India
[d] Oncology Division, Department of Internal Medicine, Faculty of Health Sciences, University of the Witwatersrand, Private Bag 3, Wits, 2050, Johannesburg, South Africa
[e] Computational Systems Biology Group, Faculty of Medicine and Health Technology, Tampere University and BioMediTech, Tays Cancer Center, Tampere University Hospital, P.O. Box 553, 33101, Tampere, Finland
[f] Institute for Systems Biology, 1441N 34th Street, Seattle, WA, 98103-8904, USA

ARTICLE INFO

Keywords:
Indoline derivatives
Apoptosis
Gene expression
EGFR
Docking
ADME
QSAR

ABSTRACT

Indoline derivatives functions as an inhibitors of epidermal growth factor receptor (EGFR) with the anticancer potential against various cancers. We aim to investigate anti-breast cancer effects and mechanism of action of novel indoline derivatives. Molecular docking of seven indoline derivates with EGFR revealed, *N*-(2-hydroxy-5-nitrophenyl (4′-methylphenyl) methyl) indoline (HNPMI) as the top lead compound. RT-PCR analysis showed the downregulation of PI3K/S6K1 genes in breast cancer cells through the activation of EGFR with HNPMI. This compound found to have higher cytotoxicity than Cyclophosphamide, with the IC_{50} of 64.10 μM in MCF-7 and 119.99 μM in SkBr3 cells. HNPMI significantly reduced the cell proliferation of MCF-7 and SkBr3 cells, without affecting non-cancerous cells, H9C2. Induction of apoptosis was analyzed by Caspase-3 and -9, DNA fragmentation, AO/EtBr staining and flow cytometry assays. A fold change of 0.218- and 0.098- for caspase-3 and 0.478- and 0.269- for caspase-9 in MCF7 and SkBr3 cells was observed, respectively. Caspase mediated apoptosis caused DNA fragmentation in breast cancer cells upon HNPMI treatment. The structural elucidation of HNPMI by QSAR model and ADME-Tox suggests, a bi-molecular interaction of HNPMI-EGFR which is related to antiproliferative and apoptotic activity. The data concludes that, HNPMI-induced the apoptosis via EGFR signaling pathway in breast cancer cells. Thus, HNPMI might serve as a scaffold for developing a potential anti-breast cancer therapeutic agent.

1. Introduction

Breast cancer is ranked as the second most common cancer worldwide. Report from Global statistics found that among the various types of cancers diagnosed, 12% of the patients were reported with breast cancer(Age standardized (World) incidence rates, breast, all ages, 2018). Though there are multiple factors involved in the cause of disease, lifestyle changes and the environmental factors plays a significant role. Prognosis and the overall survival are uncomplimentary, due to the limited treatment response and drug toxicity. Understanding on the heterogeneity of the breast cancer, numerous advances have been made in the treatment (Musa et al., 2018; Tong et al., 2018; Vaiyapuri et al., 2015). One such development is the use of small molecule targeted therapy in combination with standard chemotherapeutic agents. The current treatment regimens include the myriads of newly approved drugs for treating different subtypes of breast cancer. Despite the advanced treatment, lack of potential drugs or combinations, urges to discover the novel drug for inhibiting the proliferation and metastatic properties of the breast cancer cells.

Indole derivatives function as the inhibitor of epidermal growth factor receptor (EGFR) with the anticancer potential. EGFR is one of the well-studied and vital targets identified against breast cancer. EGFR is a mediator of a wide variety of signal transduction events controlling cell proliferation, migration and their survival (Ali and Wendt, 2017). It is

* Corresponding author. Molecular Signaling Lab, Faculty of Medicine and Health Technology, Tampere University and BioMediTech, Tays Cancer Center, Tampere University Hospital, P.O. Box 553, 33101, Tampere, Finland.
E-mail address: meenakshisundaram.kandhavelu@tuni.fi (M. Kandhavelu).

https://doi.org/10.1016/j.ejphar.2020.173195
Received 6 March 2020; Received in revised form 9 May 2020; Accepted 11 May 2020
Available online 21 May 2020

found to be overexpressed in majority of the breast cancers(Masuda et al., 2012). Since EGFR is the major signaling mediator for PI3 kinase, Ras-Raf-MAPK, JNK, and PLC(Downward et al., n.d.), the search for the potent EGFR inhibitors is of interest. Recently, we have synthesized numerous indolines and morpholines derivatives and evaluated its effect against different cancers (Doan et al., 2016; Karjalainen et al., 2018; Palanivel et al., 2020b, 2020a). However, the molecular mechanism of action of the HNPMI against breast cancer is not well studied. The present study is focused to reveal the best indoline derivatives based on its potential interaction with bind to EGFR protein. We performed in-silico screening of seven indoline derivatives that profoundly inhibits the growth of cancer cells.

N-(2-Hydroxy-5-Nitrophenyl (4′-Methylphenyl) Methyl) Indoline (HNPMI) was found to have best interaction with EGFR. We also have investigated the effect of HNPMI on downstream pathway genes of EGFR pathway in breast cancer cell lines. Also, the cytotoxicity and apoptotic induction of the HNPMI was found to be promising. QSAR study was performed to compare the structure and its activity relationship. ADME/Tox analysis was done to understand the drug-likeliness property of the HNPMI, which gives an idea about its bioavailability. These studies explore HNPMI as a potent antiproliferative and apoptosis inducer in breast cancer cells.

2. Materials and methods

2.1. Cell lines, materials

The study was aimed to identify the effect of indoline derivatives in inducing the cell death in breast cancer cells through the activation of EGFR signaling. Hence, EGFR overexpressed human breast cancer cells, MCF-7 and SkBr3 (NCCS, Pune, India) were chosen for the study. Cells cultured in DMEM medium, with 10% Fetal Bovine Serum, at 37 ˚C, 5% CO_2 in a humidified atmosphere. The non-cancerous cells, H9C2 (cardiomyocyte), were also maintained in the same medium as above. All the cell lines used in the study was EGFR (+).

2.2. Indoline derivatives

Seven indoline derivatives were selected for studying the anti-breast cancer effect and their mechanism of action. The list of selected compounds as follows: *N*-(2-hydroxy-5-nitrophenyl(4′-methylphenyl)methyl)indoline (HNPMI); (2-(3,4-dihydroquinolin1(2H)-yl)(p-tolyl)methyl)phenol); 2-(indolin-1-yl(4-methoxyphenyl)methyl)phenol; 2-(indolin-1-yl(4-methoxyphenyl)methyl)-4-nitrophenol; 2-(indolin-1-yl (phenyl)methyl)-4-nitrophenol; 2-(indolin-1-yl(phenyl)methyl)-4-nitrophenol; 2-(indolin-1-yl(p-tolyl)methyl)-4-nitrophenol.

2.3. Virtual screening and synthesis of chemical compounds

Molecular docking was performed to identify the best potent inhibitor of EGFR among the seven indoline derivatives using *i*GEMDOCK (Hsu et al., 2011). The seven indoline structures were drawn using ACD/Chemsketch (Fig. 1A) (Hunter, 1997). The structures were cleaned and energy minimization was done using Frog2 online tool (Leite et al., 2007). The EGFR structure was retrieved from PDB database and its active site residues were identified. The interaction profiles was analyzed for these ligands and the interaction poses were visualized using Pymol (Schrödinger, 2015). AEE788 (Traxler et al., 2004) and Gefitinib (Pao et al., 2004), an EGFR inhibitor(s) were used as a reference compounds. From the docking score, the compound (HNPMI) with the lowest binding energy was chosen for the synthesis. The compound HNPMI was synthesized (Fig. 1D) using the salicylaldehyde as the carbonyl component in the Petasis-borono Mannich reaction in glycerol at 50 ˚C by a previously established methodology (Rosholm et al., 2015) starting from salicylaldehyde and the corresponding boronic acid. After the completion of the reaction, good yield of HNPMI was obtained by flash chromatography by diluting the reaction media with water and saturated $NaHCO_3$ solution and finally extracted with diethyl ether. Despite the mass transfer issues in reactions observed in high viscosity glycerol, raising the reaction temperature to 50 ˚C or 80 ˚C was enough to ensure the formation of the desired compound after 24 h or 48 h. NMR characterization was performed as previously explained (Supplementary file: Spectral data) (Doan et al., 2016)and further used for in-vitro analysis.

2.4. RNA extraction and cDNA synthesis

MCF-7 and SkBr3 cells were grown as described above and once the cells reaches 75% confluence, they were treated with the IC_{50} concentration of HNPMI for 24 h. Total RNA from the untreated and HNPMI treated MCF-7 cells were extracted using One step-RNA Reagent (Biobasic Inc.). RNA was extracted, air dried and dissolved in DEPC water and used for cDNA synthesis. It was reverse transcribed with Easy Script Plus™ Reverse Transcriptase. For RT-PCR reaction, 1–2 µg of RNA and 2 µl of oligo-dT was incubated at 65 ˚C for 5 min and chilled immediately on ice. To this, 4 µlof 1X reverse transcriptase buffer, 2 µl of 2.5 mM dNTP mix, and 0.5 µl of RNase inhibitor (40 U/µL) were added and incubated for 5 min at 42 ˚C. To this mixture, 1 µl Easy Script reverse transcriptase (200 U/µL) was added and the reaction was left at 42 ˚C for 50 min followed by 70 ˚C for 10 min and chilled on ice.

2.5. RT-PCR analysis

The expression of target genes EGFR, PI3K, and S6K1 along with housekeeping gene, β-actin were analyzed using RT-PCR. The specific forward and reverse primers were used as follows: EGFR (F: 5′ TCCC CGTAATTATGTGGTGACAGATC 3′ and R: ACCCCTAAATGCCACCGGC 3′); *PI3K* (F: 5′ AACACAGAAGACCAATACTC 3′ and R: 5′ TTCGCCAT CTACCACTAC 3′); *S6K1* (F: 5′CACATAACCTGTGGTCTGTTGCTG 3′ and R: 5′ AGATGCAAAGCGAACTTGGGATA 3′); and *β-actin* (F: 5′ CACCCG CGAGTACAACCTT 3′ and R: 5′ CCCATACCCACCATCACACC 3′), were synthesized commercially and used for PCR. The PCR mixture contains 1X Taq Buffer (with $MgCl_2$), 0.2 mM dNTPs, 2.5 mM $MgCl_2$, 0.3 µM Forward and Reverse primers, template cDNA and 1U Taq Polymerase. The PCR cycle was set up as follows; Initial denaturation (94 ˚C - 2min), denaturation (94 ˚C −30s), annealing (Ta-1min), extension (72 ˚C - 1min 20s), final extension (72 ˚C - 7min) and hold at 4 ˚C. The cycle was repeated for 32 times. Ta for β-actin- 54 ˚C; EGFR – 56 ˚C; PI3K – 54 ˚C; S6K1 - 56 ˚C. After the reaction, the products were separated on 1.5% agarose gel. 100bp DNA ladder was used for reference. The gene expression was quantified by measuring the intensity of the DNA band using the ImageJ program.

2.6. Cell viability/proliferation assay

The cell cytotoxicity was measured using MTT assay in all three cell lines (Mosmann, 1983). Briefly, the cells were plated in 96 well plates with a cell density of approximately 1.2×10^4 cells/well. At 70% confluence, the cells were treated with varying concentrations of HNPMI (10, 25, 50, 75, and 100 µM). Untreated cells were also maintained as a control. After 24 h of incubation, 10µlof MTT (5 mg/ml) was added and incubated for 4 h at 37 ˚C. 100 µl of DMSO was added to dissolve the formazan crystals that are formed, and the absorbance was read at 570 nm in a microtiter plate reader. Cyclophosphamide was used as a positive control (Bang et al., 2000; Mamounas et al., 2005). Dose response curve was plotted to calculate the IC_{50} concentration using concentration-effect curve function of Graphpad Prism 6. Three technical and biological repeats were performed for each condition and the data are presented as mean of 3 independent ± standard error of the mean.

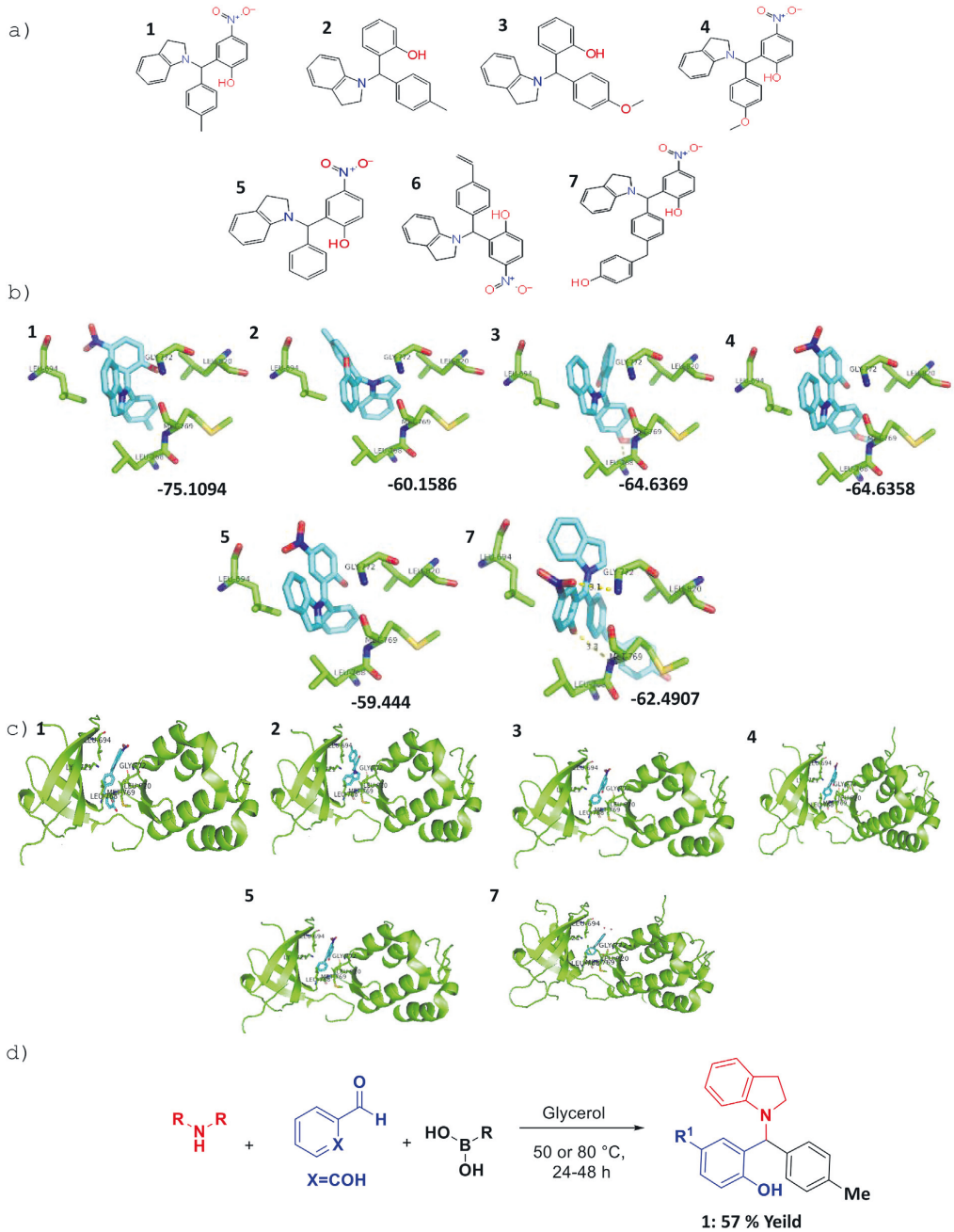

Fig. 1. Compound structure and their interaction with EGFR (A) 2D structure of indoline derivatives (B) Molecular docking analysis of indoline derivatives with EGFR. The surface-docking model of HNPMI in the EGFR active site. The docking score is represented for each model. The ligand is represented as sticks; and the protein active sites are represented as lines. Hydrogen bond interaction are shown in dotted lines (Red) and the interacting residues are labelled (C) Ligand-receptor interaction (D)Synthesis of top ligand, N-(2-hydroxy-5-nitrophenyl(4′-methylphenyl) methyl) indoline HNPMI. (For interpretation of the references to color in this figure legend, the reader is referred to the Web version of this article.)

Table 1
List of Training set and Test set of compounds used for QSAR model.

Training Set			
S.No	Compound Name	$IC_{50\ (\mu M)}$	References
1	N-(2-hydroxy-5-nitrophenyl(4′-methylphenyl)methyl)indoline	64.10	Present Study
2	TAMOXIFEN	6,05	Mokhtari et al. (2012)
3	4-((5-bromo-2-oxoindolin-3-ylidene)methyl)benzonitrile	6	
4	N-(2-fluoro-4-((2-oxoin dolin-3-ylidene) methyl)phenyl)acetamide	9,3	
5	3-(4-((4-methylpiperazin-1-yl)methyl)benzylidene)indolin-2-one	42,07	
6	3-((5-(4-fluorophenyl)pyridin-3-yl)methylene)indolin-2-one	8,54	
7	4-(2-oxo-5-(trifluoromethoxy)indolin-3-ylideneamino)benzamide	27,2	
8	4-(5, 7-dichloro-2-oxoindolin-3-ylideneamino)benzamide	65,86	
9	7-(Hy d roxymethy l ene) - 2 - m e t hy l - 5, 7, 8, 9, 1 0, 1 1 -hexahydrocycloocta[b]indol-6-one	27,34	Vairavelu and Prasad KJ (2016))
10	2-C hl or o - 7 - (hy d roxymethy l e n e) - 5, 7, 8, 9, 1 0, 1 1 -hexahydrocycloocta[b]indol-6-one	21,96	
11	7-(Hy d roxymethy l ene) - 4 - m e t hy l - 5, 7, 8, 9, 1 0, 1 1 -hexahydrocycloocta[b]indol-6-one	37,79	
12	7-(Hydroxymethylene)-5,7,8,9,10,11-hexahydrocycloocta[b] indol-6-one	49,45	
13	9-Methyl-4,5,6,7-tetrahydropyrazolo[3′,4′:8,7]-12Hcycloocta[b]indole	30,41	
14	9-Chloro-4,5,6,7-tetrahydropyrazolo[3′,4′:8,7]-12Hcycloocta[b]indole	15,98	
15	11-Methyl-4,5,6,7-tetrahydropyrazolo[3′,4′:8,7]-12Hcycloocta[b]indole	35,77	
16	4,5,6,7-Tetrahydropyrazolo[3′,4′:8,7]-12H- cycloocta[b]indole	47,56	
17	9-Methyl-4,5,6,7-tetrahydroisoxazolo[3′,4′:8,7]-12Hcycloocta[b]indole	29,96	
18	9-Chloro-4,5,6,7-tetrahydroisoxazolo[3′,4′:8,7]-12Hcycloocta[b]indole	21,96	
19	11-Methyl-4,5,6,7-tetrahydroisoxazolo[3′,4′:8,7]-12Hcycloocta[b]indole	37,14	
20	4,5,6,7-Tetrahydroisoxazolo[3′,4′:8,7]-12H-cycloocta[b]indole	48,26	
21	9-Methyl-1-phenyl-4,5,6,7-tetrahydropyrazolo[3′,4′:8,7]-12Hcycloocta[b]indole	50,41	
Test Set			
S.No	**Compound Name**	**IC_{50} (μM)**	**References**
1	9-Chloro-1-phenyl-4,5,6,7-tetrahydropyrazolo[3′,4′:8,7]-12Hcycloocta[b]indole	27.23	Vairavelu and Prasad KJ (2016)
2	11-Methyl-1-phenyl-4,5,6,7-tetrahydropyrazolo[3′,4′:8,7]-12Hcycloocta[b]indole	25.22	
3	1-Phenyl-4,5,6,7-tetrahydropyrazolo[3′,4′:8,7]-12Hcycloocta[b]indole	54.61	
4	2-Hydroxy-10-methyl-5,6,7,8-tetrahydropyrimido[5′,6′:8,7]-13H-cycloocta[b]indole	30.13	
5	2-Hydroxy-10-chloro-5,6,7,8-tetrahydropyrimido[5′,6′:8,7]-13Hcycloocta[b]indole	11	
6	2-Hydroxy-12-methyl-5,6,7,8-tetrahydropyrimido[5′,6′:8,7]-13H-cycloocta[b]indole	32	
7	2-hydroxy-5,6,7,8-tetrahydropyrimido[5′,6′:8,7]-13H-cycloocta[b]indoles	45	
8	2-Mercapto-10-methyl-5,6,7,8-tetrahydropyrimido[5′,6′:8,7]-13H-cycloocta[b]indole	31	
9	2-Mercapto-10-chloro-5,6,7,8-tetrahydropyrimido[5′,6′:8,7]-13H-cycloocta[b]indole	12.35	
10	2-Mercapto-12-methyl-5,6,7,8-tetrahydropyrimido[5′,6′:8,7]-13H-cycloocta[b]indole	34	
11	2-Mercapto-5,6,7,8-tetrahydropyrimido[5′,6′:8,7]-13Hcycloocta[b]indole	46	

2.7. Caspases 3 and caspases 9 activity assays

Drug induced cell apoptosis was measured by estimating caspase-3 and caspase-9 level by chromogenic assays following the manufacturer's protocol (Calbiochem, Merck). The MCF-7 and SkBr3 were treated with HNPMI for 24 h and lysed using Lysis buffer (50 mM HEPES, 100 mM NaCl, 0.1% CHAPS, 1 mM DTT, 100 mM EDTA). The cytosolic extracts were collected by centrifugation of the lysate, and the concentration of the protein was determined by Bradford assay using BSA as a standard. To each reaction sample 50 μl of cell lysate containing 100–200 μg of total protein was added. Cellular extracts were incubated with 5 μl of the 4 mM p-nitroanilide (pNA) substrates, DEVD-pNA (caspase- 3 activity) for 2 h at 37 °C. The amount of free pNA was calculated by measuring the absorbance cleaved substrates at 405 nm in a plate reader. Relative Caspase-3 and 9 activities were calculated based on the absorbance of free pNA from treated cells to untreated cells.

2.8. DNA isolation and agarose gel electrophoresis

The DNA fragmentation analysis was performed in MCF-7 cell line in order validate the apoptosis using gel electrophoresis (Basnakian and James, 1994). MCF-7 cells were grown in appropriate culture medium and at 75% confluence the cells were treated with IC_{50} concentration of HNPMI for 24 h. The HNPMI treated and control cells were lysed using lysis buffer. After incubation and centrifugation, phenol: chloroform: isoamylalcohol mixture was added to the supernatant to spool out DNA in the aqueous phase. DNA was precipitated using ammonium acetate and ice-cold isopropanol. After a repeated wash with 70% ethanol, the isolated DNA was stored in 20–50 μl of TE buffer. Samples were loaded in 2% agarose gel (w/v) and run at 50 V. DNA Ladder Mix (1 kb) was used as marker and DNA was detected using ethidium bromide under UV transilluminator.

2.9. Fluorescence activated cell sorting analysis

Translocation of membrane phosphatidylserine (PS) is a phospholipid which is translocated from the internal plasma membrane to the surface of the lipid layer is the hallmark in identifying apoptotic cells. Annexin V is a phospholipid-binding protein that has high affinity for PS. The fluorochrome-labelled Annexin V was used for the detection of translocated PS using Fluorescence activated cell sorting (FACS). The induction of apoptosis in MCF-7 cell line after the treatment with HNPMI was determined by FACS analysis(Vermes et al., 1995). MCF-7 cells at the confluence of 75% were treated with HNPMI in three different concentrations viz. 59.10 μM, 64.10 μM and 69.10 μM and the control well was left untreated. The cells were incubated for 24 h, trypsinised and the cell pellet was suspended in PBS. The cells were washed with 1X binding buffer at a concentration of 1×10^6 cells/ml. To this suspension, 5 μl of FITC Annexin V and 5 μl propidium iodide were added and vortexed gently. Cells were further incubated at 25 °C for 15 min in dark. Treated and control cells were mixed with 400 μl of 1X Binding Buffer and the apoptotic cell were analyzed by flow cytometry within 1 h.

2.10. Acridine orange/ethidium bromide dual staining

Dual staining was performed in MCF-7 cells to visualize the potential of the HNPMI induced apoptosis. MCF-7 cells were grown on six

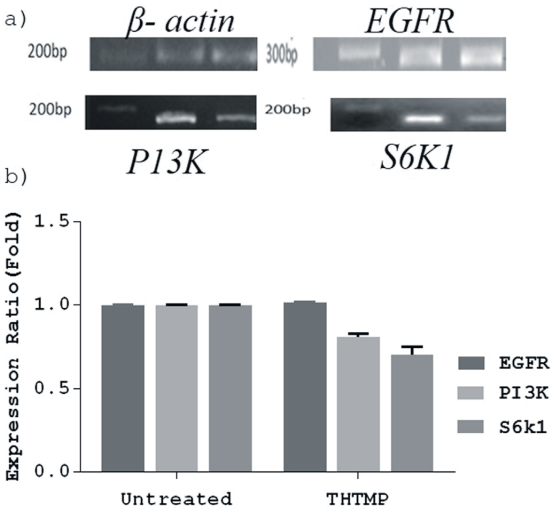

Fig. 2. Gene expression analysis of EGFR downstream signaling genes. (A) PCR amplification of β-actin (204bp), EGFR (250bp), P13K (195bp) and S6K1 genes (180bp). (Lane 1: 100bp DNA marker, Lane 2: Control (Untreated) (B) Optical density was measured to determine the fold change of mRNA expression for EGFR, S6K1, and PI3K genes, normalised with the housekeeping gene β-actin.

well plates and treated with three different concentrations (59.10 μM, 64.10 μM and 69.10 μM) of HNPMI for 24 h and control well was left untreated. The cells were trypsinised and suspended in PBS. Staining solution (1:1) mixture of 100 μg/ml AO and 100 μg/ml EB were added to this solution and 10 μl suspension was placed on a clean microscopic slide and observed under a fluorescent microscope with a blue filter (420–495 nm) and a green filter (510–560 nm). The cells were viewed in different fields and quantified using 300 cells per well(Basikc et al., 2006).

2.11. QSAR analysis of HNPMI

The relationship between the molecular descriptors of the set of compounds of interest with their respective biological activity has been studied by using quantitative structure-biological activity/property relationship (QSAR)(Roy et al., 2015). In this study, a QSAR approach was performed quantitatively to depict and provide mechanistic insights into interactions between the chemical structures of HNPMI by considering the compounds with similar structures.

In this analysis, 32 compounds were selected those shares significant similarity with the HNPMI. Since there are very limited experimentally confirmed compounds for the target, tamoxifen (Mokhtari et al., 2012), a non-indoline derivative is also has been selected for the QSAR analysis. The total of 32 compounds and their biological activity in terms of IC_{50} were chosen from the literature (Table 1). The descriptors for the compounds was calculated using Dragon software. The Dragon software was classified into 18 groups from 1497 descriptors. DRAGON software was used to calculate the set of 18 descriptors for each molecule in the training set (Todeschini et al., 2009). To most relevant set of descriptors was selected based on the IC_{50} of the compounds, and the MLR models were built. BUILDQSAR software was used to eliminate the variables. The goodness of the correlation was assessed by the square of coefficient regression (R^2), square of cross regression (q^2), the F-test (F), and the standard deviation (Std). The number of compounds is represented as “n” and the correlation coefficient as “r”.

2.12. Prediction of ADMET properties

A computational study of synthesized compound HNPMI was performed to predict the ADMET properties. ADMET filtering was done using admetSAR (http://www.admetexp.org/predict/). We assessed drug likeliness properties that signify the compound with good Absorption, Distribution, Metabolism, Excretion and Toxicity of HNPMI in breast cancer treatment.

3. Results

3.1. HNPMI interaction with EGFR and its downstream signaling effect on breast cancer cells

The aim of the study was to elucidate the interaction of seven indoline derivatives with EGFR protein (Fig. 1A). Molecular docking was employed to understand the binding affinity of active sites of EGFR protein with the selected indoline derivatives. The crystallographic 3D structure of EGFR protein was downloaded from Protein Databank (PDB ID:1M17) with a resolution of 2.6 Å, that served as a template. The active site residues of EGFR protein were found as follow, Lys-721, Met-769, Leu-768, Leu-820, Pro-770, Leu-694 and Gly-772. Also, the ligands structure was drawn using Chemsketch and saved as.mol file. The molecular docking studies was performed using iGEMdock (version 2.1). Docking of selected seven ligands against EGFR active site revealed the binding efficiency of six ligands except the compound “2-(indolin-1-yl(phenyl)methyl)-4-nitrophenol” with the nil docking pose (Fig. 1B). The ligand receptor interaction is represented in Fig. 1C. The compound, HNPMI showed strong binding behavior among all the tested compounds against the EGFR with the minimum binding energies −75.104 kcal/mol. Molecular docking disclosed the interaction of HNPMI with EGFR receptor through the hydrogen bonding and charged residue interactions with 29 amino acids. The results revealed that in HNPMI, the ligand – receptor (EGFR) complex exhibits two hydrogen bonds, one with amino acid Gly772 and the other with amino acid Met769. Also, to validate the binding efficiency of HNPMI, reference compounds such as AEE788 and Gefitinib were also docked with the target protein, EGFR (Supplementary file: Fig. 1A and B). The compound AEE788 exhibited the binding energy of −9.5 kcal/mol with the hydrogen bond interactions at Gln767, Met769, Thr766 whereas Gefitinib showed the binding energy of −7.9 kcal/mol with the hydrogen bond interactions at Met769, Thr830, Glu738. This data revealed that HNPMI exhibited least binding energy with highest docking score than the reference compounds, thus proving HNPMI as a potential target of EGFR and it was synthesized for further invitro analysis (Fig. 1D).

To better understand the effect of HNPMI in the EGFR downstream signaling pathway, the gene expression changes of EGFR, PI3K and S6K1 was performed by RT-PCR. Firstly, EGFR (250bp), PI3K (195bp), S6K1 (180bp) and the housekeeping gene, β-actin (180bp) were amplified using the cDNA of both the drug treated and control MCF-7 cells (Fig. 2A). Gene expression level was quantified using ImageJ tool using the gel image of amplicon (Fig. 2B). There is an alteration in the relative expression level of genes PI3K and S6K1, whereas the expression of EGFR doesn't show significant change in the cells treated with IC_{50} concentration of HNPMI when compared to the control cells. There is 0.4-fold decrease in the expression of S6K1 and 0.3-fold decrease for PI3K when compared with the control cells (Fig. 2B). Thus, the HNPMI downregulates the S6K1 and PI3K via EGFR signaling activation, which might possibly induce cell death.

3.2. Cytotoxicity of HNPMI

The cytotoxic activity of HNPMI (Fig. 3A) and cyclophosphamide (Fig. 3B) as a reference compound was investigated against breast cancer cell lines, MCF-7 and SkBr3 cell lines and non-cancerous (H9C2)

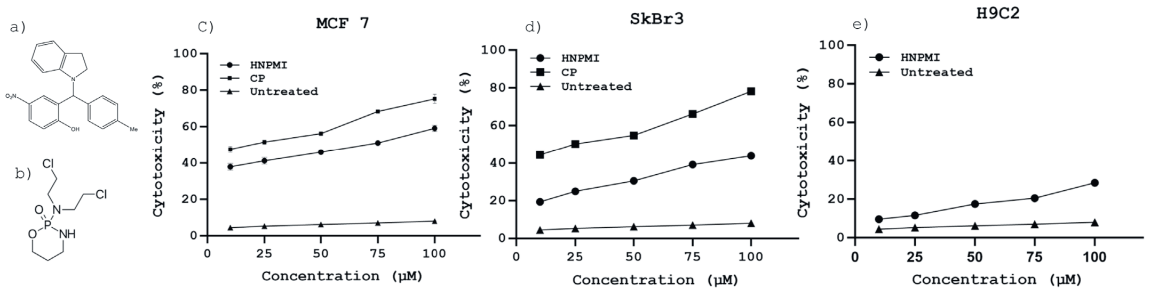

Fig. 3. Cytotoxicity effect of HNPMI in breast cancer and non-cancerous cells. (A) 2D structure of HNPMI and (B) Cyclophosphamide (CP, positive control). IUPAC: N-(2-hydroxy-5-nitrophenyl (4′-methylphenyl) methyl) indoline (M. wt – 329.443) and N, N-bis(2-chloroethyl)-2-oxo-1,3,2λ^{5}oxazaphosphinan-2-amine (M.wt.261.083) respectively, Dose dependent cytotoxicity effect of HNPMI and CP in breast cancer cells, MCF-7(C), SkBr3 (D) and H9C2 (non-cancerous cell), untreated (E). Error bar represents mean S.E.M. (n = 3 per group) with the statistical significance, p-values (*P < 0.05).

cell lines with varying concentration ranging from 10 to 100 μM. HNPMI have shown a dose-dependent reduction in the viability of these cells. The results show 33.96% and 50.93% cytotoxicity against MCF-7 cells whereas 14.64% and 39.07% toxicity for SkBr3 cells at 10 μM and 100 μM, respectively. HNPMI have the toxicity against MCF-7 (Fig. 3C) and SkBr3 (Fig. 3D) cell lines with IC_{50} values of 64.10 μM and 119.99 μM respectively. The IC_{50} value of the cyclophosphamide was found to be 21.37 μM in MCF7 and 38.34 μM in SkBr3. Interestingly, the HNPMI showed negligible level of cytotoxicity in non-cancerous cell, H9C2 when compared to the untreated cells (Fig. 3E).

3.3. Effects of HNPMI on caspases induction

The effect of anticancer drug on activation of caspase 3 and 9 is considered as the crucial in assessing the cytotoxicity. On treatment with HNPMI, MCF-7 and SkBr3 have shown an increased fold change of Caspase 3 and 9. At IC_{50} concentration, caspase 3 activity is elevated by a fold of 0.218 and 0.098 in MCF-7 and SkBr3, respectively (Fig. 4A), when compared to untreated cells. Similarly, caspase 9 activity has been increased by a fold of 0.478 and 0.269 in MCF-7 and SkBr3, respectively (Fig. 4B). The observed fold changes for both caspase 3 and 9 in treated conditions are statistically significant (*P ≤ 0.005) than the untreated condition.

3.4. HNPMI induces apoptosis mediated DNA fragmentation in MCF-7 cells

Caspase activation triggers cascade of downstream pathways that induces DNA fragmentation. To investigate the ability of HNPMI inducing apoptosis mediated cell death, the DNA laddering assay was performed. The DNA of the MCF-7 cells were exposed with IC_{50} concentration of HNPMI that leads to DNA fragmentation, whereas the untreated cells did not provide ladders of DNA (Fig. 5A). These results confirmed that HNPMI caused internucleosomal DNA fragmentation in the MCF-7 cells exhibiting the characteristic features of apoptosis causing cell death.

To gain more insight into the mode of action of apoptotic cell death by HNPMI, the phosphatidylserine externalization was detected by FACS. On treating MCF-7 cells with HNPMI for 24 h, around 54% of the cells were found to be viable, 1.06% cells are at early apoptotic cells, 39.61% of cells are at late apoptotic cells and 2.31% of cells are necrotic cells (Fig. 5B, C and D).

Induction of apoptosis was independently validated by AO/EtBr staining. The morphological evidences for apoptosis were also observed using dual staining. Apoptotic cells were marked by granular yellow-orange nuclear staining. The cells were characterized with nuclear shrinkage and blebbing of the nuclear membrane but in-contrast, necrotic cells showed uniform orange under fluorescent microscopy. The untreated cells appeared to have normal and green color nuclear staining (Fig. 6A-D). Dose dependent treatment with 59.10 μM, 64.10 μM and 69.10 μM HNPMI showed increased percentage of apoptosis of about 12%, 43% and 40% of apoptotic cells respectively (Fig. 6E). All the above observations suggested that HNPMI treatment induced apoptosis mediated cell death in MCF-7 cells.

3.5. Biological activity of HNPMI and its ADMET property

The anticancer activity of HNPMI was tested against the biological activity using built QSAR. The biological properties of the chemical molecules based on their chemical structure was analyzed. The QSAR model was built and the best compound which fits well with the model

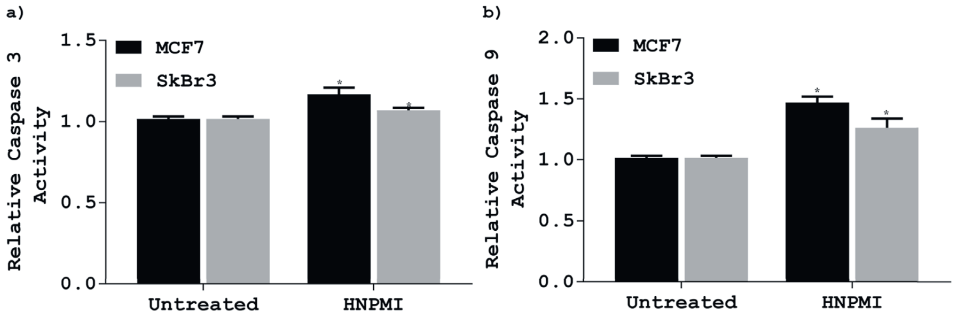

Fig. 4. Caspase 3 and Caspase 9 activity in breast cancer cells treated with IC_{50} concentration of HNPMI. (A) Relative caspase 3 activity of HNPMI in MCF7 cells and SKBr3 cells in treated and untreated conditions (B) relative caspase 9 activity as similar condition (A). Data represents mean ± S.E.M. of two individual experiments (n = 3 with the statistical significance, p-values (Two-way anova, *P ≤ 0.005).

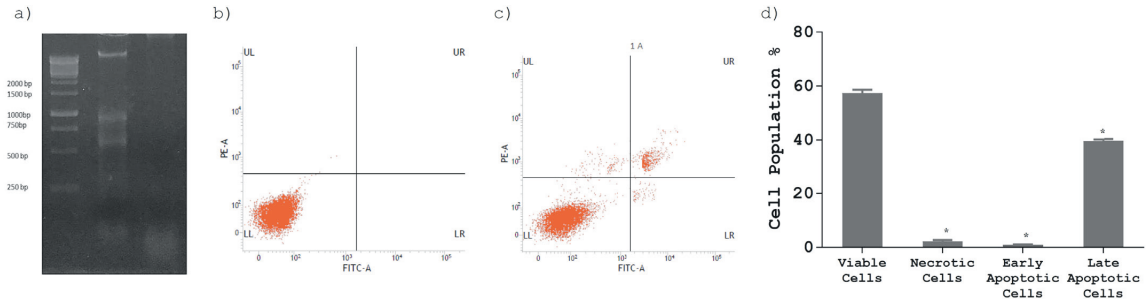

Fig. 5. Apoptosis induction in cells treated with IC_{50} concentration of HNPMI (A) 1.5% agarose gel electrophoresis of DNA extracted from HNPMI treated and untreated cells MCF-7 cells, Lane 1- 1 Kb Ladder; Lane 2 - DNA of cells treated with HNPMI; Lane 3- DNA of untreated cells. FACS assessment of cell apoptosis using Annexin/PI staining (B) untreated MCF-7 cells (C) HNPMI treated MCF-7 cells, UL- Necrotic cells, UR- Late apoptotic cells, LL - Viable cells, LR – Early apoptotic cells; (D) Percentage of cell population at different stages of cell death. Data represents mean ± S.E.M. of two individual experiments (n = 3 with the statistical significance, p-values (Two-way anova, *P ≤ 0.005).

was considered to show better biological activity when compared with the other compounds. Kennard-Stone algorithm was employed to divide the studied compounds, which comprised 32 compounds into a training set of 21 compounds and a test set of 11 compounds (Table 1). Multi-linear regression model was used to generate the QSAR model, in which the compounds were considered as outliers that has the significant deviation from the regression line. The correlation coefficient value (r) of the QSAR model was 0.947 and the test set value was 0.993 (Fig. 7) and this helps in predicting the anticancer activity of the QSAR model. The model generated using QSAR emphasized the presence of the indole ring, the aromaticity and certain other substituents like nitrogen and oxygen ascertain to the biological activity of the compounds.

From the ADMET analysis, it has been proven that HNPMI has good pharmacokinetic properties and obeyed the drug likeliness rules. The end points activity, calculated activities of the inhibitors and the accuracy value for each compound were reported in Table 2. The *in-silico* prediction of oral bioavailability and ADMET risk profiling are within their acceptable limit for HNPMI. It has good absorption properties, predicted to cross blood-brain barrier, CaCO-2 permeability and good intestinal absorption. It was predicted to be localized in mitochondria of the cell. The metabolism and toxicity parameters are also in acceptable limit for the compound. In terms of metabolism, it was found to act as a substrate and noninhibitor of CYP450. The compound by itself has no carcinogenicity property. The result elucidates that HNPMI has good drug likeliness property. Thus, HNPMI can be suggested as a to develop as a new drug candidate that possess unique ADMET properties.

4. Discussion

Indoline derivatives have gained importance as an anti-breast cancer drug and hence the synthesis of pharmacologically potential indoline derivatives is of immense interest in recent years. HNPMI is a novel indole derivatives characterized as a potent anticancer compound against bone cancer (Doan et al., 2017) and brain tumor (Doan et al., 2019). We have investigated the ability of the HNPMI to inhibit breast cancer cell proliferation and apoptosis induction in cancerous cells. Previously, indole derivates, diindolylmethanes flouro and cyano derivatives have cytotoxic effect towards tumor MCF7, NCI–H460, and SF-268 cells (Hong et al., 2002; Mousavi et al., 2011). HNPMI induced reduction in the cell viability of both cells, MCF-7 and SKBr3 without affecting the non-cancerous cells, H9C2 in a dose dependent manner.

The HNPMI used in the present study contains nitro group. Previous studies have reported the presence of nitro groups as a toxicophoric

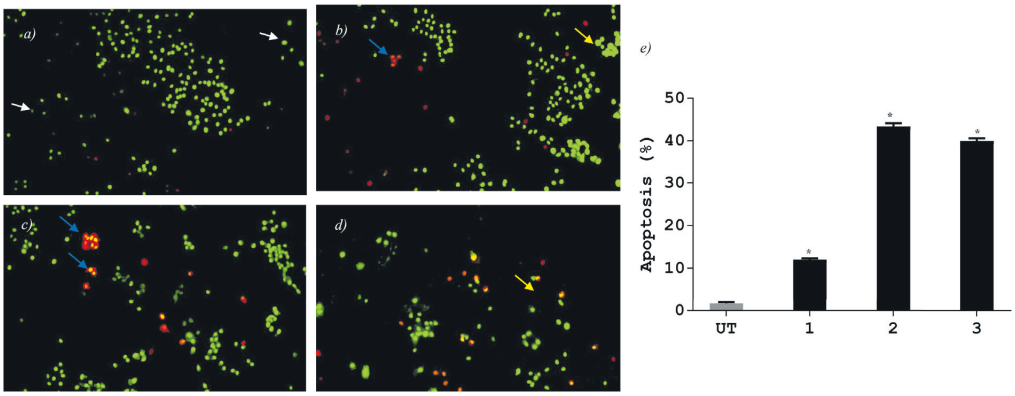

Fig. 6. Fluorescence microscopy images of AO-EtBr staining for deduction of apoptosis in. MCF7 cells (A) Untreated cells (B) MCF7 cells treated with 59.10 μM HNPMI (C) 64.10 μM (D) 69.10 μM. Appearance of green fluorescence (white arrow) in untreated control cells represents viable cells with normal morphology whereas visualization of bright yellow green color (yellow arrow) and reddish yellow/orange staining (blue arrow) in the treated cells shows the presence of early and late apoptotic cells. Necrotic cells appear a uniform orange stain; (E) percentage of. apoptosis in treated and untreated MCF-7 cells with different concentration of HNPMI where 1 is 59.10 μM; 2 is 64.10 μM; and 3 is 69.10 μM. Data represents mean ± S.E.M. of two individual experiments (n = 3 with the statistical significance, p-values (Two-way anova, *P ≤ 0.005). . (For interpretation of the references to color in this figure legend, the reader is referred to the Web version of this article.)

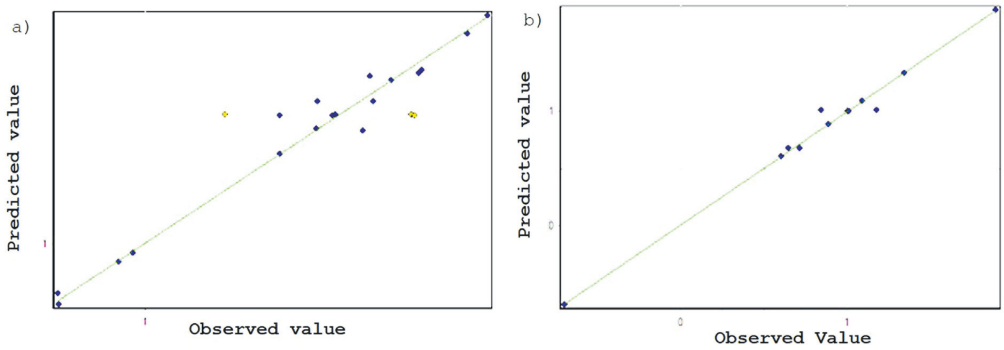

Fig. 7. Correlation of biological activity and physicochemical parameters of (A) training set (R2 = 0.947) and (B) test set (Q2 = 0.993).

Table 2
ADME properties of the ligand HNPMI.

Descriptor(s)	HTS Data	Accuracy
Blood-Brain Barrier	BBB+	0,8003
Human Intestinal Absorption	HIA+	0,9971
Caco-2 Permeability	Caco2+	0,5375
P-glycoprotein Substrate	Non-substrate	0,7583
P-glycoprotein Inhibitor	Non-inhibitor	0,6068
	Non-inhibitor	0,9278
Renal Organic Cation Transporter	Non-inhibitor	0,8148
Subcellular localization	Mitochondria	0,6819
CYP450 2C9 Substrate	Non-substrate	0,6246
CYP450 2D6 Substrate	Non-substrate	0,8092
CYP450 3A4 Substrate	Substrate	0,6311
CYP450 1A2 Inhibitor	Inhibitor	0,7358
CYP450 2C9 Inhibitor	Inhibitor	0,651
CYP450 2D6 Inhibitor	Non-inhibitor	0,8645
CYP450 2C19 Inhibitor	Non-inhibitor	0,5508
CYP450 3A4 Inhibitor	Non-inhibitor	0,7413
CYP Inhibitory Promiscuity	High CYP Inhibitory Promiscuity	0,7253
Human Ether-a-go-go-Related Gene Inhibition	Strong inhibitor	0,5167
	Non-inhibitor	0,7336
AMES Toxicity	AMES toxic	0,9402
Carcinogens	Non-carcinogens	0,6772
Fish Toxicity	High FHMT	0,9583
Tetrahymena Pyriformis Toxicity	High TPT	0,9846
Honey Bee Toxicity	Low HBT	0,513
Biodegradation	Not ready biodegradable	0,9604
Acute Oral Toxicity	Category III	0,7048
Carcinogenicity (Three-class)	Warning	0,4551

compound. However, extensive studies were conducted in exploring compounds containing nitro groups as anticancer agents, antitubercular agents, and antiparasitic agents. These compounds induce cell death by various mechanisms like topoisomerase inhibition, histone deacetylase inhibition, DNA alkylation, or tubulin polymerization inhibition, and have significantly demonstrated hypoxia-induced effects that are attributed to their bio-reductive activation potential. Some of the compounds are selectively toxic to bacteria, parasites, or tumor cells without harming the host organism or normal cells because of their nitroaromatic and heteroaromatic compounds(Nepali et al., 2019). In this aspect, our compound even though it bears nitro group, its cytotoxicity was higher in breast cancer cells than the non-cancerous cells.

Indole-based anticancer agents have been explored as a potential drug for regulating multiple signaling pathways of the cancer cells. Recently, a indole derivative, trisubstituted, shows cytotoxicity against MCF-7 cells by regulating MMP-2/MMP-9 molecule(Bakar et al., 2016). So far, the indole derivative Brassinin is shown to down-modulate the constitutive PI3K/Akt/mTOR in prostate cancer cells (Chripkova et al., 2014). Here, HNPMI was reported as a modulator of PI3K signaling pathway especially by downregulating S6K1 gene in breast cancer. Although, the HNPMI did not alter the expression of EGFR, it downregulates the PI3K/S6K1 genes down the cascade.

Apoptosis represent one of the important features of malignant cells and majority of available anti-breast cancer drugs depends on the apoptosis induction. It was found that HNPMI have induced the apoptosis in MCF7 cells through DNA fragmentation. Previous studies on indole derivatives have also proven their role in cell death induction by apoptosis in MCF-7 cells (Weng et al., 2008). Also, PI3K genes are found to be overexpressed in the cancerous condition which prevents the cells entering apoptosis (Chikh et al., 2016). Here, HNPMI down-regulates the expression of these genes and stops the cells from entering cellular proliferation signaling pathway and also induces the apoptosis. ADMET analysis has also been performed to prove the compound's structural feature as suitable drug candidate. The relative analysis of QSAR model exhibits a strong harmonization in the biological activity and the physicochemical property of the compound. Overall, these results suggest that the HNPMI have potential effect against the growth of breast cancer cells through the apoptosis induction, which can be subjected to pre-clinical trials for breast cancer treatment.

5. Conclusion

Our results conclude that the HNPMI induce caspase mediated apoptosis through EGFR mediated downstream signaling pathway. HNPMI downregulates the S6K1 and PI3K via EGFR signaling activation. HNPMI act as a potential anti-breast cancer compound, which inhibits the growth of MCF-7 and SkBr3 cells without affecting the non-cancerous cells. QSAR further supports the quantitative structural relationship with it is biological significance. Also, considering the long-term administration of this drug as an anti-breast cancer agent, its excellent safety profile has been proved using ADMET studies. Overall, HNPMI is a promising candidate for executing further phase clinical trials with pharmacological importance for the treatment of breast cancer.

Ethical approval

This article does not contain any studies with human participants performed by any of the authors.

Compliance with ethical standards

The authors declare that they have no conflict of interest.

CRediT authorship contribution statement

Suresh Palanivel: Data curation, Formal analysis, Writing - original

draft. **Akshaya Murugesan:** Formal analysis, Data curation, Writing - review & editing. **Kumar Subramanian:** Data curation, Formal analysis. **Olli Yli-Harja:** Project administration, Writing - review & editing. **Meenakshisundaram Kandhavelu:** Conceptualization, Project administration, Investigation, Writing - review & editing.

Acknowledgement

We would like to thank Prof. Nuno R. Candeias, Faculty of Engineering and Natural Sciences, Tampere University for gift of synthesized compounds.

Appendix A. Supplementary data

Supplementary data to this article can be found online at https://doi.org/10.1016/j.ejphar.2020.173195.

References

Age Standardized (World) Incidence Rates, Breast, All Ages.
Ali, R., Wendt, M.K., 2017. The paradoxical functions of EGFR during breast cancer progression. Signal Transduct. Target. Ther. 2, 16042. https://doi.org/10.1038/sigtrans.2016.42.
Bakar, F., Kilic-Kurt, Z., Caglayan, M.G., Olgen, S., 2016. The effects of 1,3,5-trisubstituted indole derivatives on cell growth, apoptosis and MMP-2/9 mRNA expression of MCF-7 human breast cancer cells. Anticancer. Agents Med. Chem. 17, 762–767. https://doi.org/10.2174/1871520616666160802115737.
Bang, S.M., Heo, D.S., Lee, K.H., Byun, J.H., Chang, H.M., Noh, D.Y., Choe, K.J., Bang, Y.J., Kim, S.R., Kim, N.K., 2000. Adjuvant doxorubicin and cyclophosphamide versus cyclophosphamide, methotrexate, and 5-fluorouracil chemotherapy in premenopausal women with axillary lymph node positive breast carcinoma: results of a randomized controlled trial. Cancer. https://doi.org/10.1002/1097-0142(20001215)89:12<2521::AID-CNCR2>3.0.CO;2-F.
Basikc, D., Papovic, S., Ristic, P., Arsenijevic, N., 2006. Analysis of cycloheximide-induced apoptosis in human leukocytes: fluorescence microscopy using annexin V/propidium iodide versus acridin orange/ethidium bromide. Cell Biol. Int. 30, 924–932. https://doi.org/10.1016/j.cellbi.2006.06.016.
Basnakian, A.G., James, S.J., 1994. A rapid and sensitive assay for the detection of DNA fragmentation during early phases of apoptosis. Nucleic Acids Res. 22, 2714–2715.
Chikh, A., Ferro, R., Abbott, J.J., Piñeiro, R., Buus, R., Iezzi, M., Ricci, F., Bergamaschi, D., Ostano, P., Chiorino, G., Lattanzio, R., Broggini, M., Piantelli, M., Maffucci, T., Falasca, M., 2016. Class II phosphoinositide 3-kinase C2β regulates a novel signaling pathway involved in breast cancer progression. Oncotarget. https://doi.org/10.18632/oncotarget.7761.
Chripkova, M., Drutovic, D., Pilatova, M., Mikes, J., Budovska, M., Vaskova, J., Broggini, M., Mirossay, L., Mojzis, J., 2014. Brassinin and its derivatives as potential anticancer agents. Toxicol. Vitro 28, 909–915. https://doi.org/10.1016/J.TIV.2014.04.002.
Doan, P., Karjalainen, A., Chandraseelan, J.G., Sandberg, O., Yli-Harja, O., Rosholm, T., Franzen, R., Candeias, N.R., Kandhavelu, M., 2016. Synthesis and biological screening for cytotoxic activity of N-substituted indolines and morpholines. Eur. J. Med. Chem. 120, 296–303. https://doi.org/10.1016/j.ejmech.2016.05.024.
Doan, P., Musa, A., Candeias, N.R., Emmert-Streib, F., Yli-Harja, O., Kandhavelu, M., 2019. Alkylaminophenol induces G1/S phase cell cycle arrest in glioblastoma cells through p53 and cyclin-dependent kinase signaling pathway. Front. Pharmacol. https://doi.org/10.3389/fphar.2019.00330.
Doan, P., Nguyen, T., Yli-Harja, O., Candeias, N.R., Kandhavelu, M., 2017. Effect of alkylaminophenols on growth inhibition and apoptosis of bone cancer cells. Eur. J. Pharmaceut. Sci. 107, 208–216. https://doi.org/10.1016/j.ejps.2017.07.016.
Downward, J., Parker, P., Waterfield, M.D., n.d. Autophosphorylation sites on the epidermal growth factor receptor. Nature 311, 483–485.
Hong, C., Firestone, G.L., Bjeldanes, L.F., 2002. Bcl-2 family-mediated apoptotic effects of 3,3′-diindolylmethane (DIM) in human breast cancer cells. Biochem. Pharmacol. https://doi.org/10.1016/S0006-2952(02)00856-0.
Hsu, K.-C., Chen, Y.-F., Lin, S.-R., Yang, J.-M., 2011. iGEMDOCK: a graphical environment of enhancing GEMDOCK using pharmacological interactions and post-screening analysis. BMC Bioinf. 12, S33. https://doi.org/10.1186/1471-2105-12-S1-S33.
Hunter, A.D., 1997. ACD/ChemSketch 1.0 (freeware); ACD/ChemSketch 2.0 and its tautomers, dictionary, and 3D plug-ins; ACD/HNMR 2.0; ACD/CNMR 2.0. J. Chem. Educ. 74, 905. https://doi.org/10.1021/ed074p905.
Karjalainen, A., Doan, P., Chandraseelan, J.G., Sandberg, O., Yli-Harja, O., Candeias, N.R., Kandhavelu, M., 2018. Synthesis of phenol-derivatives and biological screening for anticancer activity. Anticancer. Agents Med. Chem. 17, 1710–1720. https://doi.org/10.2174/1871520617666170327142027.
Leite, T.B., Gomes, D., Miteva, M.A., Chomilier, J., Villoutreix, B.O., Tuffery, P., 2007. Frog: a FRee Online druG 3D conformation generator. Nucleic Acids Res. 35, W568–W572. https://doi.org/10.1093/nar/gkm289.
Mamounas, E.P., Bryant, J., Lembersky, B., Fehrenbacher, L., Sedlacek, S.M., Fisher, B., Wickerham, D.L., Yothers, G., Soran, A., Wolmark, N., 2005. Paclitaxel after doxorubicin plus cyclophosphamide as adjuvant chemotherapy for node-positive breast cancer: results from NSABP B-28. J. Clin. Oncol. https://doi.org/10.1200/JCO.2005.10.517.
Masuda, H., Zhang, D., Bartholomeusz, C., Doihara, H., Hortobagyi, G.N., Ueno, N.T., 2012. Role of epidermal growth factor receptor in breast cancer. Breast Canc. Res. Treat. 136, 331–345. https://doi.org/10.1007/s10549-012-2289-9.
Mokhtari, S., Mosaddegh, M., Hamzeloo Moghadam, M., Soleymani, Z., Ghafari, S., Kobarfard, F., 2012. Synthesis and cytotoxic evaluation of novel 3-substituted derivatives of 2-indolinone. Iran. J. Pharm. Res. IJPR 11, 411–421.
Mosmann, T., 1983. Rapid colorimetric assay for cellular growth and survival: application to proliferation and cytotoxicity assays. J. Immunol. Methods 65, 55–63.
Mousavi, S.H., Moallem, S.A., Mehri, S., Shahsavand, S., Nassirli, H., Malaekeh-Nikouei, B., 2011. Improvement of cytotoxic and apoptogenic properties of crocin in cancer cell lines by its nanoliposomal form. Pharm. Biol. https://doi.org/10.3109/13880209.2011.563315.
Musa, A., Tripathi, S., Kandhavelu, M., Dehmer, M., Emmert-Streib, F., 2018. Harnessing the biological complexity of Big Data from LINCS gene expression signatures. PloS One. https://doi.org/10.1371/journal.pone.0201937.
Nepali, K., Lee, H.Y., Liou, J.P., 2019. Nitro-group-containing drugs. J. Med. Chem. https://doi.org/10.1021/acs.jmedchem.8b00147.
Palanivel, S., Murugesan, A., Yli-Harja, O., Kandhavelu, M., 2020a. Anticancer activity of THMPP: downregulation of PI3K/S6K1 in breast cancer cell line. Saudi Pharmaceut. J. https://doi.org/10.1016/j.jsps.2020.02.015.
Palanivel, S., Yli-Harja, O., Kandhavelu, M., 2020b. Alkylamino phenol derivative induces apoptosis by Inhibiting EGFR Signaling Pathway in Breast Cancer Cells. Anticancer. Agents Med. Chem. https://doi.org/10.2174/1871520620666200213101407.
Pao, W., Miller, V., Zakowski, M., Doherty, J., Politi, K., Sarkaria, I., Singh, B., Heelan, R., Rusch, V., Fulton, L., Mardis, E., Kupfer, D., Wilson, R., Kris, M., Varmus, H., 2004. EGF receptor gene mutations are common in lung cancers from "never smokers" and are associated with sensitivity of tumors to gefitinib and erlotinib. Proc. Natl. Acad. Sci. U.S.A. https://doi.org/10.1073/pnas.0405220101.
Rosholm, T., Gois, P.M.P., Franzen, R., Candeias, N.R., 2015. Glycerol as an efficient medium for the Petasis borono-mannich reaction. ChemistryOpen 4, 39–46. https://doi.org/10.1002/open.201402066.
Roy, K., Kar, S., Das, R.N., Roy, K., Kar, S., Das, R.N., 2015. Validation of QSAR models. Underst. Basics QSAR Appl. Pharm. Sci. Risk Assess. 231–289. https://doi.org/10.1016/B978-0-12-801505-6.00007-7.
Schrödinger, L.L.C., 2015. The {AxPyMOL} Molecular Graphics Plugin for {Microsoft PowerPoint}, vol. 8 Versiõn1.
Todeschini, R., Consonni, V., Todeschini, R., 2009. Wiley InterScience (Online service). Molecular Descriptors for Chemoinformatics. Wiley-VCH.
Tong, C.W.S., Wu, M., Cho, W.C.S., To, K.K.W., 2018. Recent advances in the treatment of breast cancer. Front. Oncol. 8, 227. https://doi.org/10.3389/fonc.2018.00227.
Traxler, P., Allegrini, P.R., Brandt, R., Brueggen, J., Cozens, R., Fabbro, D., Grosios, K., Lane, H.A., McSheehy, P., Mestan, J., Meyer, T., Tang, C., Wartmann, M., Wood, J., Caravatti, G., 2004. AEE788: a dual family epidermal growth factor receptor/ErbB2 and vascular endothelial growth factor receptor tyrosine kinase inhibitor with antitumor and antiangiogenic activity. Canc. Res. https://doi.org/10.1158/0008-5472.CAN-03-3681.
Vairavelu, Leena, Prasad KJ, Rajendra, 2016. An expedient general synthesis of quinolino and pyrrolocycloocta[b]indoles. Organic Chem. Curr. Res. 5 (2), 1–4. https://doi.org/10.4172/2161-0401.1000165.
Vaiyapuri, P.S., Ali, A.A., Mohammad, A.A., Kandhavelu, J., Kandhavelu, M., 2015. Time lapse microscopy observation of cellular structural changes and image analysis of drug treated cancer cells to characterize the cellular heterogeneity. Environ. Toxicol. https://doi.org/10.1002/tox.21950.
Vermes, I., Haanen, C., Steffens-Nakken, H., Reutelingsperger, C., 1995. A novel assay for apoptosis. Flow cytometric detection of phosphatidylserine expression on early apoptotic cells using fluorescein labelled Annexin V. J. Immunol. Methods 184, 39–51.
Weng, J.-R., Tsai, C.-H., Kulp, S.K., Chen, C.-S., 2008. Indole-3-carbinol as a chemopreventive and anti-cancer agent. Canc. Lett. 262, 153–163. https://doi.org/10.1016/j.canlet.2008.01.033.

PUBLICATIONS

IV

Molecular interaction study of novel indoline derivatives with EGFR-kinase domain using multiple computational analysis

Palanivel S, Yli-Harja O, and Kandhavelu M

Journal of Biomolecular Structure and. Dynamics; 22March 2021, 1-10.

. doi: 10.1080/07391102.2021.1900917

Molecular interaction study of novel indoline derivatives with EGFR-kinase domain using multiple computational analysis

Suresh Palanivel[1,2]*, Olli Yli-Harja[2,3,4], Meenakshisundaram Kandhavelu[1,2]

[1]*Molecular Signaling Lab, Faculty of Medicine and Health Technology, Tampere University and BioMediTech, Tays Cancer Center, Tampere University Hospital, P.O. Box 553, 33101 Tampere, Finland.*

[2]*Institute of Biosciences and Medical Technology, Tampere, Finland*

[3]*Computational Systems Biology Group, Faculty of Medicine and Health Technology, Tampere University and BioMediTech, Tays Cancer Center, Tampere University Hospital, P.O. Box 553, 33101 Tampere, Finland.*

[4]*Institute for Systems Biology, 1441N 34th Street, Seattle, WA 98103-8904, USA*

** E-mail: suresh.palanivel@tuni.fi*

**Phone: (+91) 9677118756*

ABSTRACT:

Epidermal growth factor receptors are constitutively overexpressed in breast cancer cells, which in turn stimulate many downstream signaling pathways that are involved in many carcinogenic processes. This makes EGFR a striking target for cancer therapy. This study focuses on the EGFR kinase domain inactivation by novel synthesized indoline derivatives. The compounds used are N-(2-hydroxy-5-nitrophenyl (4'-methyl phenyl) methyl) indoline (HNPMI), alkylaminophenols - 2-((3,4-Dihydroquinolin-1(2H)-yl) (p-tolyl) methyl) phenol (THTMP) and 2-((1, 2, 3, 4-Tetrahydroquinolin-1-yl) (4 methoxyphenyl) methyl) phenol (THMPP). To get a clear insight into the molecular interaction of EGFR and the three compounds, we have used ADME/Tox prediction, Flexible docking analysis followed by MM/GB-SA, QM/MM analysis, E-pharmacophore mapping of the ligands and Molecular dynamic simulation of protein-ligand complexes. All three compounds showed good ADME/Tox properties obeying the rules of drug-likeliness and showed high human oral absorption. Molecular docking was performed with the compounds and EGFR using Glide Flexible docking mode. This showed that the HNPMI was best among the three compounds and had interactions with key residue Lys 721. The protein-ligand complexes were

stable when simulated for 100ns using Desmond software. The interactions were further substantiated using QM/MM analysis and MM-GB/SA analysis in which HNPMI was scored as the best molecule. All the analyses were carried out with a reference molecule – Gefitinib which is a known standard inhibitor of EGFR. Thus, the study elucidates the potential role of the indoline derivatives as an anti-cancer agent against breast cancer by effectively inhibiting EGFR.

Keywords: EGFR inhibitors, Indolines, Computational analysis, molecular targets, ADME/Tox, QM/MM, Protein-ligand complex

Introduction:

Among the available cancer treatment options, Chemotherapy is the most knock-down tool to kill cancer cells. Emergence of new anticancer drugs constitutes a prominent level of research in cancer therapeutics. Despite the rapid advancement in drug discovery, the lack of efficacy, safety, and selectivity in currently available anticancer drugs, persisted as the major unsolved issue. Among the various chemotherapeutic methods, Targeted therapy is gaining importance. This is a mechanism to control and kill a specific gene or protein that is involved in carcinogenesis[1]. Targeting cancer cells without affecting normal cells will reduce the side effects caused due to chemotherapy in cancer patients. Better understanding and advancements in cancer molecular biology and signaling pathways have enhanced the research in this field of study.

One of such targets, which are involved in the major tumorigenic process, is the Epidermal Growth Factor Receptor (EGFR). EGFR is a transmembrane protein that belongs to the receptor tyrosine kinases family. It mediates cell proliferation, apoptosis, angiogenesis and metastasis in many cancers by mediating various signaling pathways including PI3K-AKT-mTOR, JAK-STAT, ERK-MAPK pathways[2], [3]. EGFR is one of the most common molecules that is altered in cancers and is mostly over-expressed[4]. The two domains of EGFR protein include the tyrosine kinase domain and the ligand (EGF) binding domain. Both the domains are studied widely in multiple cancers including non-small lung cancer, prostate cancer, breast cancer and so on[2], [5], [6]. Myriads of small molecules are studied as inhibitors targeting both domains. Some of the EGFR inhibitors have produced impressive therapeutic benefits to responsive types of cancers viz. Erlotinib, Gefitinib, and Lapatinib[7], [8]. Primarily, the inhibitors targeting Tyrosine kinase activity of EGFR turned successful in the cancer treatment[9]. This is due to the fact that the kinase activity of EGFR is predominantly involved in promoting cell proliferation compared to cell survival[8].

The eliciting problem with the existing EGFR inhibitors as anticancer drugs is that the EGFR overexpressing cancer cells does not respond to the EGFR - kinase domain inhibitors. Though, it is non-deniable that the emergence of novel drug molecules increases, there is always a demand to anticipate for molecules that overcome resistance in EGFR over-expressed cancer cells.

The current study was initiated to address this issue. Our research group has synthesized seven indoline derivatives and conducted *in vitro* studies in breast cancer cells. It was obvious from our

earlier results that three molecules out of seven showed good anticancer activity. They exhibited potent anti-proliferative activity and induced apoptosis in breast cancer cell lines. We have also performed the protein and gene expression studies and concluded that the molecules inhibit EGFR kinase activity thereby possessing anti-cancer activity.

With these background experimental data, we further incline to examine the molecular insights of the drug and target interactions. As a prelude, this research article discusses the complete computational analysis carried out including molecular docking and molecular dynamic simulation to better understand the interaction of the inhibitors with the EGFR tyrosine kinase domain.

Materials and Methods:

Computational software:

All the computational experiments in this study were executed on a workstation with the following specifications: Linux Ubuntu 20.04 LTS Operating System, Intel (R) Core (TM) i5-6200U CPU @2.30GHz 2.40GHZ Processor, 8GB RAM, NVIDIA GeForce 940M card. Furthermore, Molecular Dynamics (MD) simulations were conducted on a Linux-based workstation equipped with an NVIDIA Tesla K20 GPU card. Maestro (Maestro version 12.5.139, Schrödinger, LLC, New York, NY, USA) was used for all the steps involved in the ligand preparation (LigPrep), receptor grid generation, and docking (Glide). Protein preparation wizard and MM-GB/SA were performed using Prime module andE-pharmacophore derived using Phase (Schrödinger Release 2020-4: Phase, Schrödinger, LLC, New York, NY, 2020.). ADME/Tox analysis was carried out using Qikprop (Schrödinger Release 2020-4: QikProp, Schrödinger, LLC, New York, NY, 2020). Density-functional theory (DFT) was performed using Jaguar (Density-functional theory (DFT). MD simulation was performed using DESMOND (Schrödinger Release 2020-4: Desmond Molecular Dynamics System, D. E. Shaw Research, New York, NY, 2020).

Target protein - Retrieval and Energy minimization:

The three-dimensional crystal structure of epidermal growth factor receptor (EGFR) protein was retrieved from the RCBS PDB database with PDB ID - 1M17. Optimization of the target structure was performed using protein preparation wizard to remove inconsistencies in the structure such as missing hydrogen, incorrect bond orders, the orientation of the different functional groups of the amino acids. Energy was minimized using OPLS_2005 (optimized potentials for liquid simulations) force-field[10]. The structure also includes a ligand named Erlotinib, which acts as an inhibitor to this kinase domain. The inhibitor was removed from the protein structure and energy was minimized using the protein preparation wizard. All the images were visualized using Pymol (The PyMOL Molecular Graphics System, Version 2.0 Schrödinger, LLC).

Ligand preparation:

The structures of synthesized ligands were drawn using Chemdraw. The Ligands were converted to their three-dimensional structures and optimized using Ligprep tool of Maestro. Ligprep is used to generate tautomers for each ligand, optimize and neutralize the charge on the ligands. pH 7.0 was selected and all default parameters were maintained. Partial atomic charges were computed using the OPLS_2005 force field and the ligands were energy minimized[11].

ADME/Tox analysis:

The ADME/Tox (absorption, distribution, metabolism, and excretion/ Toxicity) attributes of the synthesized ligands were calculated using the QikProp program. Qikprop predicts physically significant descriptors accurately and indicates pharmaceutically relevant properties of organic molecules. For calculating Qikprop scores the energy minimized ligands (using Ligprep) were given as input in Qikprop. Using this tool, nearly fifty chemical and biological descriptors with relevance to drug-likeliness were analyzed for the indoline derivatives considered in this study[12].

Molecular docking:

To determine the interaction of the ligands with the EGFR kinase domain, docking was performed in Glide "Extra Precision" (XP) mode of the Schrodinger suite. Glide has three modes of docking, among them XP mode is preferred as it provides elimination of false positives as accomplished by more extensive sampling and advanced scoring, resulting in even higher enrichment. The protein grid box of size 10 Å × 10 Å × 10 Å was defined and confined to the active site key residues of 4 Å present in the tyrosine kinase domain of EGFR for docking the ligands. The scale factor of 0.8 for van der Waals radii was applied to atoms of protein with absolute partial charges less than or equal to 0.15. In XP mode, the atoms of ligands are flexible, permitting their conformational and positional freedom during their interaction with the active site of the protein. The Glide Score function used here is a more sophisticated version of ChemScore with force field-based components and additional terms accounting for solvation and repulsive interactions. The choice of the best binding pose is made using a model energy score (Emodel) that combines the energy grid score, glide score and the internal strain of the ligand[13]. The docking protocol was validated by re-docking the ligand which co-exist in crystal protein. The results are given in a supplementary file (Figure S1).

MM-GB/SA Analysis:

After performing GLIDE XP docking, MM-GB/SA (Molecular mechanics-generalized-Born/ surface area) was calculated to estimate the binding free energy of ligand-protein complexes. The output file of XP docking was given as an input for the MM-GB/SA tool of Prime Module. The docked poses were energy minimized using the OPLS-AA3 force field and the energies of protein-ligand complexes were calculated using generalized-Born/surface area (GB/SA). The free energy binding affinity (ΔG bind) was calculated as mentioned below[14]

$$\Delta G_{bind} = \Delta E + \Delta G_{solv} + \Delta G_{SA}$$

Where E, G_{solv}, G_{SA} represents the minimized energy of the protein-ligand complex, solvation free energies and surface area energies and the delta represents the difference in energy between protein-ligand complex, protein, and that of the ligand.

E-pharmacophore mapping:

E-pharmacophore map was generated from the ligands using Phase software. The pharmacophore sites were generated automatically based on the default settings applied for refinement and scoring. The map includes chemical features like hydrogen bond acceptor (A), HB donor (D), hydrophobic (H) region, positive ionizable(P), negative ionizable(N) atoms and aromatic ring(R). Each of the pharmacophore feature sites is assigned with an energy value equal to the sum of XP contributions of the atoms comprising the sites, which allows sites to be ranked on the basis of energy values obtained[15].

QM/MM Methodology

Density-functional theory (DFT) is a computational quantum mechanical modeling method used to predict the biological activity and molecular level activity of chemical compounds. The parameters such as electron density, molecular electrostatic map frontier molecular orbital HOMO and LUMO were measured for quantum mechanical calculation. We employed the use of the QSITE program for QM/MM calculations. QSITE constructs the interface between QM and MM regions by utilizing the molecular orbitals along with covalent bonds. The molecular orbitals HOMO and LUMO help to understand the spatial distribution of electronic features in the charge transfer mechanism. The density functional theory (DFT) method plays a significant role in representing the QM region, MESP is calculated at each configuration and the outputs are analyzed. The Jaguar version10.4 was used to calculate the DFT calculations. The optimization of the QM wave-function is carried out by integrating the MM point charges, which are accountable for the polarization of the ligand charge distribution.

Molecular dynamics – Simulation

The molecular dynamics simulations were performed using the Desmond module of the Schrödinger package for the docked complex of 1M17 (EGFR) with the inhibitors (HNMPI, THMPP and THTMP). A protein preparation wizard is used to prepare the protein and ligand for simulation by applying the OPLS_2005 force field. Docked complexes were embedded in the TIP3P (transferable intermolecular potential 3P) water model. The system was specified on periodic boundary conditions, the particle mesh Ewald (PME) method for electrostatics, a 10 A° cutoff for Lennard–Jones interactions and SHAKE algorithm for limiting movement of all covalent bonds involving hydrogen atoms. The system was neutralized with the addition of Na^+ and Cl^- ions. Initially, a relaxation simulation was performed to relax the system with an NPT ensemble at a 300K temperature and 1 bar pressure. The relaxed system was simulated for a simulation time of 10,000 ps (picoseconds) with a time step of 1.2 ps. Trajectories after every 8.4 ps were recorded. Berendsen thermostats and barostats were used to control the temperatures and pressures during the initial simulations. Further, 100 ns unrestrained production run with an interval of every 1.0

picoseconds was carried out. During the production run, the temperature was set to 300K and was constantly maintained by invoking the Nose–Hoover thermostat with the pressure set to 1 atom, maintained through Martyna–Tobias Klein pressure bath. RMSD of the complex and protein-ligand interactions in each trajectory was plotted against the time. The stability of EGFR- drug complexes was checked from the Root Mean Square Deviation (RMSD), and the flexibility of the system was evaluated from the Root Mean Square Fluctuations (RMSF) [16].

Results:

Structure of protein and the ligands:

The 3D structure of the EGFR tyrosine kinase domain (1M17) was downloaded from PDB. The structure was determined using X-ray crystallography with a resolution of 2.60 Å. The domain structure includes 312 residues and belongs to the alpha + beta protein class (Figure 1). [17].

The ligands chosen for study are synthesized compounds; their structures were drawn using chem sketch and converted to 3D structures in Maestro software. The ligands have a similar parental structure of indoline and their sidechain varies. Ligands are N-(2-hydroxy-5-nitrophenyl (4'-methyl phenyl) methyl) indoline (HNPMI), alkylaminophenols - 2-((3,4-Dihydroquinolin-1(2H)-yl) (p-tolyl) methyl) phenol (THTMP) and 2-((1, 2, 3, 4-Tetrahydroquinolin-1-yl) (4 methoxyphenyl) methyl) phenol (THMPP) (Figure 2a, 2b & 2c). The standard inhibitor chosen for the study is Gefitinib, whose structure was downloaded from PubChem database (compound ID: CID 123631) and is shown in Figure 2d. All the four compounds were energy minimized using Ligprep and used for further analysis.

ADME/Tox analysis:

For all three ligands, pharmacologically relevant properties were analyzed. It considers nearly 50 physical signifiers to evaluate the drug likeliness property of a compound. The descriptors evaluate the Lipinski rule of five along with many other properties including the blood-brain barrier, human oral absorption. These properties describe the biological activity of the compound at the molecular level. Upon analysis (Table 1), it was found that all three ligands followed the Lipinski rule of five and none of them violated any rule. PSA and rotatable bonds play a crucial role in the oral bioavailability of drug molecules, the value of rotatable bonds between 0-15 and the value of PSA from 7-200 Å holds greater importance on the oral bioavailability of drug molecules. The lead molecules which pass through the Caco-2 permeability filter result in good intestinal absorption. Further, the results of the QPlogkhsa indicator between -1.5 to 1.5 indicate the predicted values of human serum albumin. The QPlog descriptor plays a significant role in determining the aqueous solubility. On analyzing all the parameters, all three compounds can act as effective drug candidates.

Molecular docking:

Molecular docking was performed using Glide XP mode using the energy minimized ligands and the grid formed in the binding site of the target protein. The binding active site residues are Lys 721, Ala 719, Ile 720, Glu 738, Met 742, Leu 753, Ile 765, Thr 766, Gln 767, Leu 768, Leu 820, Gly 772, Leu 694, Asn 818, Asp 831, Phe 699, Val 702 and Met 769(Table 2). All the three ligands docked to the active site pocket with a Glide score around -5 kcal/mol and showed interactions with the key residues. Among the three, HNPMI showed the best docking score. HNPMI forms hydrogen bond interaction with Asp 831 and a π-cationic interaction with Lys 721. Similarly, THTMP and THMPP showπ-cation interaction with Lys 721(Figure 3). It is also important to note that Gefitinib interacts with the binding site with a slightly higher score and interacts with Lys 721 (Table 2). Thus, Lys 721 is considered a crucial residue for a compound to inhibit the kinase activity of EGFR protein. Our ligands also show the interaction with Lys 721 which imparts their potential to inhibit the protein. The other interactions include Hydrogen bond interaction with Ala 719 – THTMP and Met 769 – THMPP. The glide energy model is also tabulated to further substantiate the ligand interaction. Lower, the Glide XP score better is the binding capacity of a compound. This confirms the potential of the compounds to inhibit EGFR, and HNPMI is the best inhibitor among the three.

MM-GB/SA:

The MM-GB/SA analysis was performed to further confirm the binding of the ligands to active site residues. The ΔG_{bind} value was found to be between -33 kcal/mol and -42 kcal/mol (Table 2). Among the three ligands, HNPMI scored the lowest value and hence possess better inhibitory capacity among the three compounds. This is in accordance with the glide score too.

E-pharmacophore mapping:

The E-Pharmacophores method utilizes the Glide XP scoring function to accurately characterize protein-ligand interactions, resulting in improved database screening enrichments. E-Pharmacophores allow for excluded volumes that correspond to regions of space that are occupied by the receptor. It is a powerful tool for lead hopping and enables the screening of hundreds of compounds per second Using this method, the sites of HNPMI, THTMP and THMPP were identified and they include an aromatic ring, an acceptor and a donor group and hydrogen bond donor group (Figure 4). The e-pharmacophore was implemented to screen the molecules further obtained from the initial docking of the selected compounds. The hypothesis was computed by imposing Glide XP energy properties over pharmacophore sites based on the protein and ligand structural information. The initial number for pharmacophore site generation was set to default; however, a five-pharmacophore site hypothesis ADHHR was generated.

DFT Analysis:

The density functional theory was implied to study the electron donor/acceptor property of HNPMI, THTMP and THMPP. The frontier molecular orbitals or most important quantum mechanical descriptors namely HOMO and LUMO poses an understanding of the reactivity and

the active site of the molecule. HOMO-LUMO gap is termed as the energy difference between the HOMO and LUMO molecular orbitals. The better stability of the chemical compound can be determined with their lowest HOMO-LUMO gap. The HOMO and LUMO potential energy of the HNPMI, THTMP and THMPP were -0.018 and -0.010, -0.018 and 0.009, and -0.19 and -0.086 respectively (Table. 4). In all three compounds, the HOMO regions are higher in density and lower in values and the LUMO regions are lower in density and higher values. Thus, the HOMO regions are capable of donating electrons and LUMO regions are capable of accept electrons in the molecule. The lower HOMO-LUMO energy gap of HNPMI, THTMP, and THMPP are -0.17, 0.17 and 0.18, respectively. The blue region represents the positive energy surface, and the red region represents the negative energy surface in the molecular electrostatic potential (MESP) of the molecule (Figure 5).

Molecular dynamics – Simulation:

Molecular dynamics simulations were carried out for EGFR (1M17) in the native form and in complex with the three test compounds to determine the stability of the complex and the molecular interactions. The RMSD (root mean square deviation) plot (Fig. 6a, 6b, 6c, and 6d) of the ligand complexes and the native EGFR looks stable after the initial equilibration period. HNMPI- EGFR complex was stable throughout the run. The Protein-ligand contact map reveals that the hotspot residues have maintained their integrations most of the time along with the active site. In the active site region of the protein -1M17, Ala 719, Lys 721 Met 769 and Asp 831 have maintained their integrations most of the time along with HNMPI (Fig. 7a). Similarly, THTMP and THMPP with Ala 719, Lys 721 and Met 769 interactions shown in (Fig. 7b and 7c) respectively, are maintained more than 30.0% of the simulation time in the selected trajectory of 100ns. Comparing the three compounds, HNMPI- EGFR complex is more stable and the interaction of ligands with the active site residues are stronger, making more than one specific contact with the ligand and occurs longer (almost throughout) during the simulation time. The interactions well correlate with our docking results. The residues in the binding pocket - Lys 721, Met 769, Asp 831, and Ala 719 interacts with the compounds and are stable (Fig. 7). Surprisingly, the interaction map of the standard Gefitinib and EGFR shows that the compound interacts well with Leu 694 and Pro772 (Fig. 7d), though the Lys 721 residue interacts more than 30% of simulation time. Thus, our molecular dynamics simulations suggest that the protein-inhibitor complexes are stable, and the binding interactions between the inhibitor and the protein are strong, HNMPI being the best complex with the lowest RMSD and stable interactions. But the residue interaction of test compounds in the binding pocket is slightly varied from the standard Gefitinib.

Discussion:

The protein target chosen for this *in silico* study, EGFR is an important molecular target in cancer therapeutics. This is due to the role it plays in cell cycle modulation and proliferation. There are myriads of small molecules are in research, towards targeting EGFR. The perturbation is many molecules are less potent in micromolar concentration. Most of the small molecules tested *in vitro* and *in vivo*, face resistance in cancer cells after multiple usages [7], [18]. This is due to the shift in the signaling pathway by the cancer cells itself. To rectify these problems, it is always better to select molecules which target domain of a target protein. Considering this conception, we study molecular interaction with the target protein, EGFR in a domain, Tyrosine kinase. In the case of EGFR, among all the domains, the tyrosine kinase domain is crucial, as it can activate cascades of proliferation and cell cycle mediating compounds[19]. We sensed that targeting over-expressed EGFR-tyrosine kinase activity can down-regulate the PI3K and S6K1 proteins downstream. This may lead to the prohibition of cell growth considerably.

The same hypothesis was studied earlier by our group in breast cancer cell lines MCF7 and SKBr3 cells. In the earlier reports, we have clearly noted the cytotoxicity induced by these compounds in the mentioned cell lines. We have also given data on their IC_{50} values, their capacity to induce apoptosis and control cell growth. The IC_{50} value of ligands HNPMI, THMPP and THTMP in MCF-7 cells were 64.10μM, 83.23μM and 87.92μM, respectively. Similarly, in the case of SKBr3 cells the IC_{50} values were 119.99μM, 113.94μM and 172.51μM respectively. We have already performed QSAR studies based on the ligand and their IC_{50} values. We have also studied the protein expression of PI3K and S6K1, which were found to be down-regulated in treated cells[20]–[22].

In continuation with these data, we were intended to study the molecular insight into the interaction between the EGFR – Kinase residues and the ligands HNPMI, THTMP and THMPP. The results presented here illustrate the interaction, their pharmacokinetic properties, stability of the protein-ligand complex formed. From the docking analysis, we found the interaction of the compounds with the key residues of the protein EGFR. Among the three compounds, though the docking score had a little difference, HNMPI had very strong interactions and showed stability in a molecular dynamics simulation study [2], [23]. HNMPI also exhibited the lowest MM-GB/ SA energy score values, this makes us conclude that the best EGFR inhibitor among our compounds is HNMPI. The e- pharmacophore analysis explains the structural features responsible for the inhibition, the hypothesis thus arrived can be used for further virtual screening of inhibitors. Overall, these findings are crucial to understand how compounds are projected with the template by good molecular features that are potential for they are allowed as reference drugs. Also, our selected compounds are more effective to EGFR than Gefitinib, hence, they could bind the receptor active site as reference binding orientation. There are also other reports stating higher binding activity than the positive control which can lead to the discovery of better EGFR inhibitors [24].

Similar studies have been performed in advanced research aiming at finding a new drug for cancer treatment. Quinazoline-based EGFR inhibitors were studied by a research group using *in silico* methods. They have performed the QSAR model, molecular docking and ADME prediction using the Schrödinger suite in 2016[25]. The inhibitor for selectively mutated EGFR was studied *in silico* through virtual screening followed by molecular docking analysis in curcumin derivatives[26]. Many reports are depicting the similar activity of various small molecules against EGFR kinase activity including Benzothiazole derivatives[27], 2, 7-diamino-thiazolo [4,5-d] pyrimidine analogs [28], Novel 5-Deazaalloxazine Analogs[29] and so on. There is also a report on Furanocoumarin derivatives against multiple targets involved in tumorigenesis of breast cancer[30]. They have performed a structure-based docking analysis. Thus, our report goes in hand with similar literature supporting *in silico* analysis of EGFR inhibitors.

Conclusion:

The present investigation gives a clear picture on the molecular interaction of EGFR protein and three chemically synthesized indoline derivatives named shortly as HNMPI, THTMP and THMPP. The compounds showed good ADME/Tox properties with drug likeliness properties along with high human oral absorption. The compounds when docked to the active site region of the EGFR kinase domain, had hydrogen bond interaction, pi-cationic interaction and hydrophobic interactions with key residues including Lys 721, Ala 719, Met 769 and Asp 831. The interactions were stable when they were simulated for 100ns in a solvent system and the complex remained intact without deterioration. The QM-MM and MM-GB/SA analysis further substantiate the interactions and the ligands were compared to the standard inhibitor – Gefitinib. Along with that the e-pharmacophore model was also generated for each molecule, which can be used for further screening of new drugs. Thus, the article gives a complete computational analysis on the interaction of target protein and the chosen ligands.

References:

[1] L. Yan, N. Rosen, and C. Arteaga, "Targeted cancer therapies," *Chinese Journal of Cancer*, vol. 30, no. 1. Landes Bioscience, pp. 1–4, 2011.

[2] A. E. Maennling *et al.*, "Molecular targeting therapy against egfr family in breast cancer: Progress and future potentials," *Cancers (Basel).*, vol. 11, no. 12, Dec. 2019.

[3] A. M. Martelli *et al.*, "The phosphatidylinositol 3-kinase/AKT/mammalian target of rapamycin signaling network and the control of normal myelopoiesis.," *Histol. Histopathol.*, vol. 25, no. 5, pp. 669–80, 2010.

[4] S. Sigismund, D. Avanzato, and L. Lanzetti, "Emerging functions of the EGFR in cancer," *Molecular Oncology*, vol. 12, no. 1. John Wiley and Sons Ltd., pp. 3–20, Jan-2018.

[5] B. C. Liao, C. C. Lin, and J. C. H. Yang, "Novel EGFR Inhibitors in Non-small Cell Lung Cancer: Current Status of Afatinib," *Current Oncology Reports*, vol. 19, no. 1. Current Medicine Group LLC 1, Jan-2017.

[6] G. Bethune, D. Bethune, N. Ridgway, and Z. Xu, “Epidermal growth factor receptor (EGFR) in lung cancer: An overview and update,” *Journal of Thoracic Disease*, vol. 2, no. 1. AME Publications, pp. 48–51, 2010.

[7] D. Singh, B. Kumar Attri, R. Kaur Gill, and J. Bariwal, “Review on EGFR Inhibitors: Critical Updates,” *Mini-Reviews Med. Chem.*, vol. 16, no. 14, pp. 1134–1166, Aug. 2016.

[8] X. Xu *et al.*, “Research and development of anticancer agents under the guidance of biomarkers,” *Cancer Transl. Med.*, vol. 5, no. 1, p. 17, 2019.

[9] A. Ayati, S. Moghimi, S. Salarinejad, M. Safavi, B. Pouramiri, and A. Foroumadi, “A review on progression of epidermal growth factor receptor (EGFR) inhibitors as an efficient approach in cancer targeted therapy,” *Bioorg. Chem.*, vol. 99, no. March, p. 103811, 2020.

[10] G. Madhavi Sastry, M. Adzhigirey, T. Day, R. Annabhimoju, and W. Sherman, “Protein and ligand preparation: Parameters, protocols, and influence on virtual screening enrichments,” *J. Comput. Aided. Mol. Des.*, vol. 27, no. 3, pp. 221–234, Mar. 2013.

[11] L. Schrödinger, “LigPrep, Schrödinger, LLC, New York, NY,.” 2019.

[12] L. Schrödinger, “QikProp, Schrödinger, LLC, New York,.” 2019.

[13] S. K. Tripathi, R. Muttineni, and S. K. Singh, “Extra precision docking, free energy calculation and molecular dynamics simulation studies of CDK2 inhibitors.,” *J. Theor. Biol.*, vol. 334, pp. 87–100, Oct. 2013.

[14] P. D. Lyne, M. L. Lamb, and J. C. Saeh, “Accurate prediction of the relative potencies of members of a series of kinase inhibitors using molecular docking and MM-GBSA scoring,” *J. Med. Chem.*, vol. 49, pp. 4805–4808, 2006.

[15] S. L. Dixon, A. M. Smondyrev, E. H. Knoll, S. N. Rao, D. E. Shaw, and R. A. Friesner, “PHASE: A new engine for pharmacophore perception, 3D QSAR model development, and 3D database screening: 1. Methodology and preliminary results,” *J. Comput. Aided. Mol. Des.*, vol. 20, no. 10–11, pp. 647–671, Oct. 2006.

[16] L. Schrödinger, “Desmond Molecular Dynamics System, D. E. Shaw Research, New York, Maestro-Desmond Interoperability Tools, Schrödinger, New York, NY, 2020.” 2019.

[17] Schrödinger, LLC, “The {PyMOL} Molecular Graphics System, Version~1.8,” Nov. 2015.

[18] S. Crunkhorn, “Cancer: Combating resistance to EGFR inhibitors,” *Nat. Rev. Drug Discov.*, vol. 18, no. 1, p. 18, Dec. 2018.

[19] W. Pao and N. Girard, “Clinical applications of kinase inhibitors in solid tumors,” in *Handbook of Cell Signaling, 2/e*, vol. 2, Elsevier Inc., 2010, pp. 615–631.

[20] S. Palanivel, A. Murugesan, O. Yli-Harja, and M. Kandhavelu, “Anticancer activity of

THMPP: Downregulation of PI3K/ S6K1 in breast cancer cell line," *Saudi Pharm. J.*, vol. 28, no. 4, pp. 495–503, Apr. 2020.

[21] S. Palanivel, O. Yli-Harja, and M. Kandhavelu, "Alkylamino Phenol Derivative Induces Apoptosis by Inhibiting EGFR Signaling Pathway in Breast Cancer Cells," *Anticancer. Agents Med. Chem.*, vol. 20, no. 7, pp. 809–819, Jul. 2020.

[22] S. Palanivel, A. Murugesan, K. Subramanian, O. Yli-Harja, and M. Kandhavelu, "Antiproliferative and apoptotic effects of indole derivative, N-(2-hydroxy-5-nitrophenyl (4′-methylphenyl) methyl) indoline in breast cancer cells," *Eur. J. Pharmacol.*, vol. 881, p. 173195, Aug. 2020.

[23] T. Kitazaki *et al.*, "Gefitinib, an EGFR tyrosine kinase inhibitor, directly inhibits the function of P-glycoprotein in multidrug resistant cancer cells," *Lung Cancer*, vol. 49, no. 3, pp. 337–343, Sep. 2005.

[24] U. D. Bommu, K. K. Konidala, R. Pamanji, and S. Yeguvapalli, "Computational screening, ensemble docking and pharmacophore analysis of potential gefitinib analogues against epidermal growth factor receptor," *J. Recept. Signal Transduct.*, vol. 38, no. 1, pp. 48–60, 2018.

[25] G. Verma *et al.*, "Pharmacophore modeling, 3D-QSAR, docking and ADME prediction of quinazoline based EGFR inhibitors," *Arab. J. Chem.*, vol. 12, no. 8, pp. 4815–4839, Dec. 2019.

[26] N. A. Shaik, H. M. Al-Kreathy, G. M. Ajabnoor, P. K. Verma, and B. Banaganapalli, "Molecular designing, virtual screening and docking study of novel curcumin analogue as mutation (S769L and K846R) selective inhibitor for EGFR," *Saudi J. Biol. Sci.*, vol. 26, no. 3, pp. 439–448, Mar. 2019.

[27] H. V. Shahare and G. S. Talele, "Designing of benzothiazole derivatives as promising EGFR tyrosine kinase inhibitors: a pharmacoinformatics study," *J. Biomol. Struct. Dyn.*, vol. 38, no. 5, pp. 1365–1374, Mar. 2020.

[28] Q.-H. Liao, Q.-Z. Gao, J. Wei, and K.-C. Chou, "Docking and Molecular Dynamics Study on the Inhibitory Activity of Novel Inhibitors on Epidermal Growth Factor Receptor (EGFR)," *Med. Chem. (Los. Angeles).*, vol. 7, no. 1, pp. 24–31, Dec. 2010.

[29] S. Mahmoud *et al.*, "Design, Synthesis, Antitumor Activity and Molecular Docking Study of Novel 5-Deazaalloxazine Analogs," *Molecules*, vol. 25, no. 11, May 2020.

[30] R. Acharya, S. Chacko, P. Bose, A. Lapenna, and S. P. Pattanayak, "Structure Based Multitargeted Molecular Docking Analysis of Selected Furanocoumarins against Breast Cancer," *Sci. Rep.*, vol. 9, no. 1, 2019.

Figure 1: Structure of Epidermal growth factor, tyrosine kinase domain alone. Red colour represents the helices and cyan blue colour indicate the beta sheets and grey colour indicate the loops in the domain

154x185mm (150 x 150 DPI)

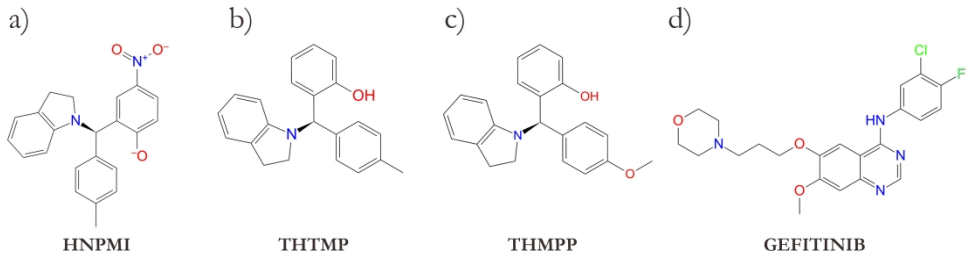

Figure 2: The 2D Chemical structure of the compounds HNMPI, THTMP, THMPP and Gefitinib

338x92mm (300 x 300 DPI)

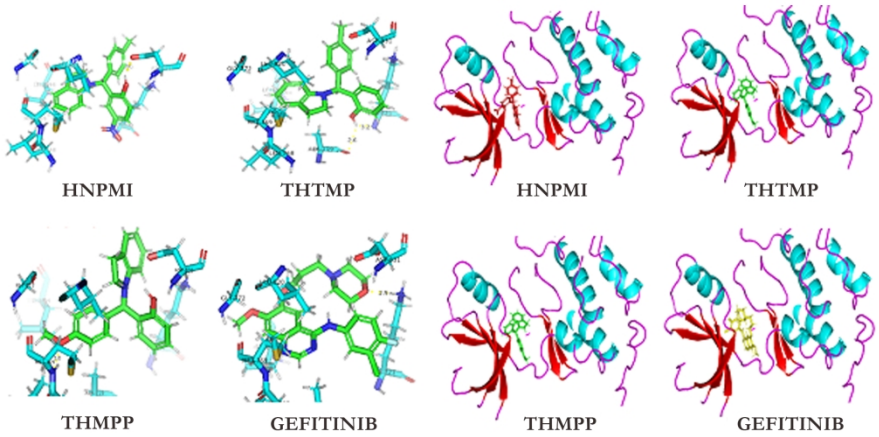

Figure 3: This figure shows the interaction and binding poses of HNMPI, THTMPP, THMPP and Gefitinib with EGFR. The hydrogen bonds formed, and their distance are shown as dashes lines (green colour). Ligands are represented as yellow coloured sticks and the interacting residues of EGFR are shown as red sticks

250x134mm (300 x 300 DPI)

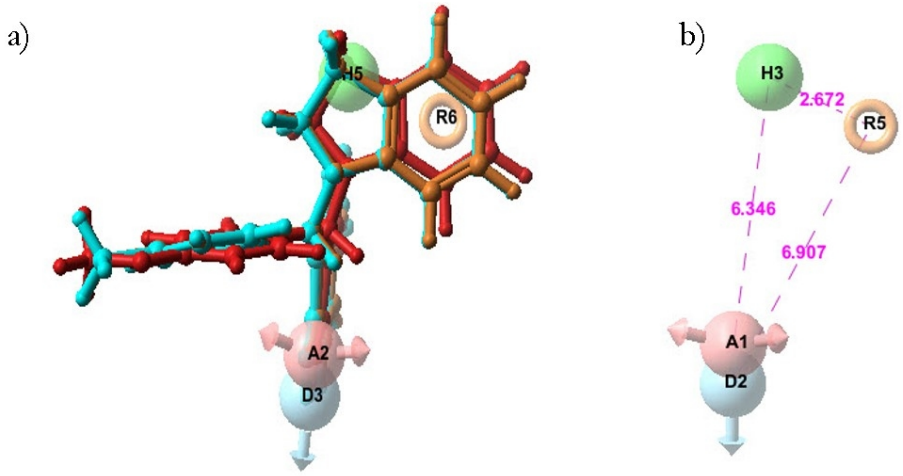

Figure 4: Structure-based pharmacophore hypotheses developed using the e- pharmacophore module of Maestro software. E-pharmacophore map of the ligands: D, A, H and R represent chemical features of hydrogen bond donor, hydrogen bond acceptor, hydrophobic regions, and aromatic ring, respectively. A) Represents the sites that are common to the three ligands, which was derived from the best hypotheses selected. Colours represented are blue for HNMPI, red for THMPP and orange for THTMP; B) Represents the measure of distance between each feature in the pharmacophore.

179x91mm (150 x 150 DPI)

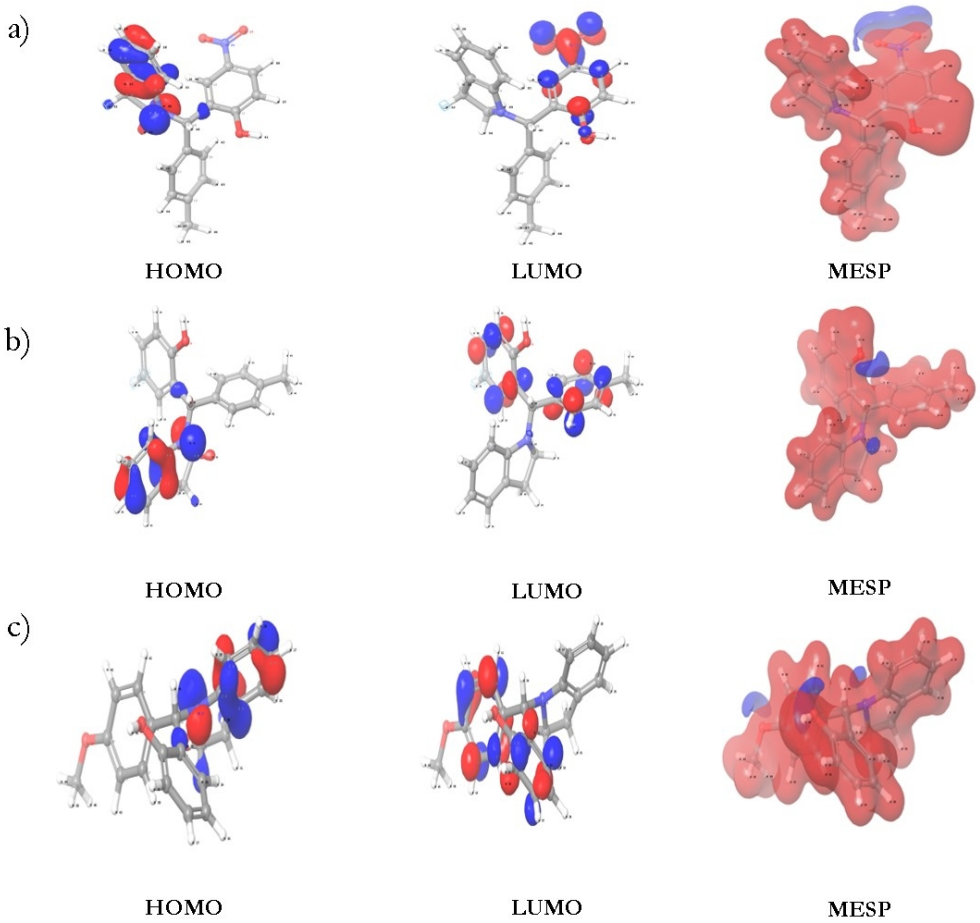

Figure 5: Contour map of HOMO, LUMO, and MESP of HNMPI, THTMP and THMPP
5a) Contour map of HOMO, LUMO, and MESP of compound HNPMI
5b) Contour map of HOMO, LUMO, and MESP of compound THTMP
5c) Contour map of HOMO, LUMO, and MESP of compound THMPP

183x175mm (150 x 150 DPI)

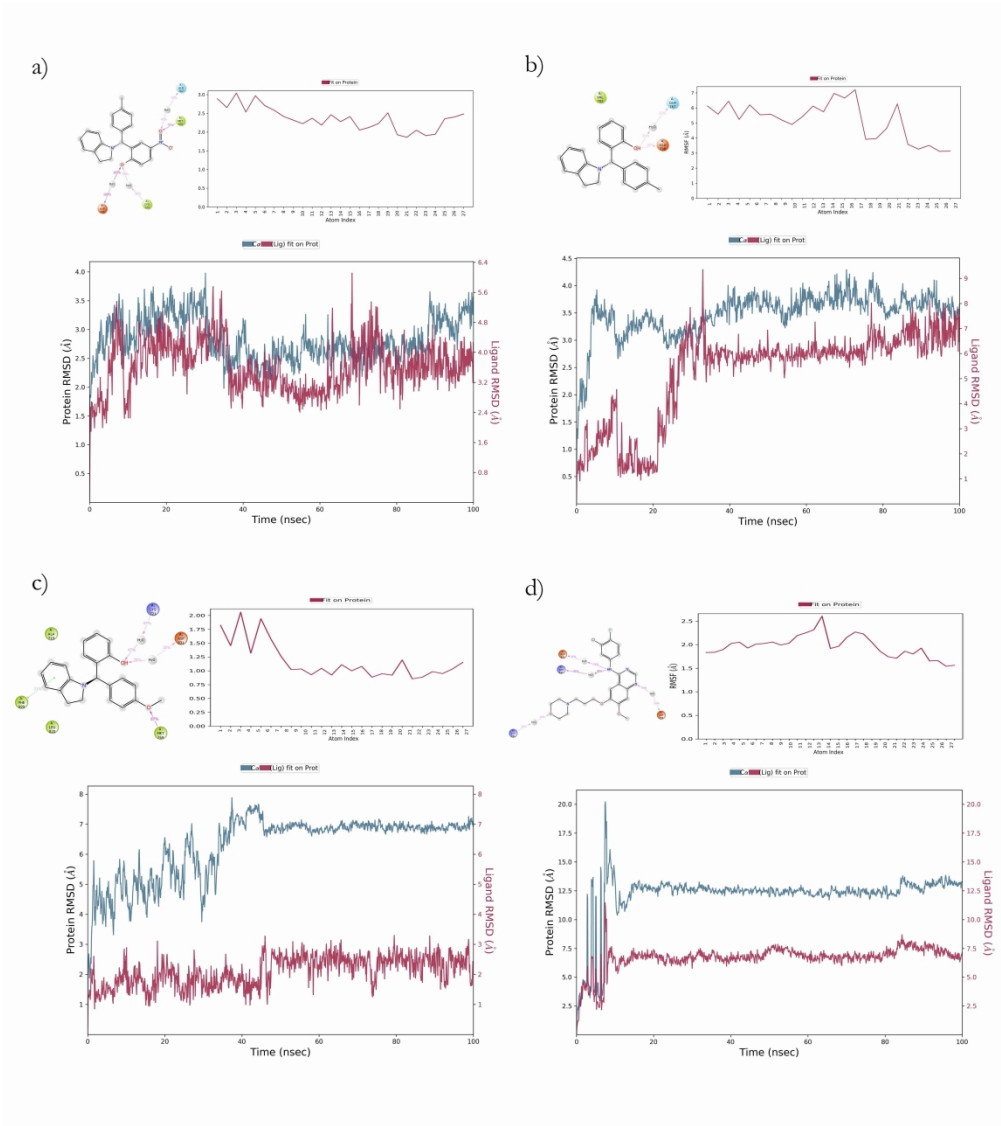

Figure 6

Figure 6: Ligand interactions with the corresponding amino acids. Root mean Square fluctuation (RMSF) of ligand obtained from 100 ns MD simulations (Pink color represents the average deviation of the ligand). Root mean square deviation (RMSD) of ligand and protein backbone obtained from 100 ns MD simulation; (Pink color represents the protein and the blue color represents the ligand).

Figure 6a: RMSD of HNMPI: Ligand Interactions, RMSF and RMSD of ligand and protein backbone obtained from 100 ns MD simulation.
Figure 6b: RMSD of THTMP: Ligand Interactions, RMSF and RMSD of ligand and protein backbone obtained from 100 ns MD simulation.
Figure 6c: RMSD of THMPP: Ligand Interactions, RMSF and RMSD of ligand and protein backbone obtained from 100 ns MD simulation.
Figure 6d: RMSD of GEFITINIB: Ligand Interactions, RMSF and RMSD of ligand and protein backbone obtained from 100 ns MD simulation.

508x571mm (300 x 300 DPI)

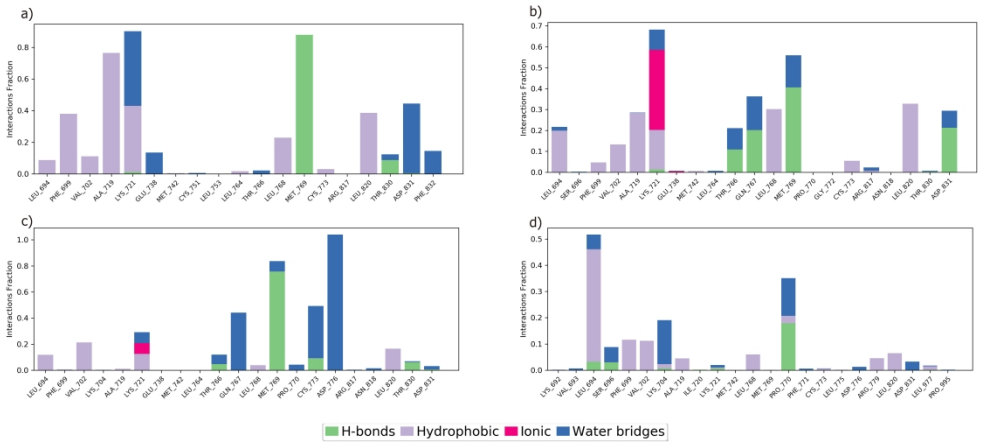

Figure 7: SIMULATION INTERACTIONS DIAGRAM - Protein interactions with the ligand can be monitored throughout the simulation. Protein-ligand interactions are categorized into four types: Hydrogen Bonds, Hydrophobic, Ionic and Water Bridges.
Figure 7a: Simulation Interactions Diagram of HNMPI
Figure 7b: Simulation Interactions Diagram of THTMP
Figure 7c: Simulation Interactions Diagram of THMPP
Figure 7d: Simulation Interactions Diagram of GEFITINIB

471x231mm (300 x 300 DPI)

Molecule	MW	Donor HB	Acceptor HB	QP logPo/w	QPlogS	QP logHERG	QPP Caco	QPlogBB	Human Oral Absorption	Percent Human Oral Absorption	Rule of Five
HNMPI	331.41	1	2.5	4.702	-4.37	-6.714	1035.938	0.287	3	100	0
THTMP	315.41	1	1.75	4.844	-4.476	-6.386	1074.949	0.373	3	100	0
THMPP	331.41	1	2.5	4.702	-4.37	-6.714	1035.938	0.287	3	100	0

Table 1: ADME properties of the ligand HNPMI, THTMP, and THMPP

Ligand name	Glide XP score (kcal/mol)	Glide energy (kcal/mol)	Interacting residues	Interactions	MM-GBSA (ΔGbind) (kcal/mol)
HNPMI	-5.345	-63.170	Asp 831 Lys 721	H bond (3.4 Å) Pi-cation	-42.534
THTMP	-5.670	-48.726	Lys 721 Ala 719	Pi-cation H bond (3.0 Å)	-33.183
THMPP	-5.797	-54.810	Lys 721 Met 769	Pi-cation H bond (2.0 Å)	-33.108
Gefitinib	-6.297	-79.051	Lys 721	H bond (2.6 Å)	-51.562

Table 2: Molecular docking analysis and Binding free energies (kcal/mol) of HNPMI, THTMP, THMPP and Gefitinib with EGFR

Ligands	HOMO	LUMO	ΔE (eV)	Iso Value
HNMPI	-0.18	-0.010	-0.17	-0.05
THTMP	-0.18	-0.009	-0.17	-0.05
THMPP	-0.19	-0.086	-0.18	-0.05

Table 3: Molecular Orbital Energy Values for HNMPI, THTMP, AND THMPP

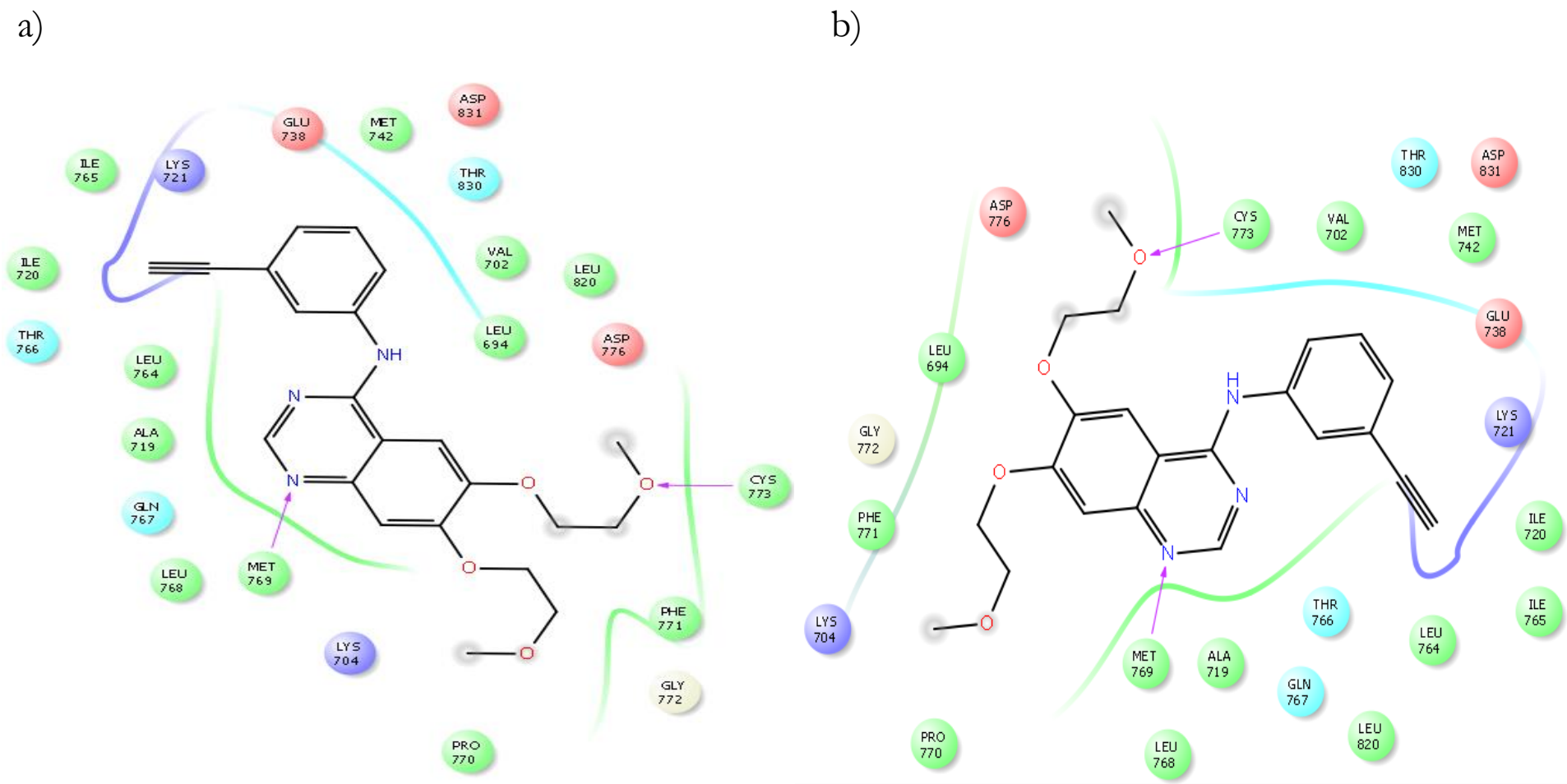

Supplementary File 1: Validation of the Docking Procedure; 1a) Ligand interaction of the ligand and the protein as in PDB (1M17) and 1b) Ligand interaction of the complex (Protein with Erlotinib) using our Glide XP procedure

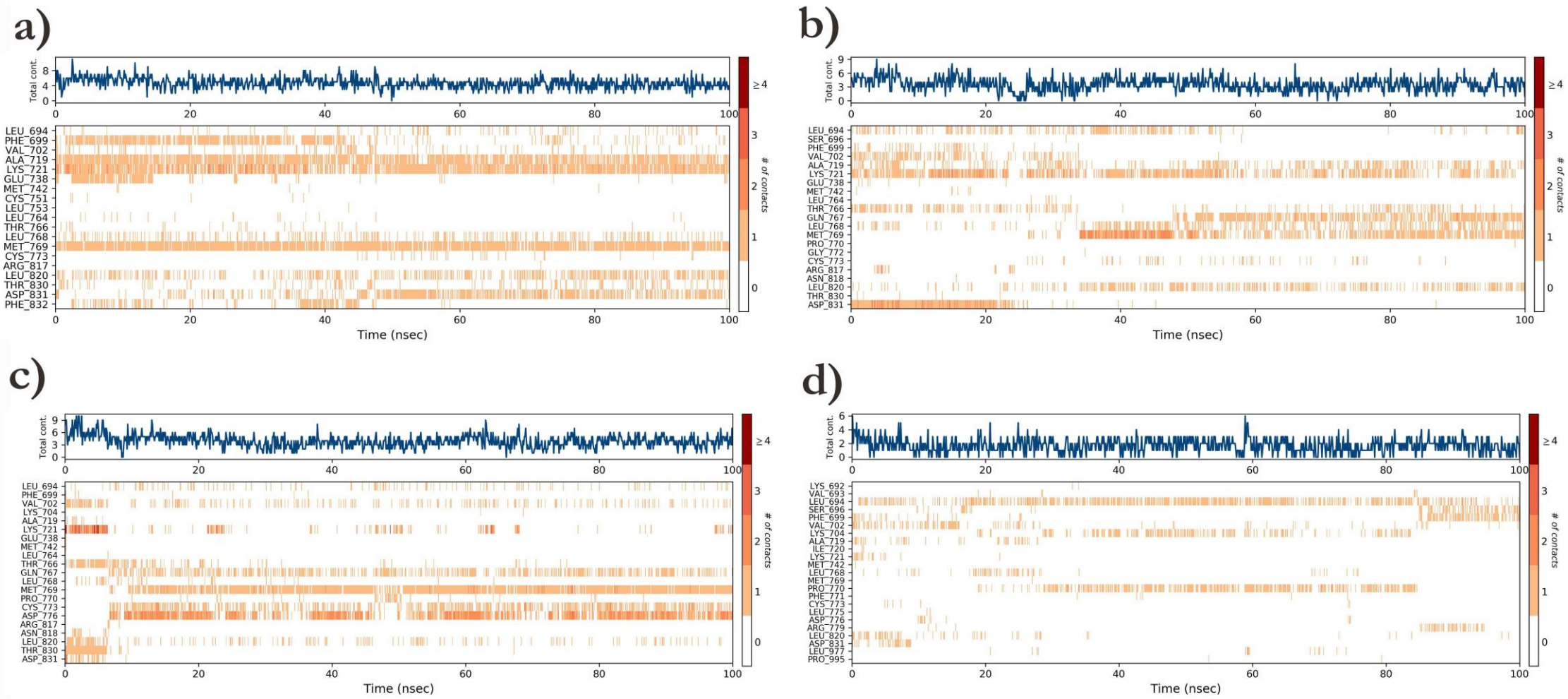

Supplementary File 2: Trajectories and Dynamics of ligand and protein backbone obtained from 100 ns MD simulation. The blue color shown in the separate chart represents the trajectory of the total number of contacts throughout the simulation. The dynamics of the protein-ligand complex interaction throughout the simulation. The X-axis represents the simulation time from 0ns to 100ns and the Y-axis represents the amino acid interactions. The orange vertical line present in the chart represents the interactions of amino acid taken place at specific timeframe.

Figure 2a: HNMPI: Trajectory and Dynamics of ligand and protein backbone obtained from 100 ns MD simulation.

Figure 2b: THTMP: Trajectory and Dynamics of ligand and protein backbone obtained from 100 ns MD simulation.

Figure 2c: THMPP: Trajectory and Dynamics of ligand and protein backbone obtained from 100 ns MD simulation.

Figure 2d: GEFITINIB: Trajectory and Dynamics of ligand and protein backbone obtained from 100 ns MD simulation.